

Oxide interfaces

Manuel Bibes

Unité Mixte de Physique CNRS / Thales, Palaiseau (FRANCE)

7th International School of Oxide Electronics (ISOE2023)

Cargèse, September 2023

<http://oxitronics.cnrs.fr>

manuel.bibes@cnrs-thales.fr



@ManuelBibes



erc

Fresco

THALES

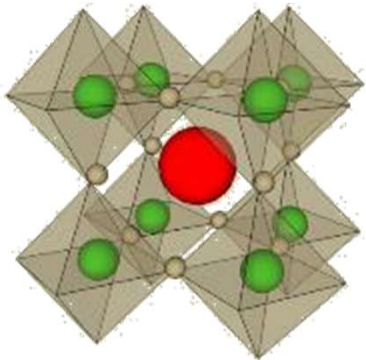


université
PARIS-SACLAY



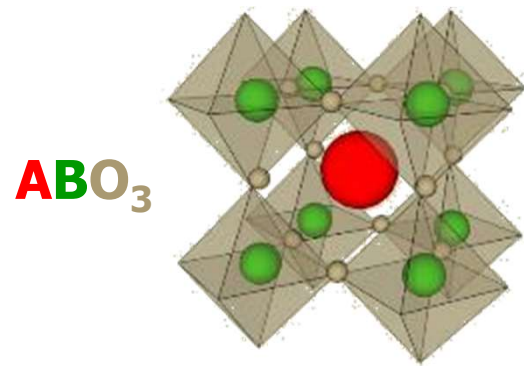
QUANTERA

Transition metal perovskite oxides

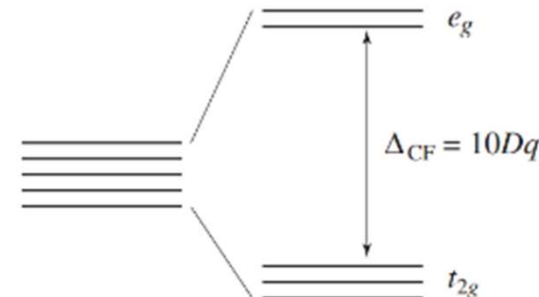
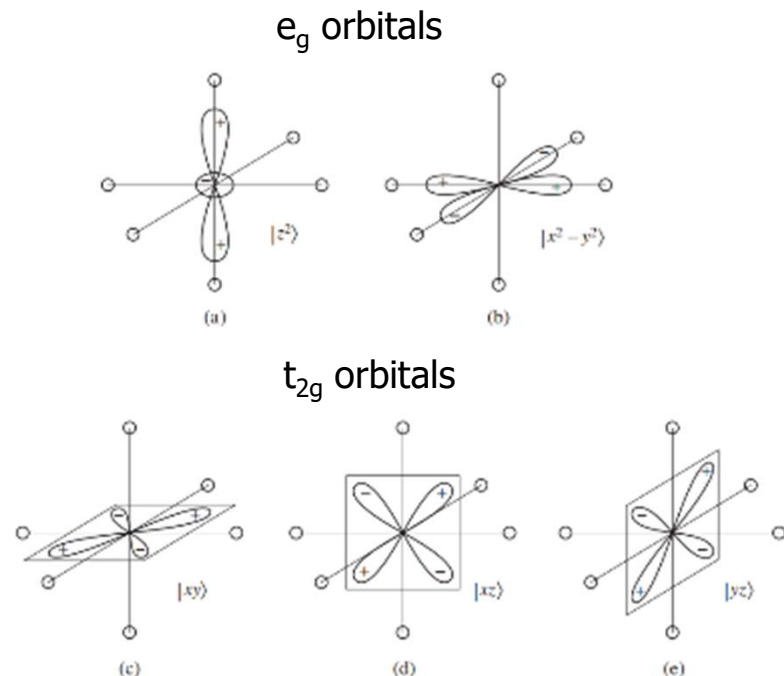


- Very **flexible** structure
doping, tuning of bond lengths and angles
- Broad range of **electronic states**
superconductivity, ferroelectricity, magnetic order, orbital order
- Competition : **giant/coupled responses**
colossal magnetoresistance, magnetoelectric coupling
- Multifunctional heteroepitaxial architectures

Transition metal perovskite oxides



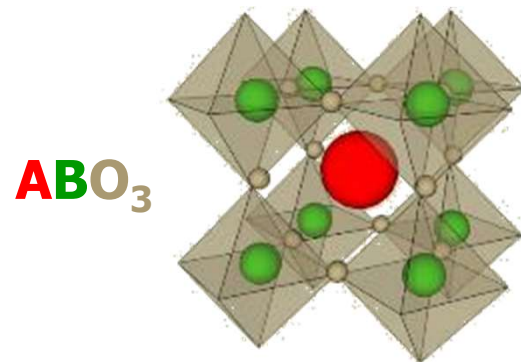
- Very **flexible** structure
doping, tuning of bond lengths and angles
- Broad range of **electronic states**
superconductivity, ferroelectricity, magnetic order, orbital order
- Competition : **giant/coupled responses**
colossal magnetoresistance, magnetoelectric coupling
- Multifunctional heteroepitaxial architectures



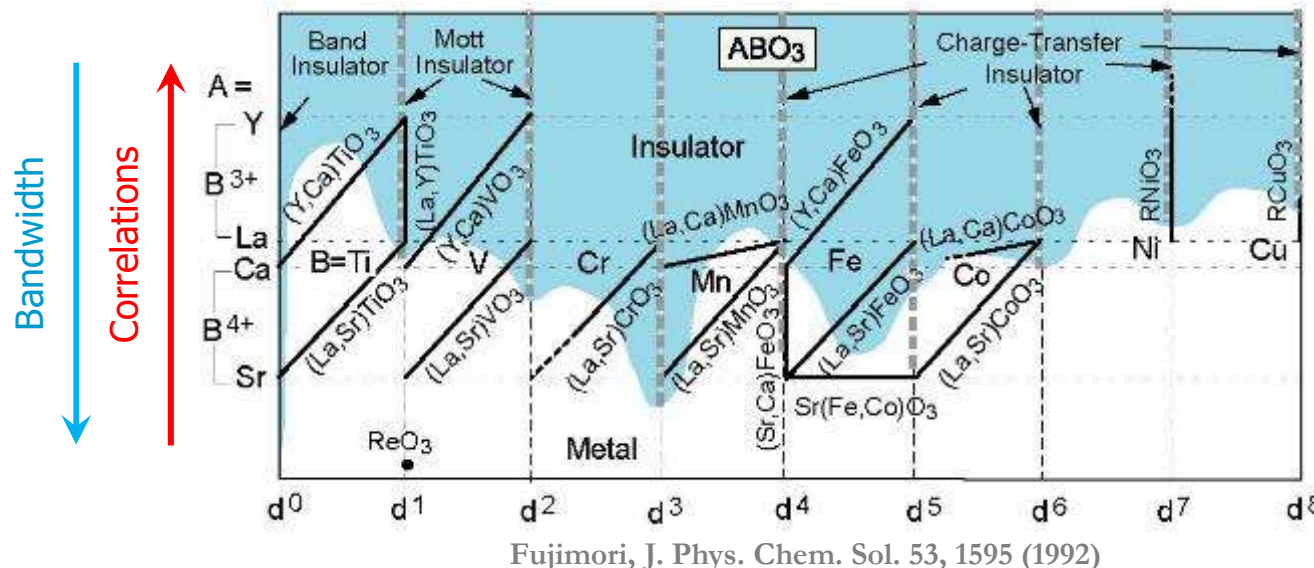
Crystal field splitting in cubic perovskites
A or B cations are too small/big
→ structural distortions → rotations of BO_6 octahedra
→ B-O-B are not straight
→ degeneracy of e_g and t_{2g} levels may be lifted
→ **huge variety of properties**

D. Khomskii, « Transition metal compounds », Cambridge Univ. Press

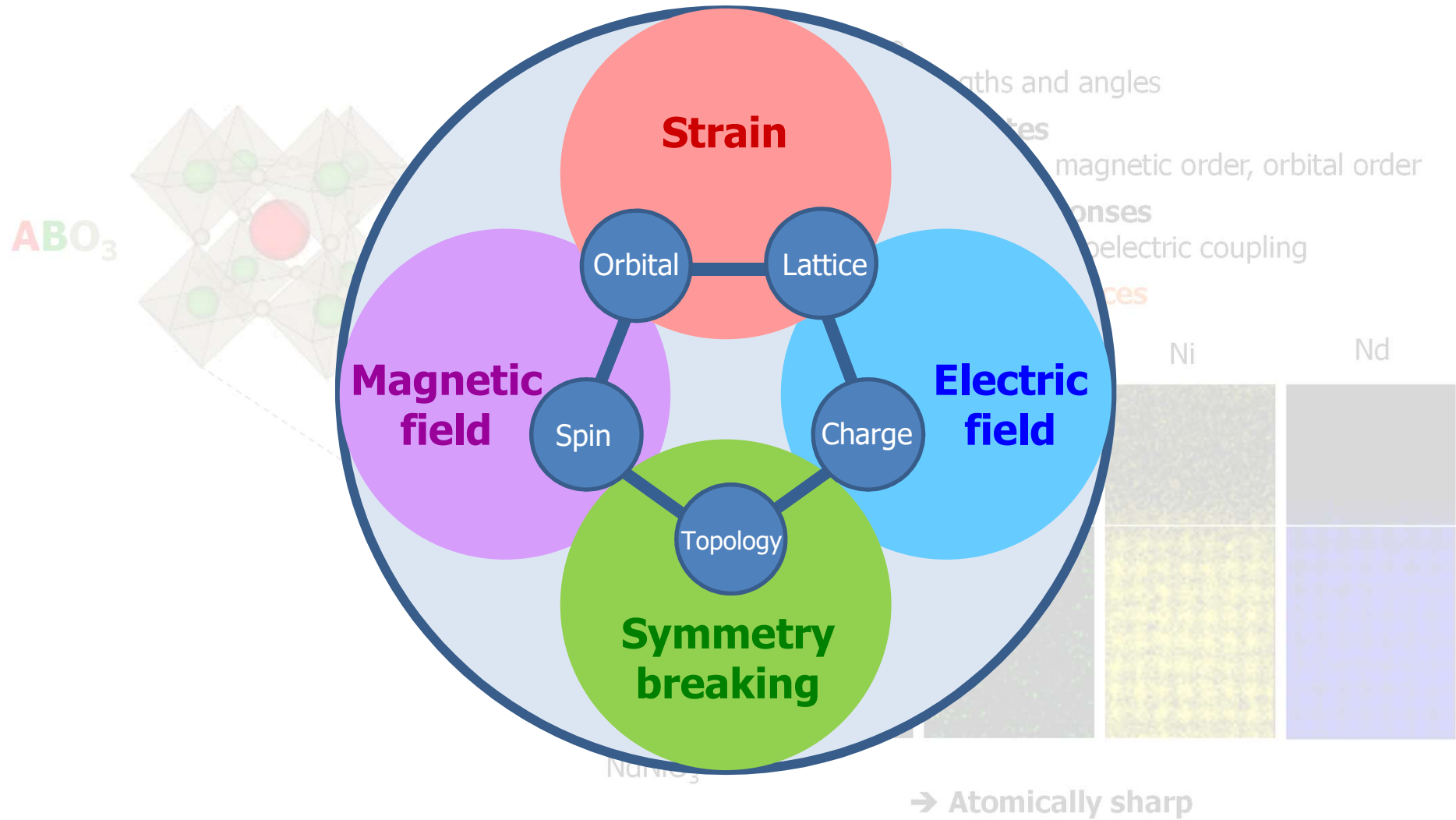
Transition metal perovskite oxides



- Very **flexible** structure
doping, tuning of bond lengths and angles
- Broad range of **electronic states**
superconductivity, ferroelectricity, magnetic order, orbital order
- Competition : **giant/coupled responses**
colossal magnetoresistance, magnetoelectric coupling
- Multifunctional heteroepitaxial architectures



Oxide interfaces : new playground for physicists



1. SrTiO₃-based 2DEGs

1.1 Physics of bulk SrTiO₃

1.2 LaAlO₃/SrTiO₃ 2DEGs

1.3 Other SrTiO₃ 2DEGs

1.4 Electronic structure of SrTiO₃ 2DEGs

1.5 Superconductivity in SrTiO₃ 2DEGs

1.5 Introducing ferroic orders into SrTiO₃ 2DEGs

2. KTaO₃-based 2DEGs

2.1 Physics of bulk KTaO₃

2.2 KTaO₃ 2DEGs

2.3 Superconductivity in KTaO₃ 2DEGs

1. SrTiO₃-based 2DEGs

1.1 Physics of bulk SrTiO₃

1.2 LaAlO₃/SrTiO₃ 2DEGs

1.3 Other SrTiO₃ 2DEGs

1.4 Electronic structure of SrTiO₃ 2DEGs

1.5 Superconductivity in SrTiO₃ 2DEGs

1.5 Introducing ferroic orders into SrTiO₃ 2DEGs

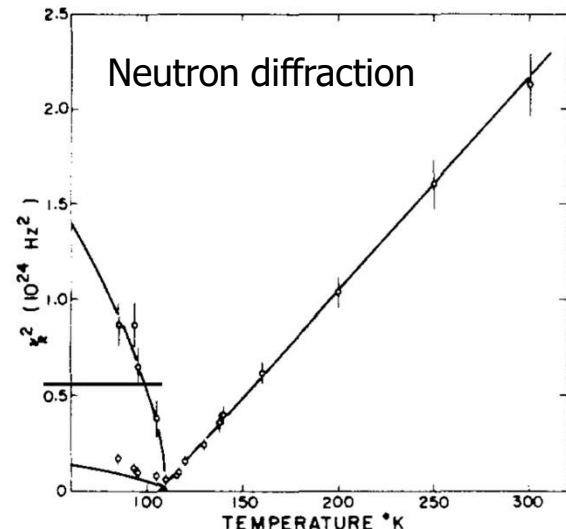
2. KTaO₃-based 2DEGs

2.1 Physics of bulk KTaO₃

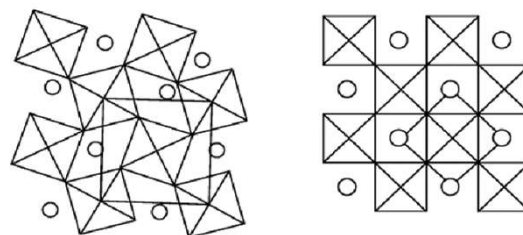
2.2 KTaO₃ 2DEGs

2.3 Superconductivity in KTaO₃ 2DEGs

Structural properties

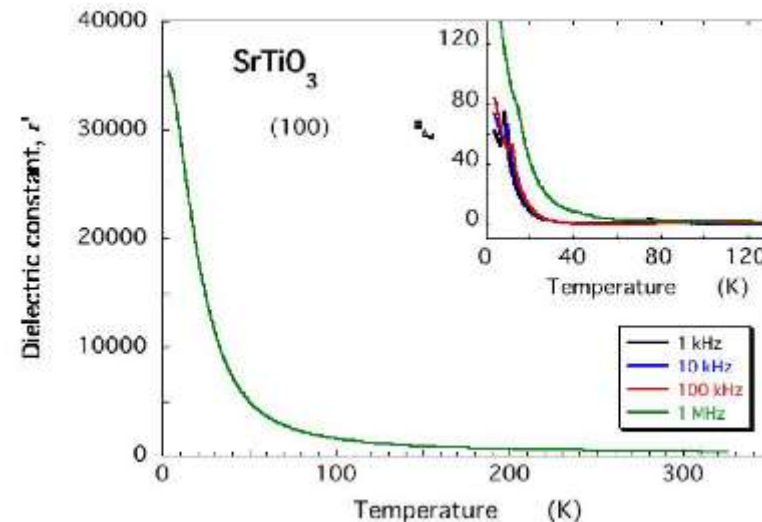


Cowley et al, Solid. State. Commun. 7, 181 (1967)



- SrTiO₃ is cubic at room temperature and above 105 K
- Below 105 K, it is tetragonal, with oxygen octahedra tilt pattern a⁰a⁰c

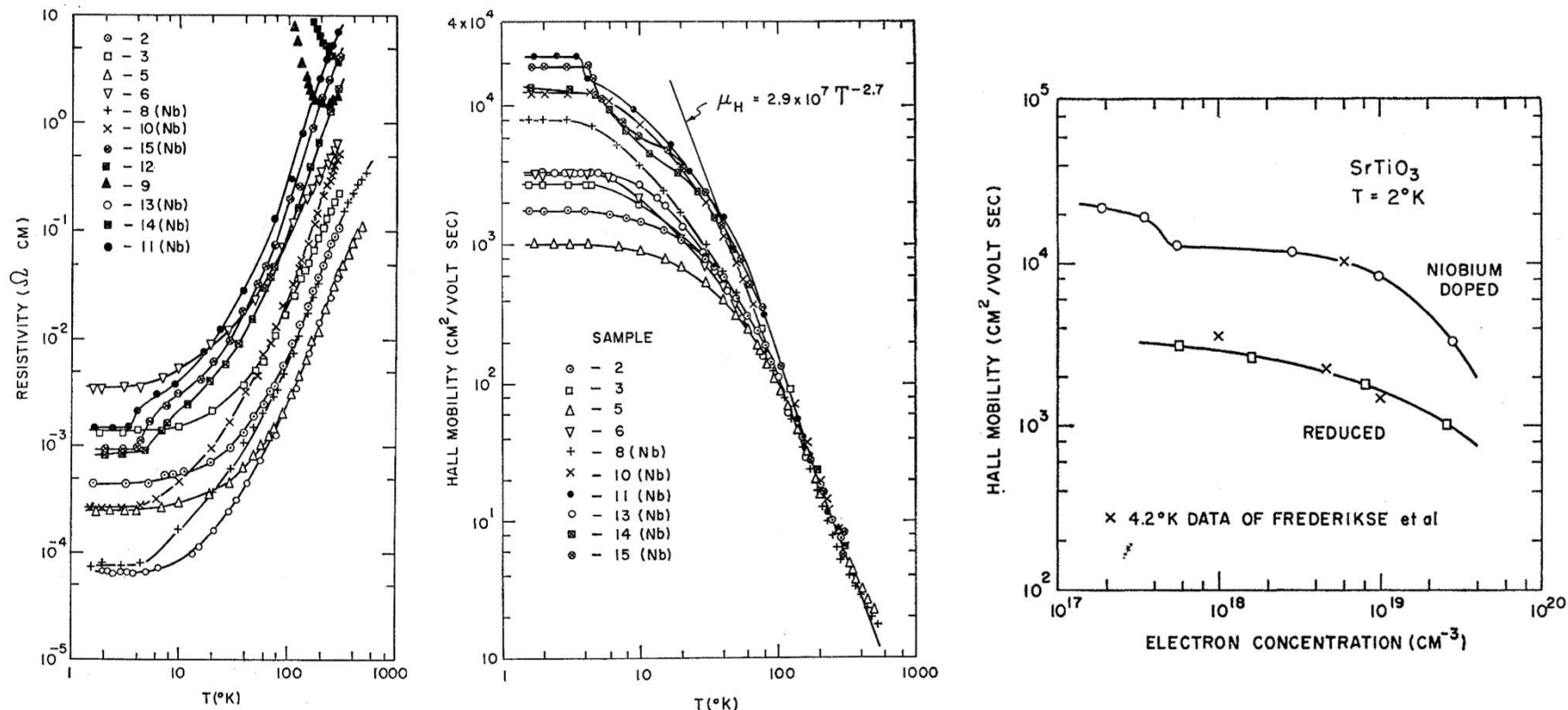
Dielectric properties



Hideshi et al, JPSJ 85, 045703 (2016)

- SrTiO₃ has a large dielectric constant that diverges at low temperature
- « Quantum paraelectric » : ferroelectric instability suppressed by quantum fluctuations

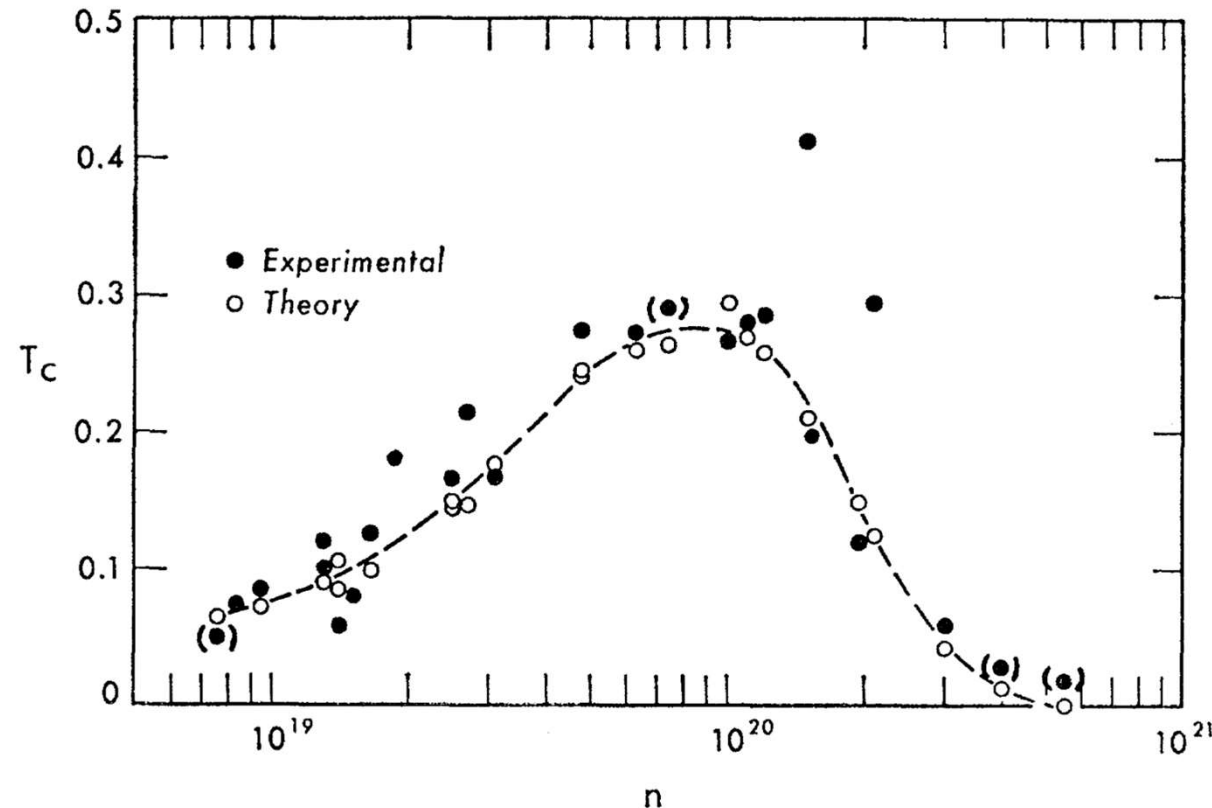
Transport properties of electron doped SrTiO₃



- SrTiO₃ can be (n-type) doped into a metal by La substitution at the Sr site, Nb substitution at the Ti site, or by the creation of oxygen vacancies
- Minute doping amounts (e.g. 10 ppm) are enough to induce metallicity
- Electron mobility is very high ($>10000 \text{ cm}^2/\text{Vs}$) at low T and decreases with doping

Tufte and Chapman PR 155, 796 (1967)

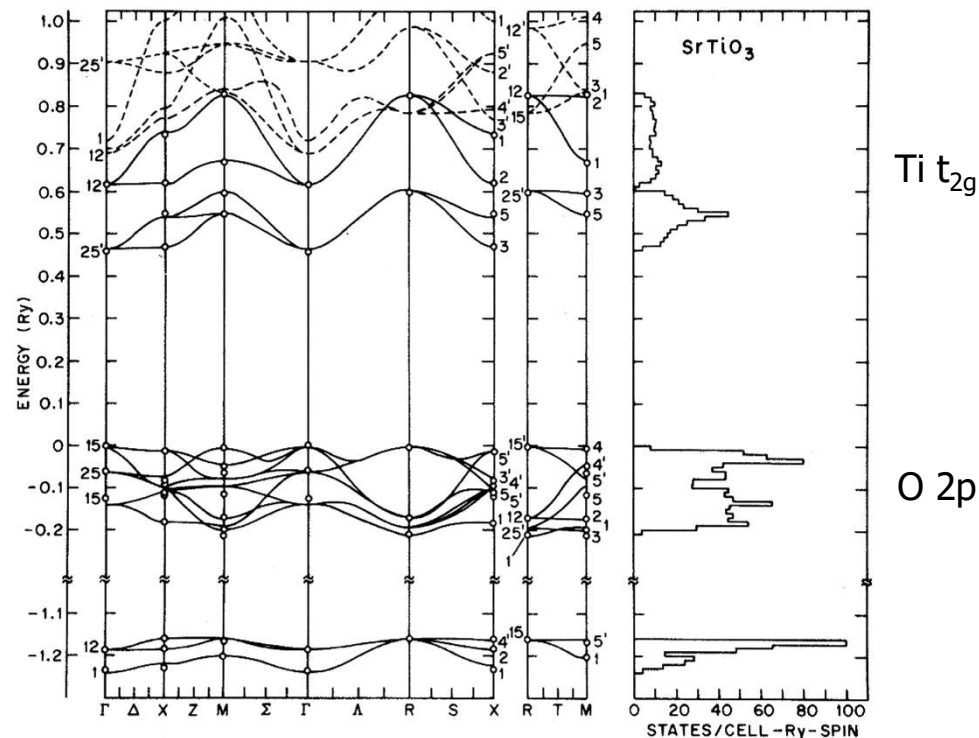
Superconductivity in electron doped SrTiO₃



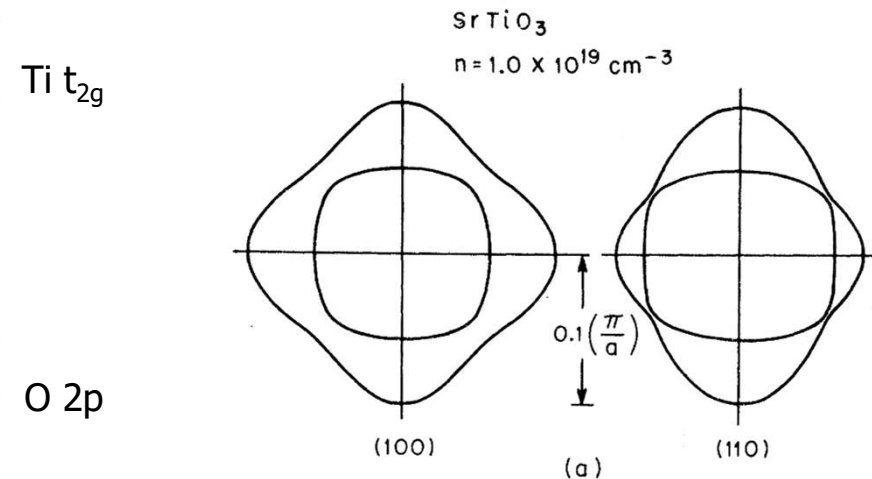
- SrTiO₃ becomes superconducting below about 300 mK for doping levels $>$ a few 10^{18} cm^{-3}
- Dome-like phase diagram as in high T_c superconductors

Koonce PR, 163, 780 (1967)

Electronic structure of SrTiO₃



Mattheiss PRB 6, 4718 (1972)



- SrTiO₃ is a band insulator, with the valence band made of O 2p states and the conduction band of Ti 3d t_{2g} states
- The gap is at the Gamma point with two degenerate bands with small and large effective masses
- The light electron band has a « circular » Fermi surface around Gamma while the heavy electron band consists of a double ellipse.

1. SrTiO₃-based 2DEGs

1.1 Physics of bulk SrTiO₃

1.2 LaAlO₃/SrTiO₃ 2DEGs

1.3 Other SrTiO₃ 2DEGs

1.4 Electronic structure of SrTiO₃ 2DEGs

1.5 Superconductivity in SrTiO₃ 2DEGs

1.5 Introducing ferroic orders into SrTiO₃ 2DEGs

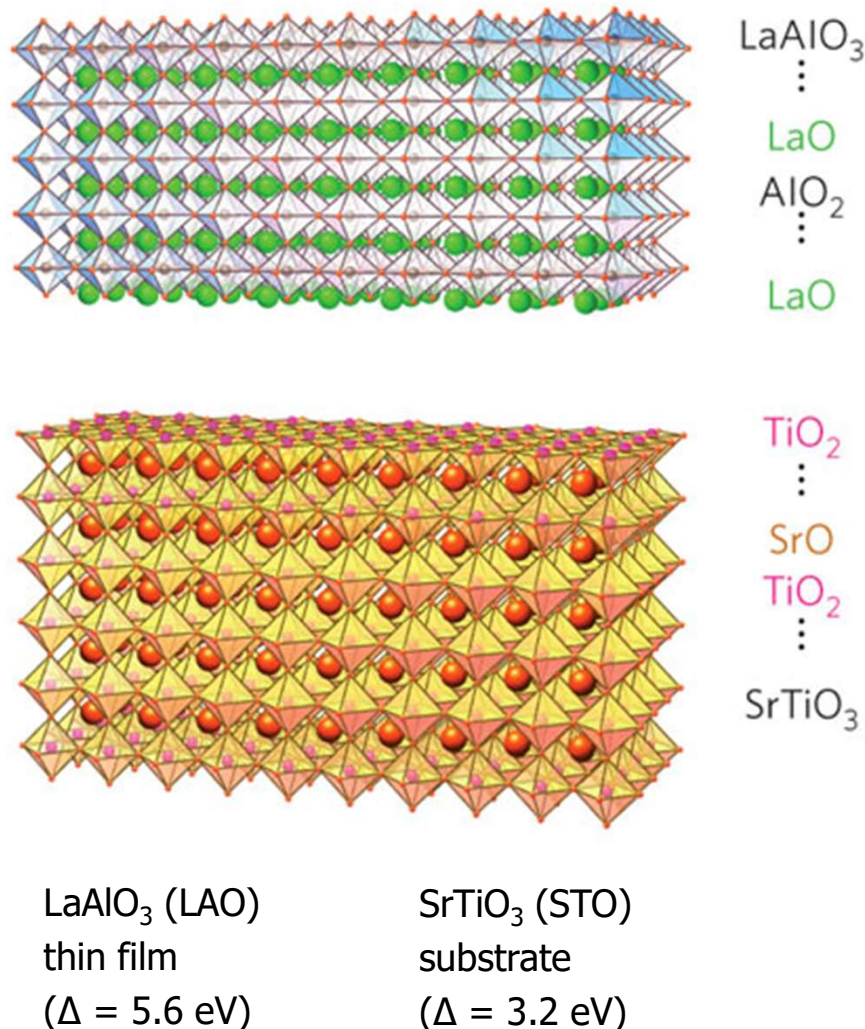
2. KTaO₃-based 2DEGs

2.1 Physics of bulk KTaO₃

2.2 KTaO₃ 2DEGs

2.3 Superconductivity in KTaO₃ 2DEGs

An unexpected discovery



- ⦿ Metallic interface despite both LAO and STO begin insulating
- ⦿ Low temperature mobility in the range of $1000 \text{ cm}^2/\text{Vs}$

A high-mobility electron gas at the LaAlO₃/SrTiO₃ heterointerface

A. Ohtomo ^{1,2,3} & H. Y. Hwang ^{1,3,4}

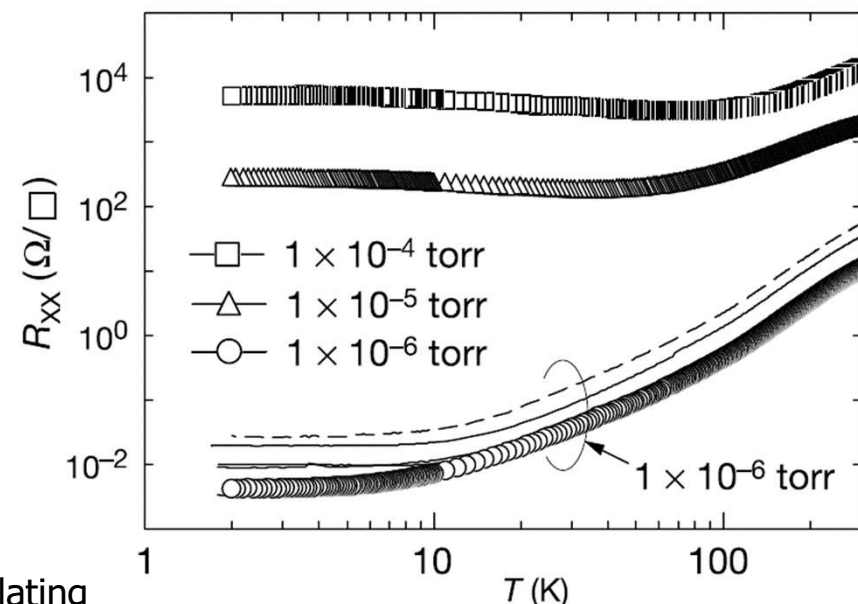
¹Bell Laboratories, Lucent Technologies, Murray Hill, New Jersey 07974, USA

²Institute for Materials Research, Tohoku University, Sendai, 980-8577, Japan

³Japan Science and Technology Agency, Kawaguchi, 332-0012, Japan

⁴Department of Advanced Materials Science, University of Tokyo, Kashiwa, Chiba, 277-8651, Japan

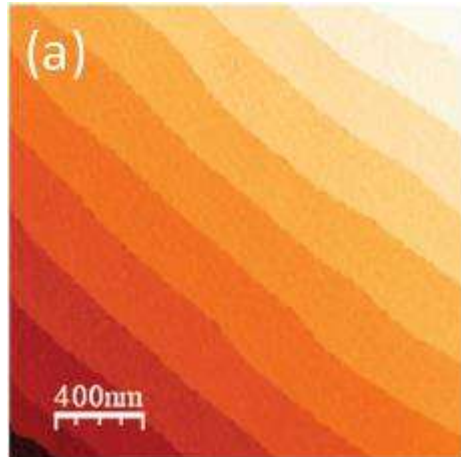
LaAlO₃ (60 Å) /SrTiO₃(001)



Ohtomo & Hwang, Nature 427, 423 (2004)

How to grow LAO/STO 2DEGs ?

TiO₂-terminated substrate

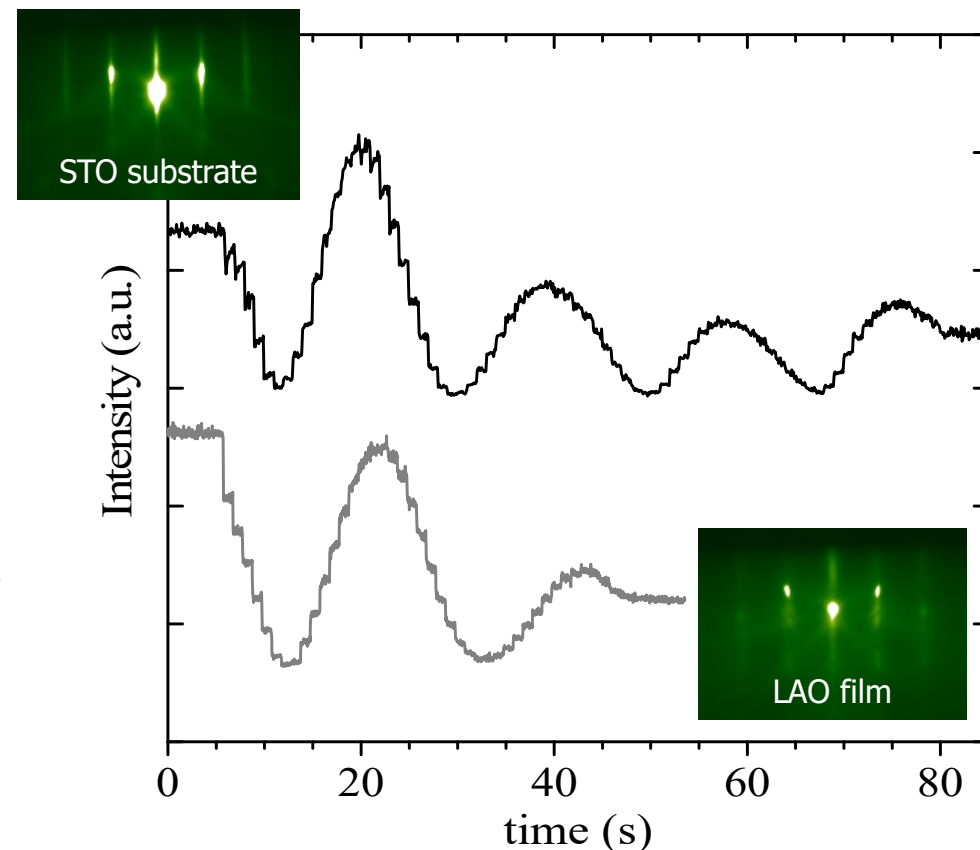


Essential steps:

- Use a TiO₂ terminated STO single crystal
- Grow an integer number of LAO unit cells ≥ 4
- Post-anneal in O₂

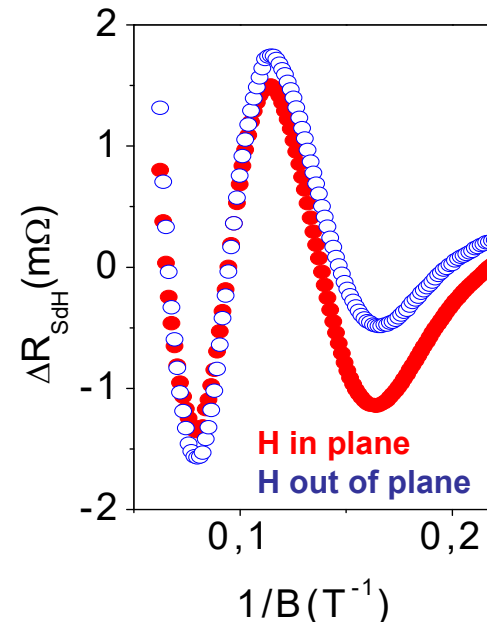
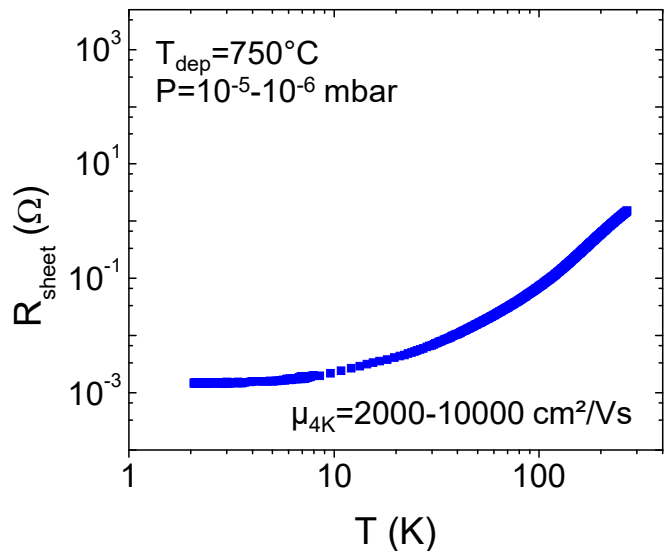
PLD growth conditions for LaAlO₃

- 700-800°C
- 2×10^{-4} mbar of O₂
- KrF excimer (248nm) – 0.6-1.2 J/cm² at 1 Hz
- in-situ annealing in high O₂ pressure (0.2-1 bar) at T \geq 500°C for 30-60'



Do we really have a 2DEG ? How to measure its thickness ?

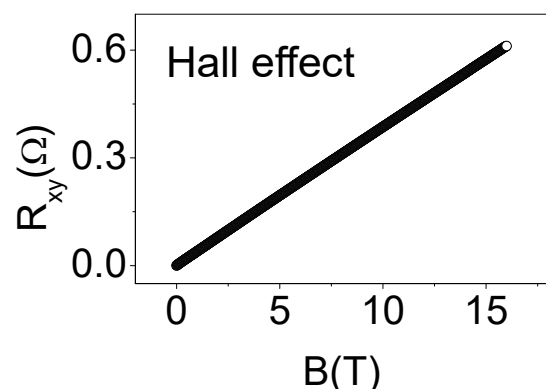
Magnetotransport measurements



High-field magnetoresistance:
 Observation of Shubnikov-de Haas oscillations

$$F_{\text{SdH}} = \frac{\hbar k_F^2}{2e} \quad n = \frac{k_F^3}{3\pi^2}$$

SdH oscillations provide the **carrier density** (cm^{-3})



Hall measurement provide the **sheet carrier density** (cm^{-2})

$$\text{SdH} \rightarrow n \times t_{\text{gas}} = (1/e) B / R_{xy} \leftarrow \text{Hall}$$

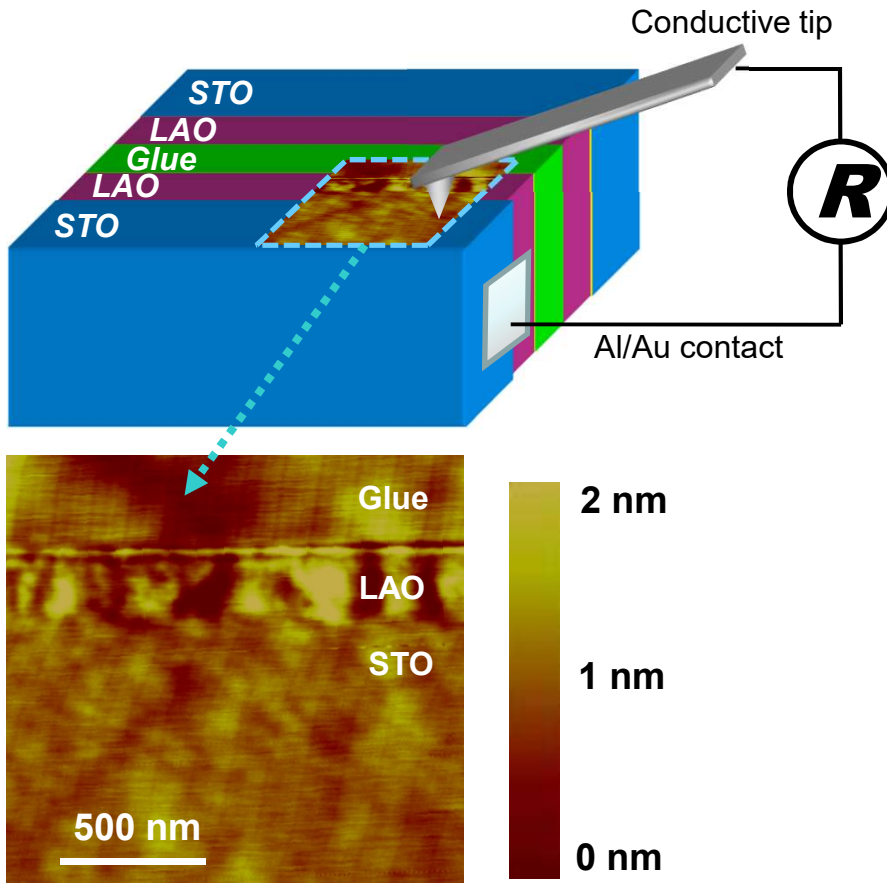
Determination of the electron gas thickness : **~500 μm**

[Herranz, MB et al, PRL 98, 216803 \(2007\)](#)

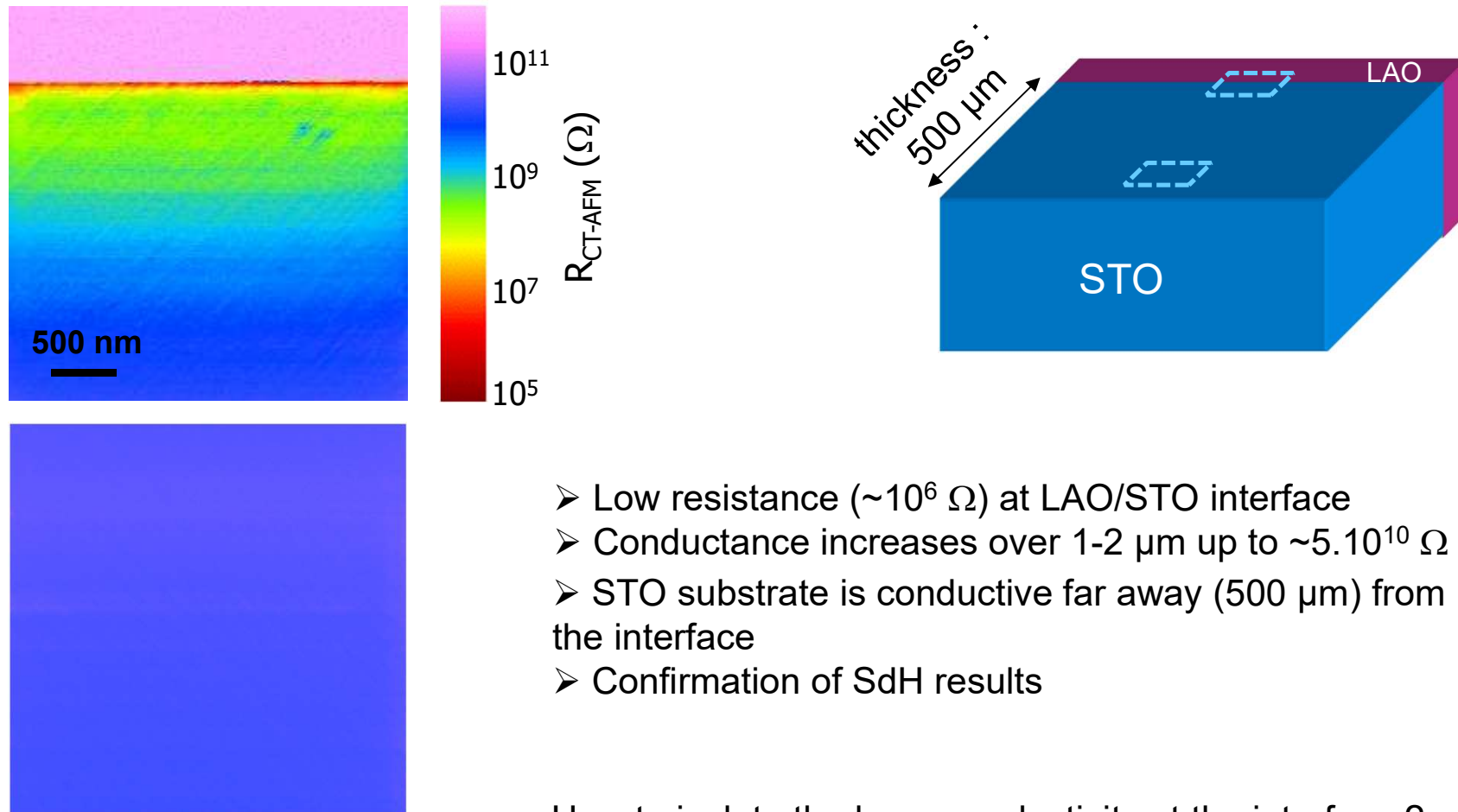
- Metallic behaviour, high mobility, quantum oscillations : nice sample !
- But : electron gas thickness is **500 μm** ! Hint : this sample was **not post-annealed in oxygen**

Conductive-tip AFM in cross-section samples

Local measurement of transport properties



Resistance mapping of non-annealed samples

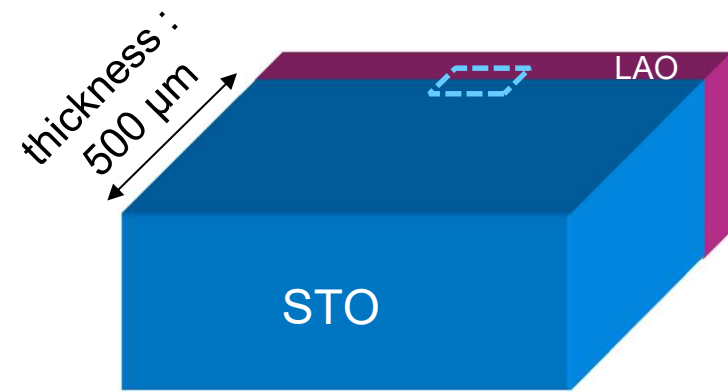
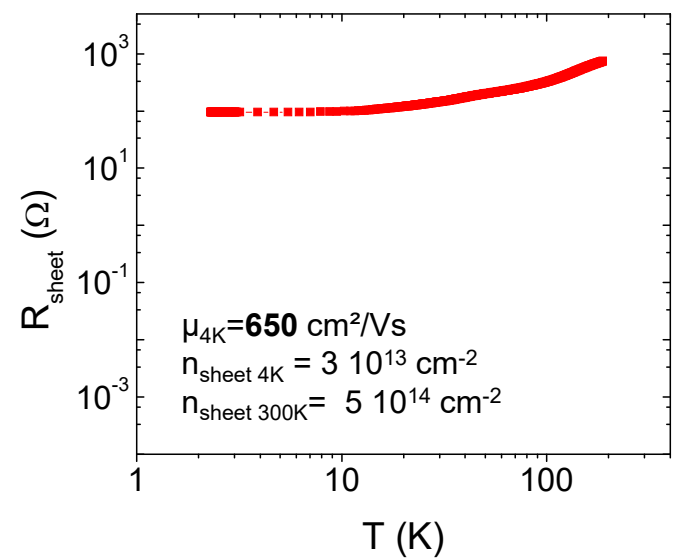


How to isolate the large conductivity at the interface ?
Get rid of oxygen vacancies : in-situ annealing

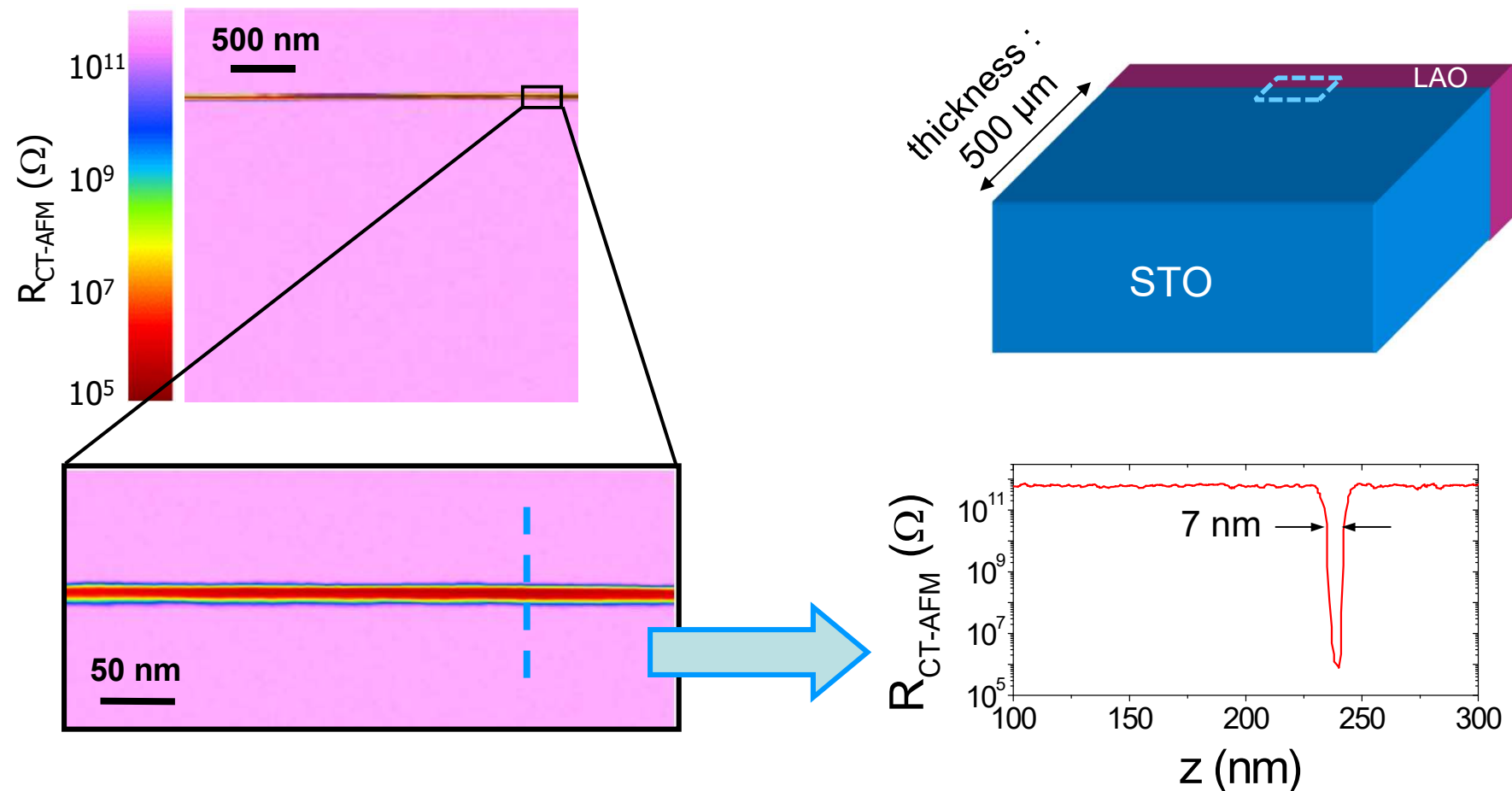
(as in Thiel et al, Science 313, 1942 (2006); Reyren et al, Science 317, 1196 (2007))

Basletic, MB, et al Nature Mater. 7, 621 (2008)

Resistance mapping of in-situ annealed sample



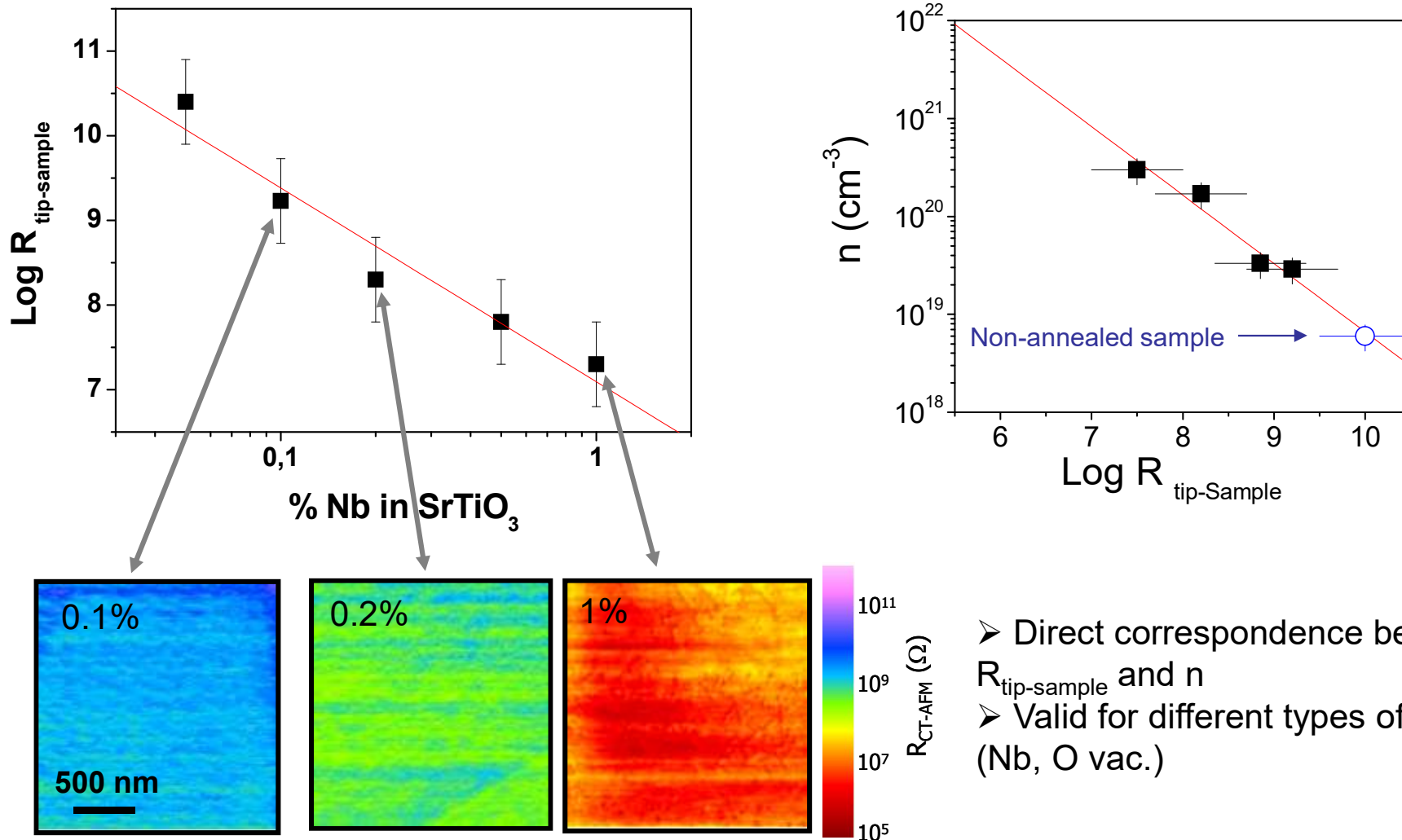
Resistance mapping of in-situ annealed sample



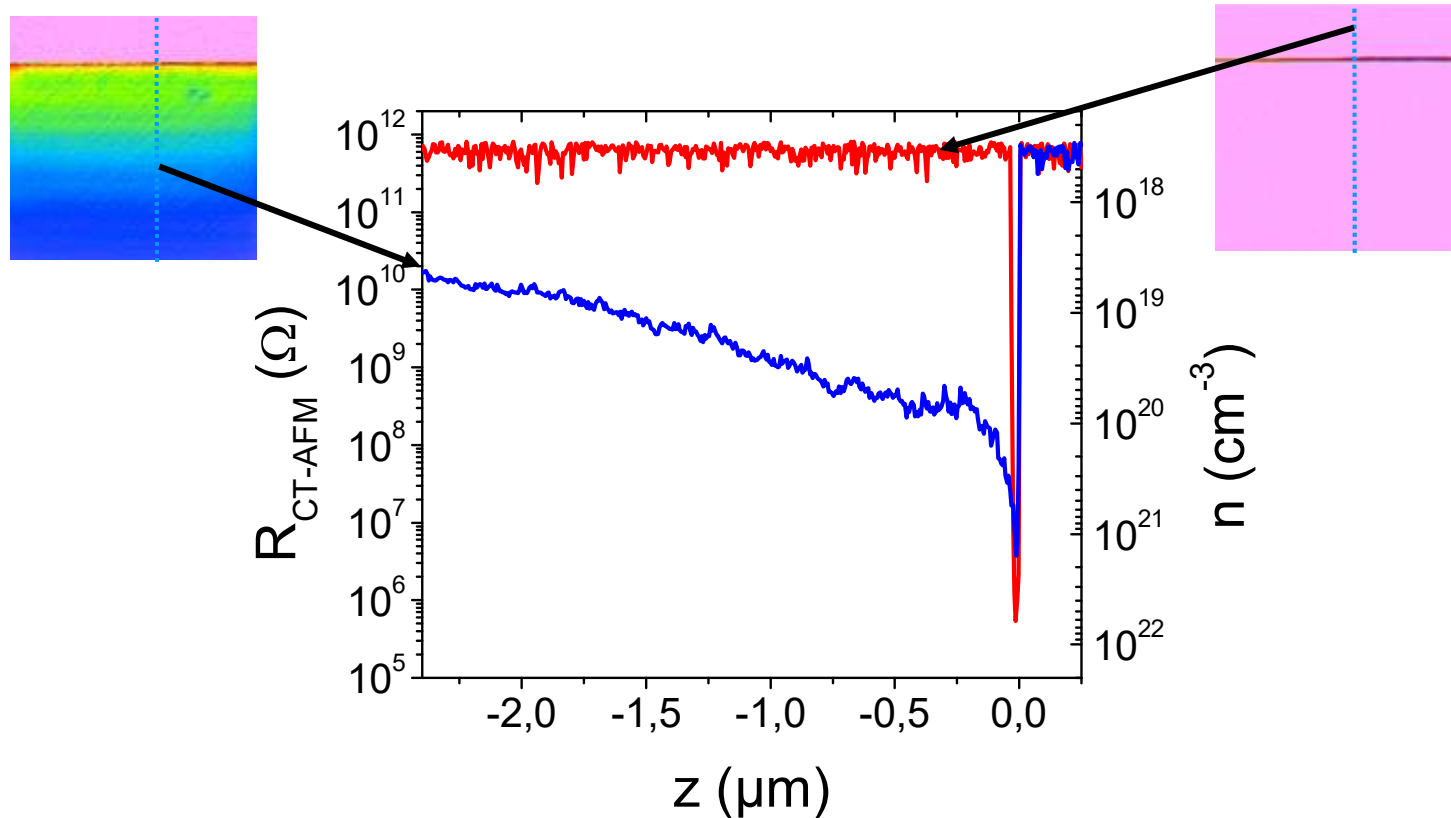
- Low resistance ($\sim 10^5 \Omega$) at LAO/STO interface
- STO substrate is highly insulating far away ($500 \mu\text{m}$) from the interface
- Conduction is **confined** at the interface
- Thickness of the metallic gas : **7 nm** (upper estimate)

Basletic, MB, et al Nature Mater. 7, 621 (2008)

Calibration of $R_{\text{tip-sample}}$ vs n using Nb-doped SrTiO₃ crystals



Local mapping of the charge carrier distribution



Non annealed sample

Carrier density away from interface : $5 \cdot 10^{18}$ cm⁻³ : $t_{\text{gas}} \approx 600$ μm

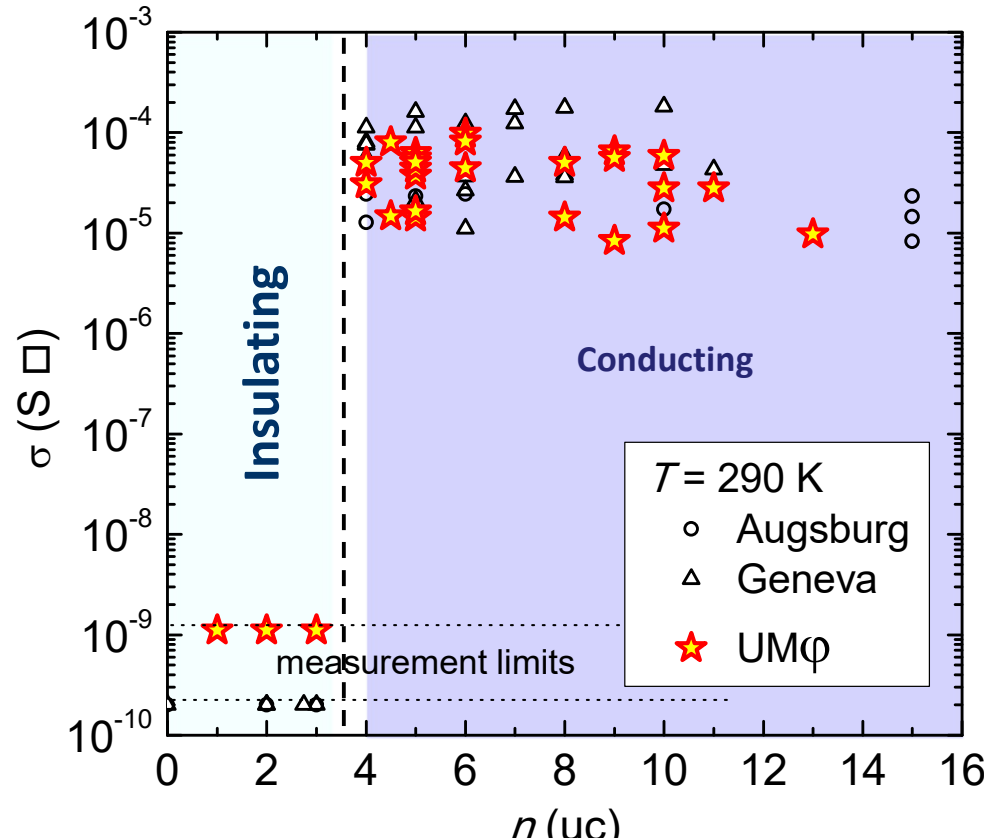
In-situ annealed sample

Carrier density at the interface : $7 \cdot 10^{21}$ cm⁻³ : $t_{\text{gas}} \approx 1$ nm

Basletic, MB, et al Nature Mater. 7, 621 (2008)

Critical thickness for conductivity

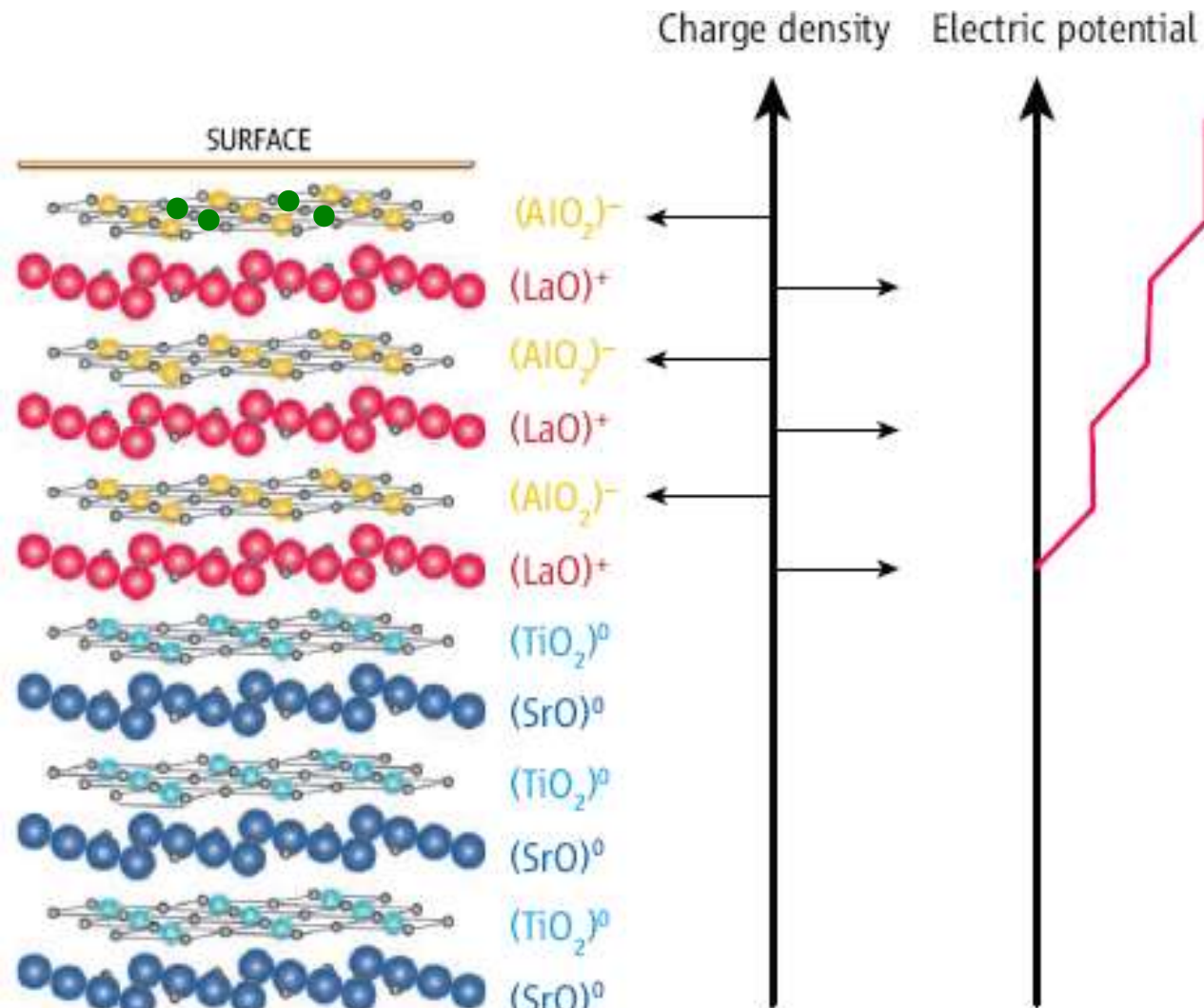
Interfacial conductivity *vs.* LAO thickness



→ **Critical thickness** threshold for conductivity =
4 unit cells (uc) of LAO

S. Thiel et al., Science 313, 1942 (2006)

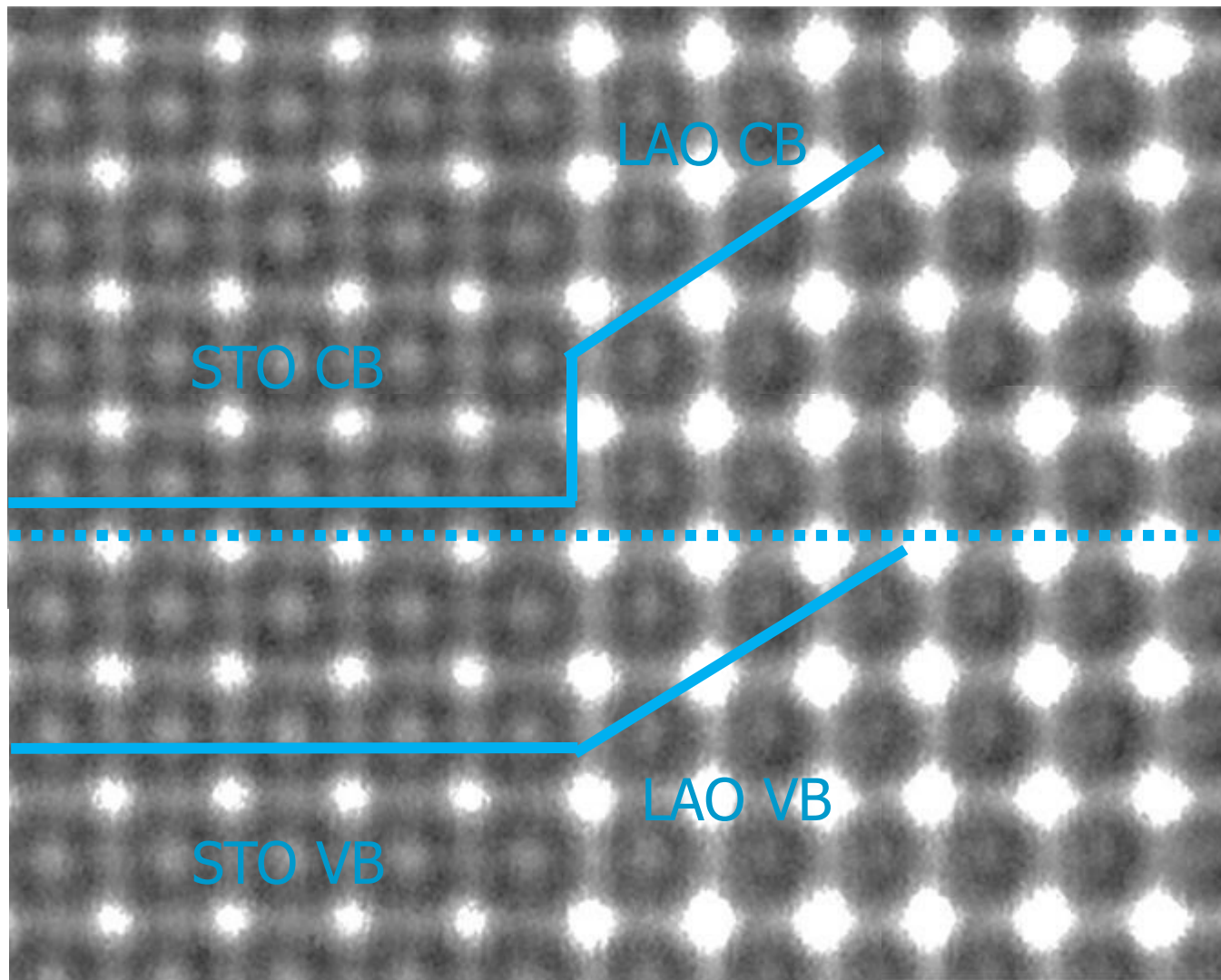
Mechanism for 2DEG formation : electronic reconstruction



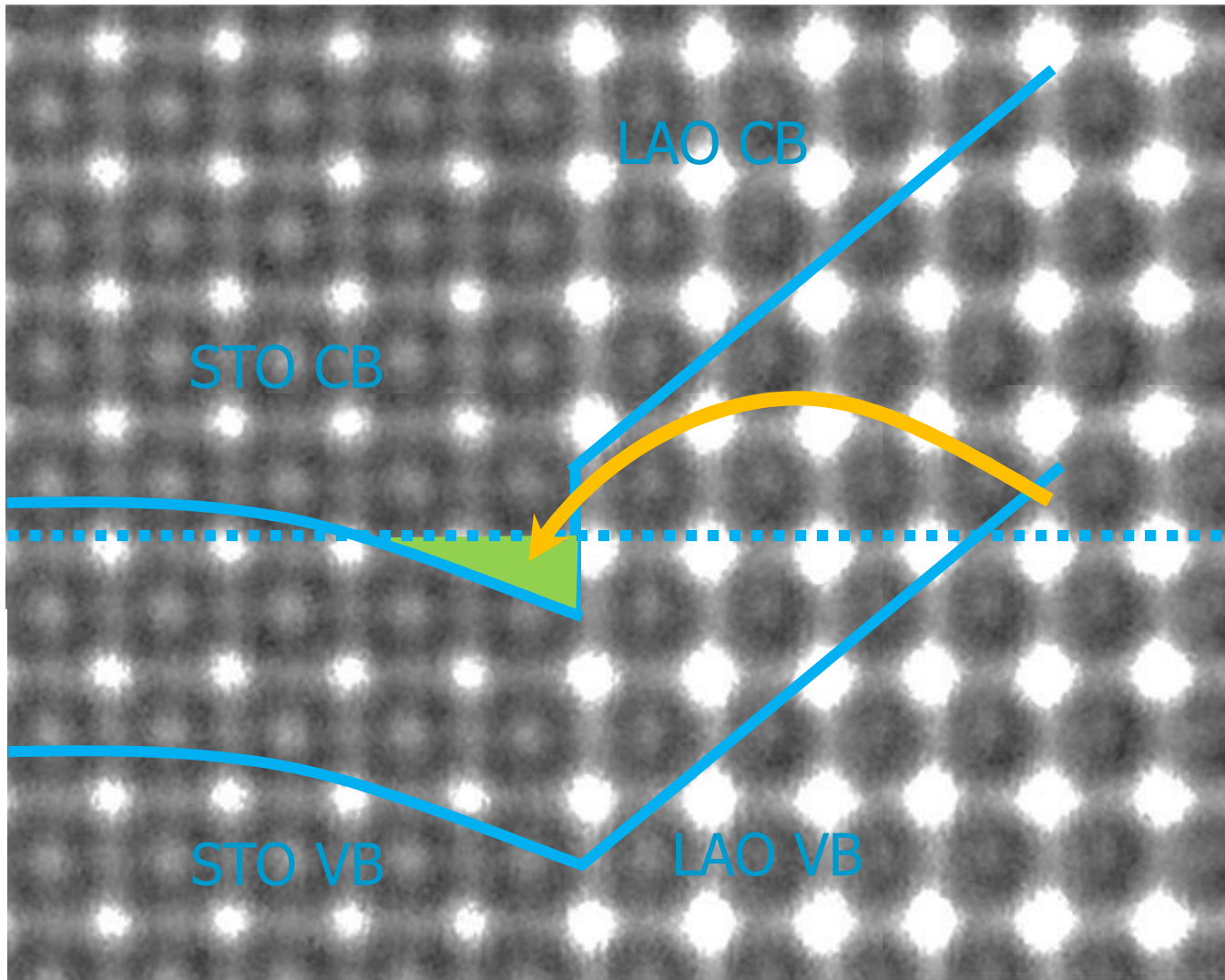
Ohtomo and Hwang, Nature Mater

© F. Milletto

Mechanism for 2DEG formation : electronic reconstruction

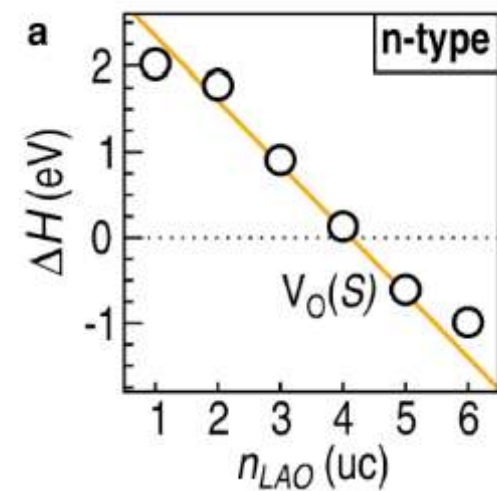
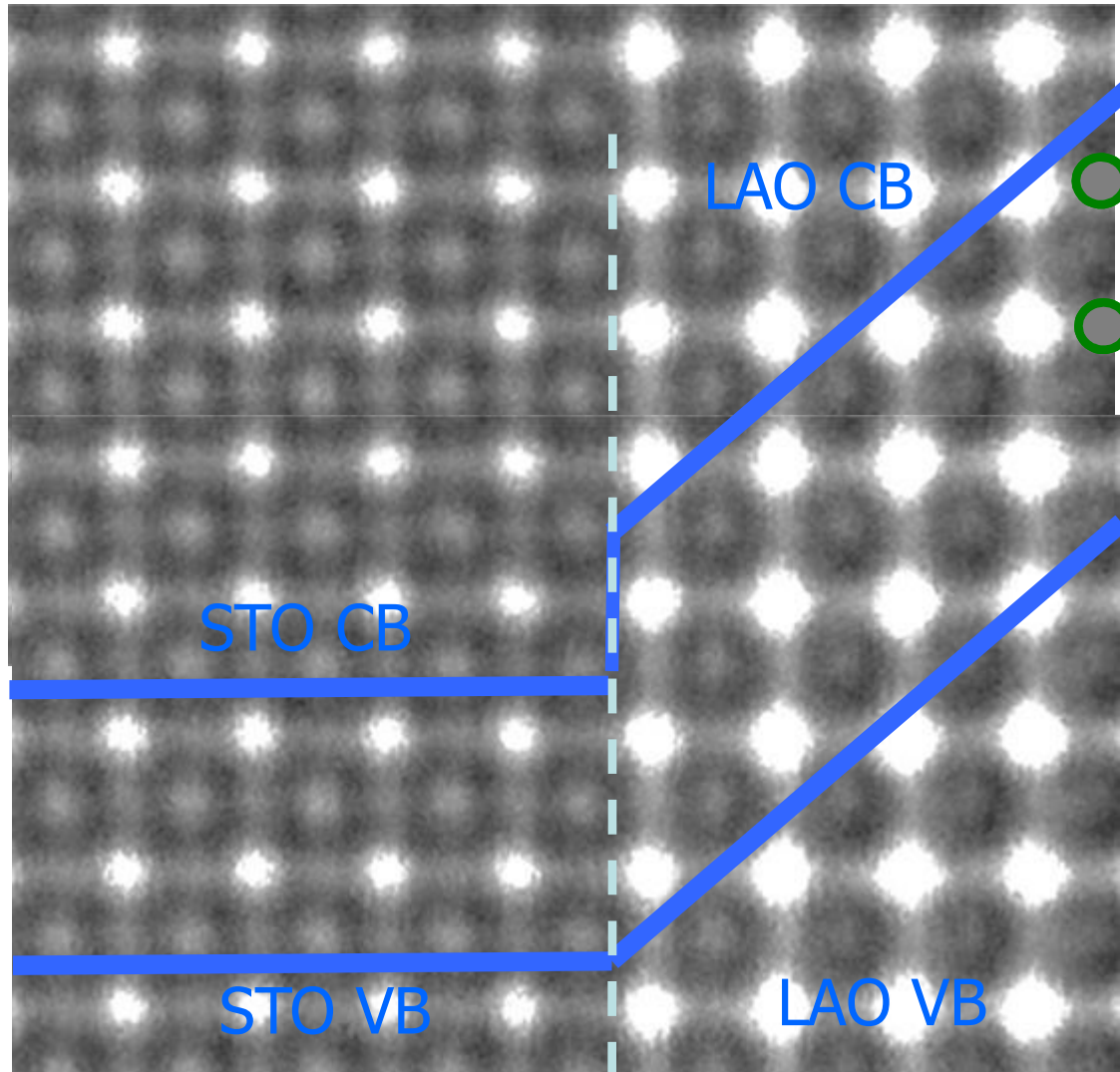


Mechanism for 2DEG formation : electronic reconstruction



Mechanism for 2DEG formation : oxygen vacancies at LAO surface

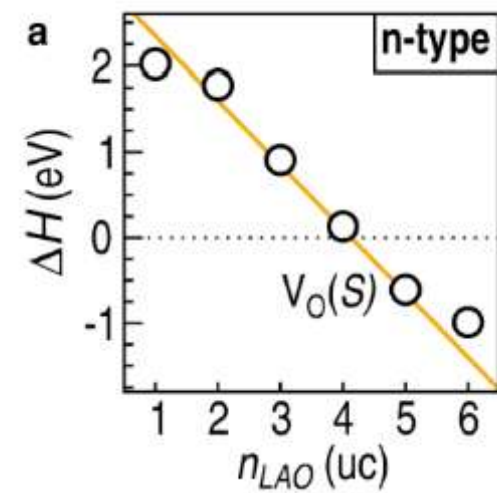
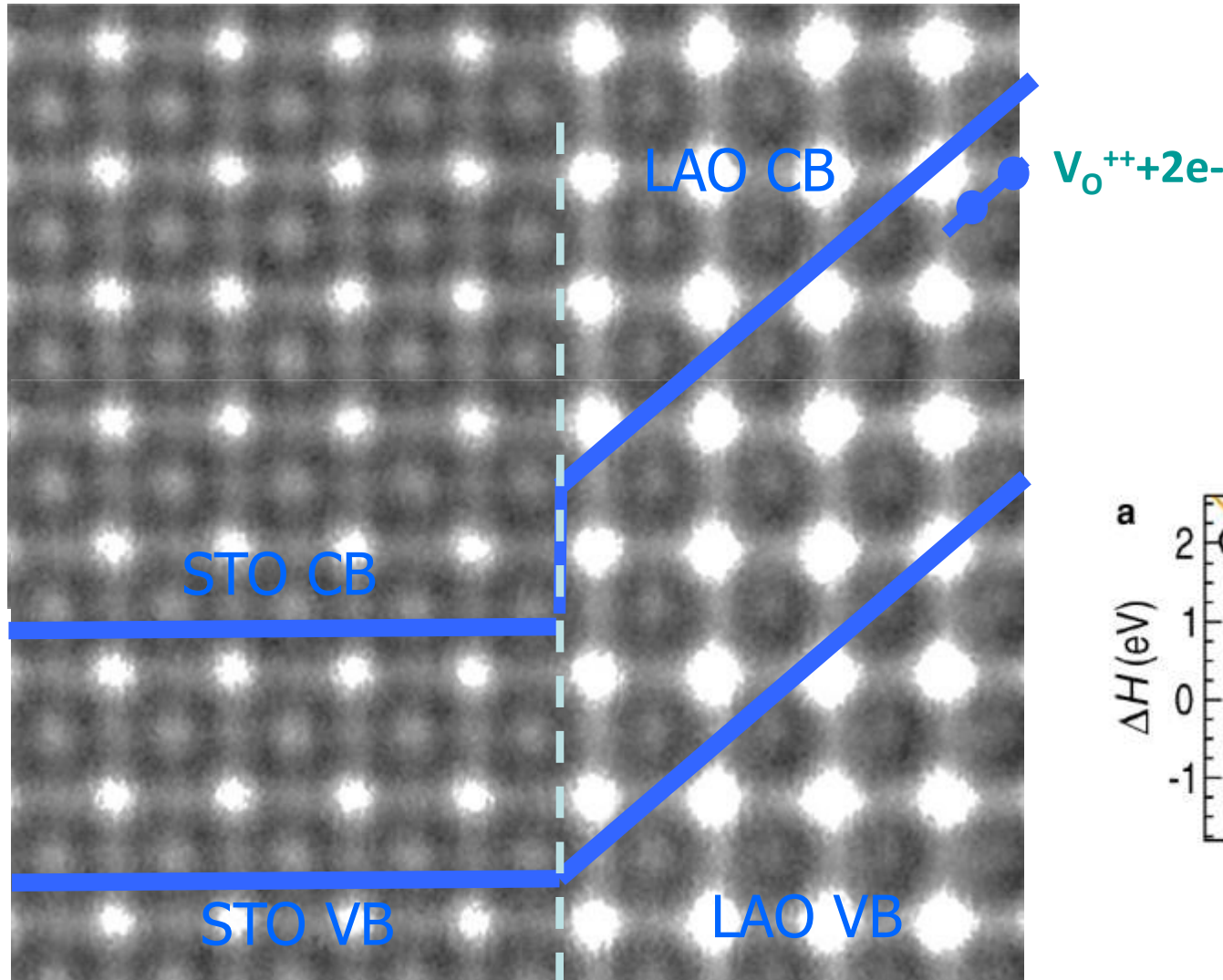
Yu and Zunger, Nature Comm. 5, 5118 (2014)



© F. Milletto

Mechanism for 2DEG formation : oxygen vacancies at LAO surface

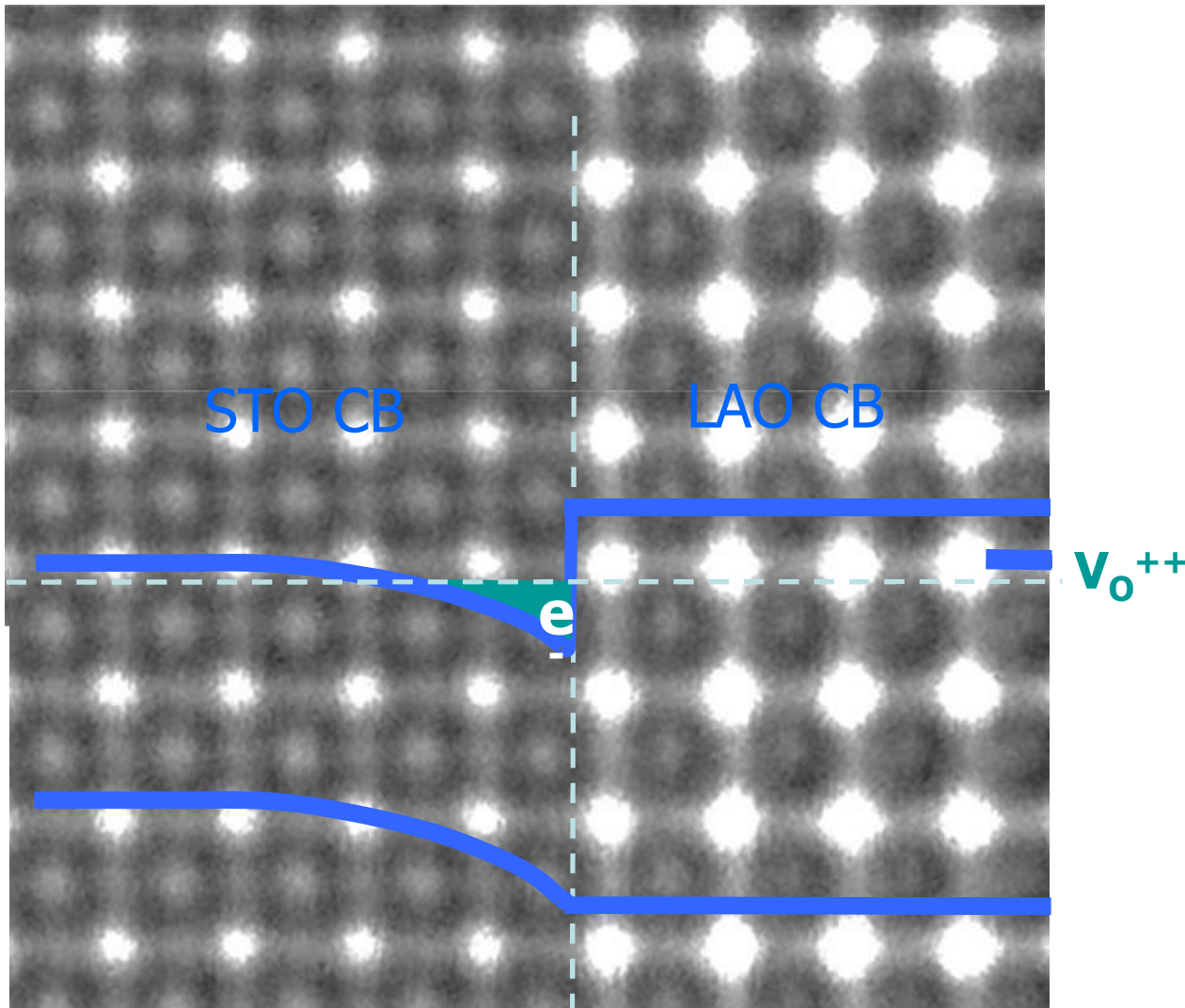
Yu and Zunger, Nature Comm. 5, 5118 (2014)



© F. Milletto

Mechanism for 2DEG formation : oxygen vacancies at LAO surface

Yu and Zunger, Nature Comm. 5, 5118 (2014)



© F. Milletto

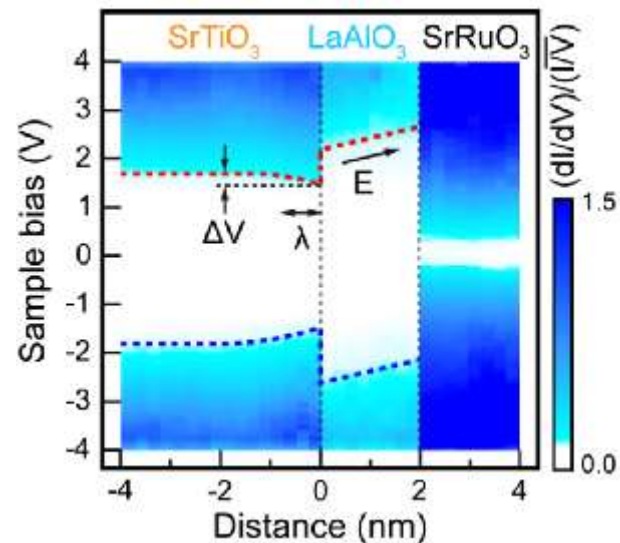
Mechanism for 2DEG formation : conclusion

So which mechanism is it ?

Hard to tell because

- Both mechanisms require a polar interface, i.e. no 2DEG for SrO-terminated STO
- Both mechanisms lead to a critical thickness of 4 unit cells
- But after 2DEG formation, there should be an E field in the 2DEG in the polar catastrophe scenario, but not in Yu and Zunger's model

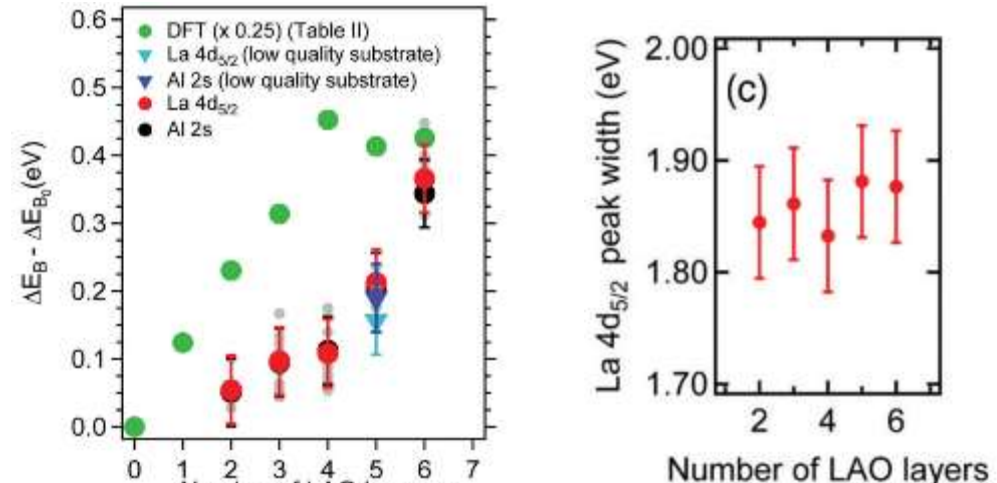
Cross section scanning tunnel spectroscopy



- Electric field visible in LAO

Huang et al, PRL 109, 246807 (2012)

Hard X-ray photoemission spectroscopy



- Core level shifts disagree with theory and no broadening

Slooten et al, PRB 87, 085128 (2013)

1. SrTiO₃-based 2DEGs

1.1 Physics of bulk SrTiO₃

1.2 LaAlO₃/SrTiO₃ 2DEGs

1.3 Other SrTiO₃ 2DEGs

1.4 Electronic structure of SrTiO₃ 2DEGs

1.5 Superconductivity in SrTiO₃ 2DEGs

1.5 Introducing ferroic orders into SrTiO₃ 2DEGs

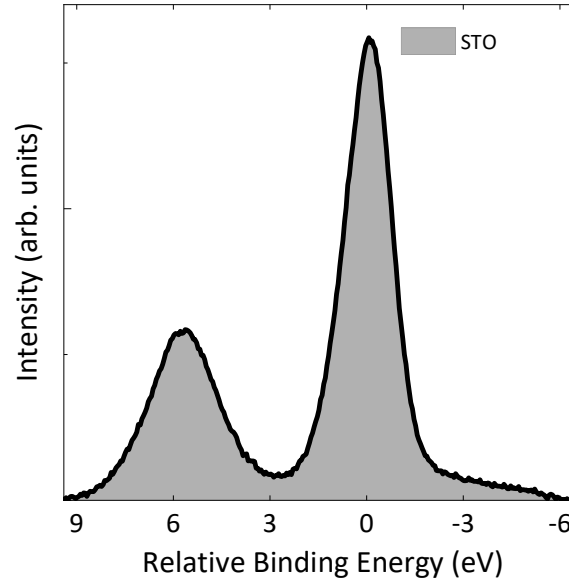
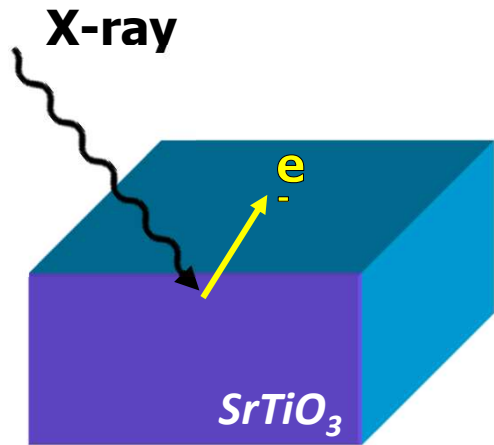
2. KTaO₃-based 2DEGs

2.1 Physics of bulk KTaO₃

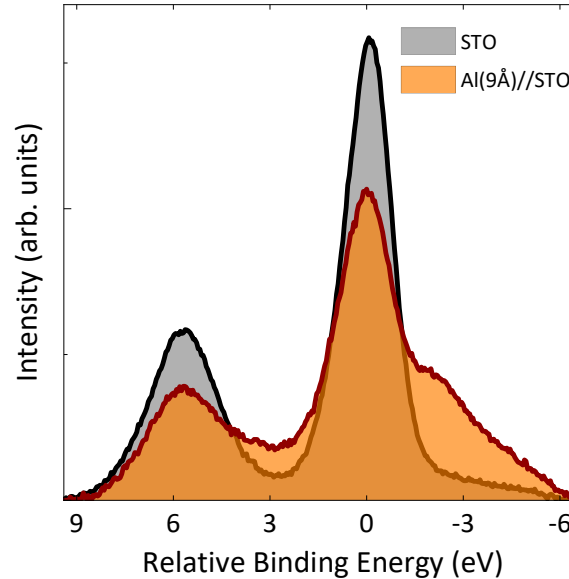
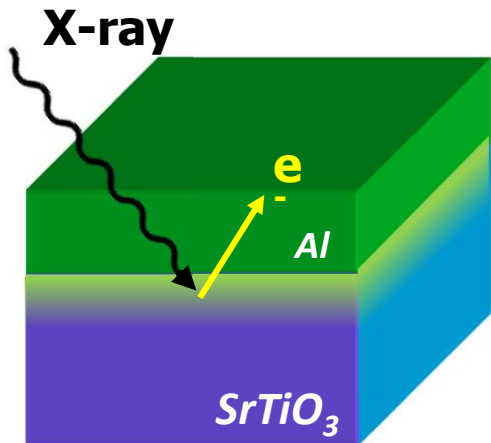
2.2 KTaO₃ 2DEGs

2.3 Superconductivity in KTaO₃ 2DEGs

A 2DEG in Al/STO

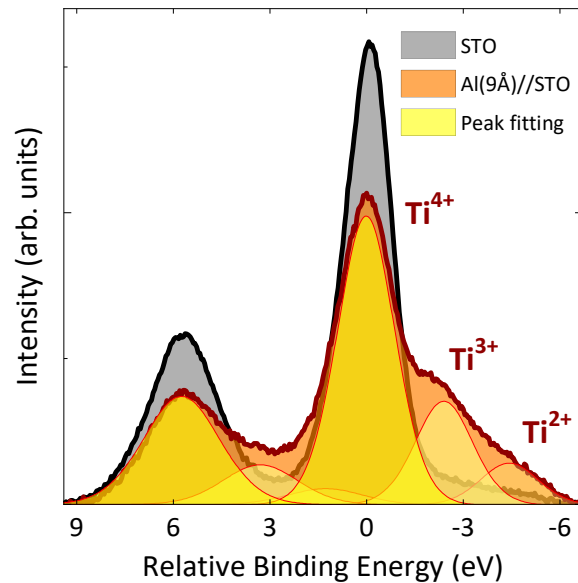
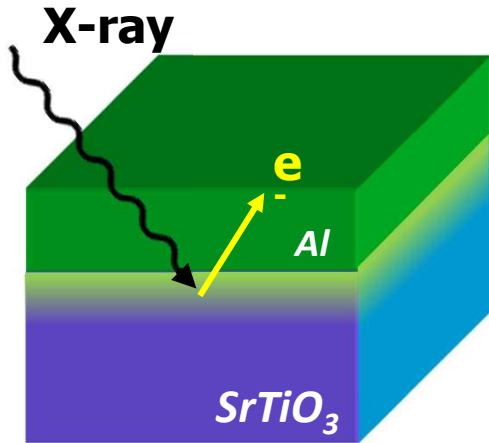


A 2DEG in Al/STO



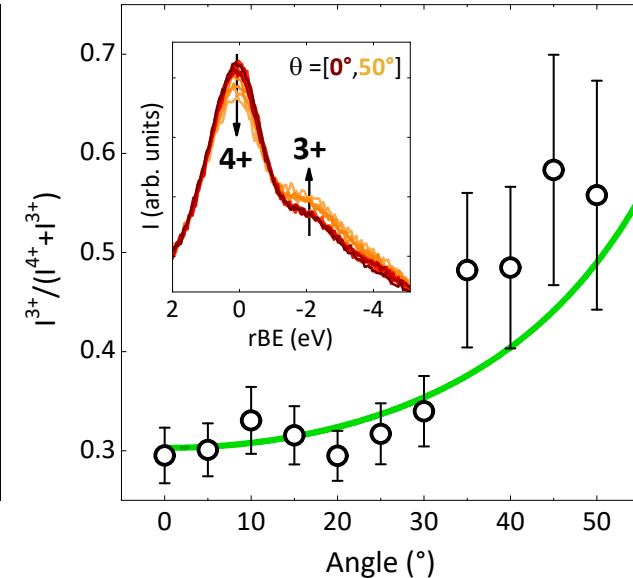
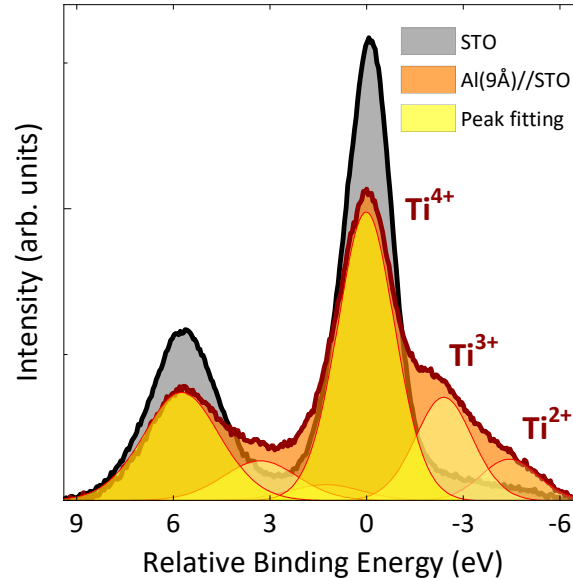
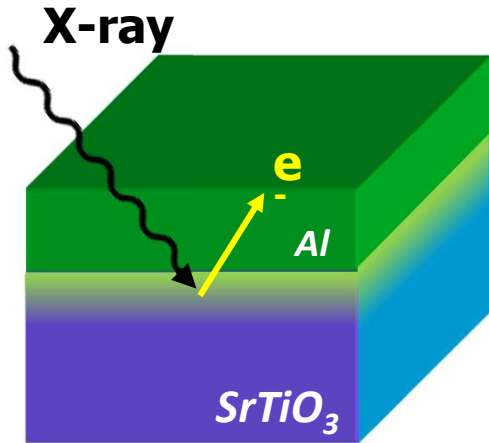
- Deposition of 9 Å of aluminum
- Aluminum pulls oxygen from the STO
- Oxygen vacancies are formed

A 2DEG in Al/STO



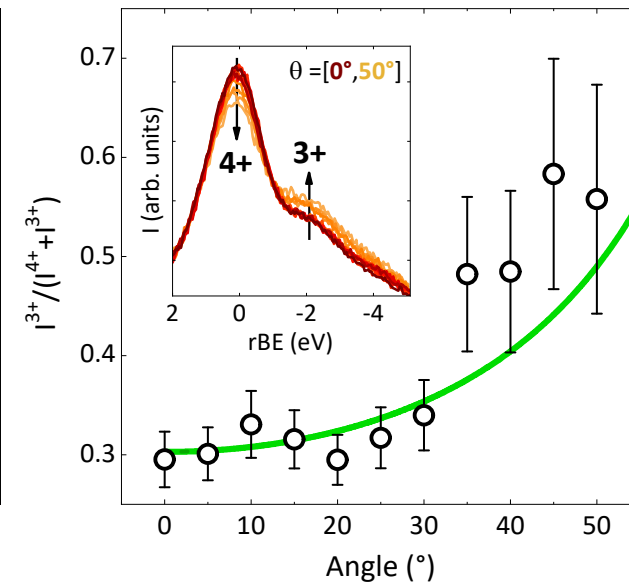
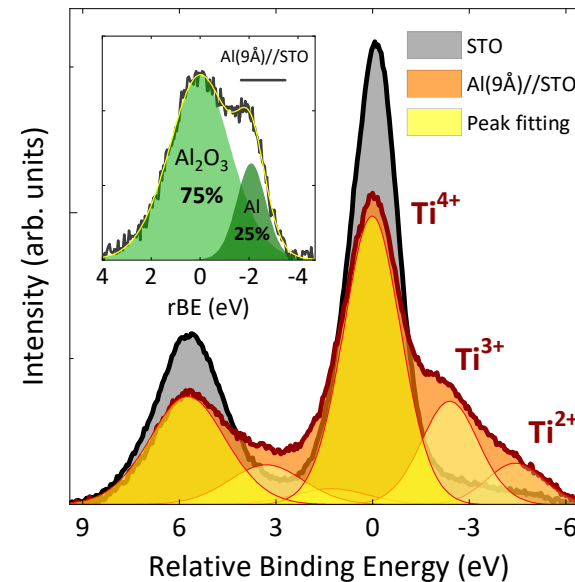
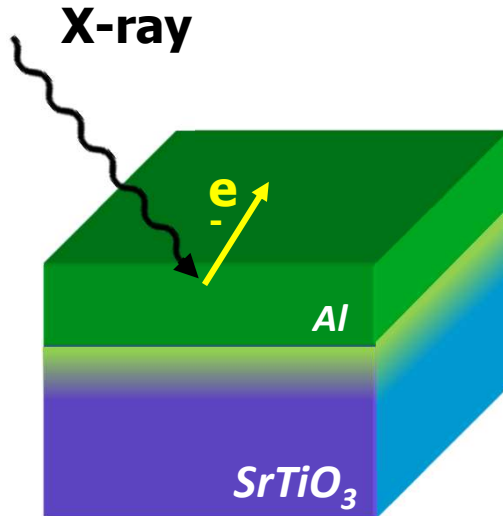
- Deposition of 9 Å of aluminum
- Aluminum pulls oxygen from the STO
- Oxygen vacancies are formed

A 2DEG in Al/STO



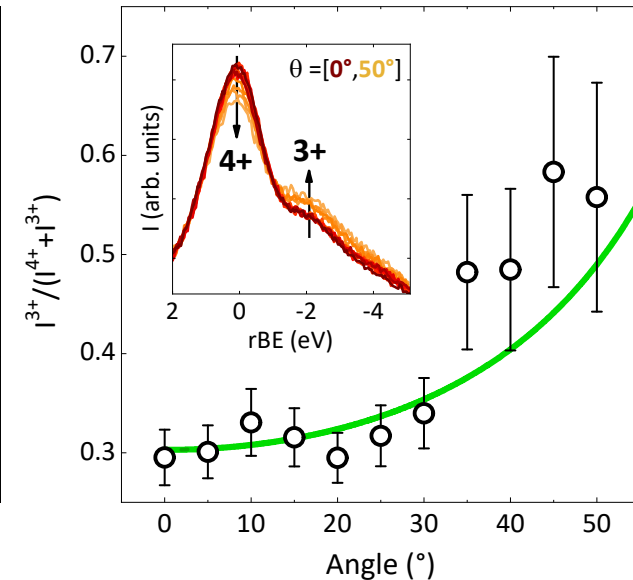
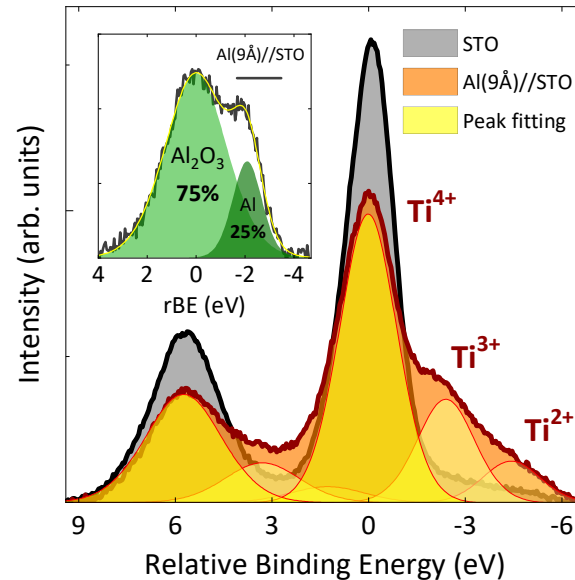
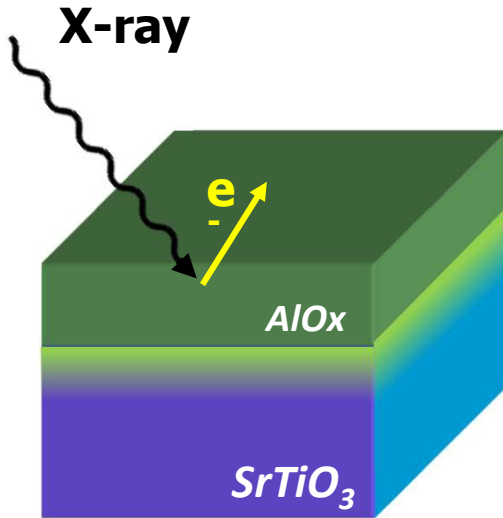
- ➊ Deposition of 9 Å of aluminum
- ➋ Aluminum pulls oxygen from the STO
- ➌ Oxygen vacancies are formed
- ➍ A 2DEG emerges at the interface

A 2DEG in Al/STO



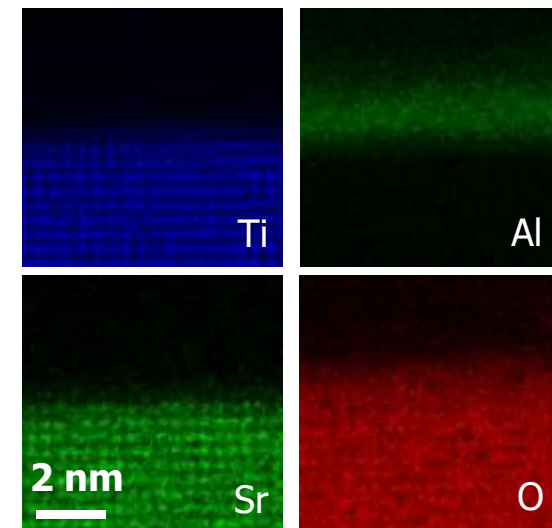
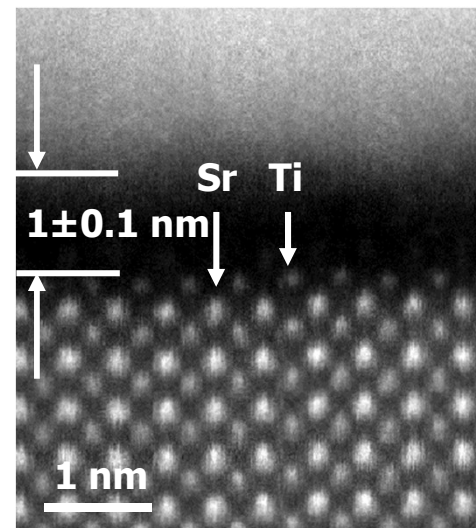
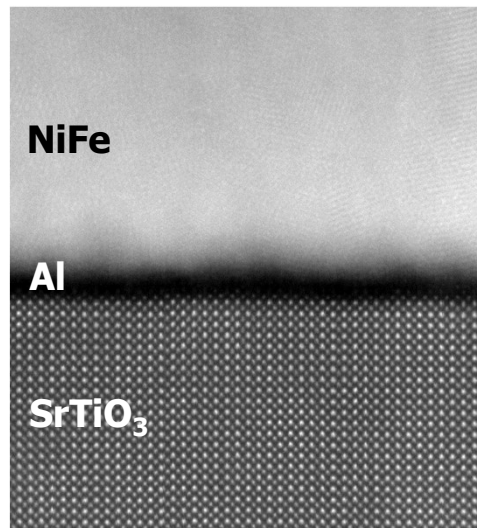
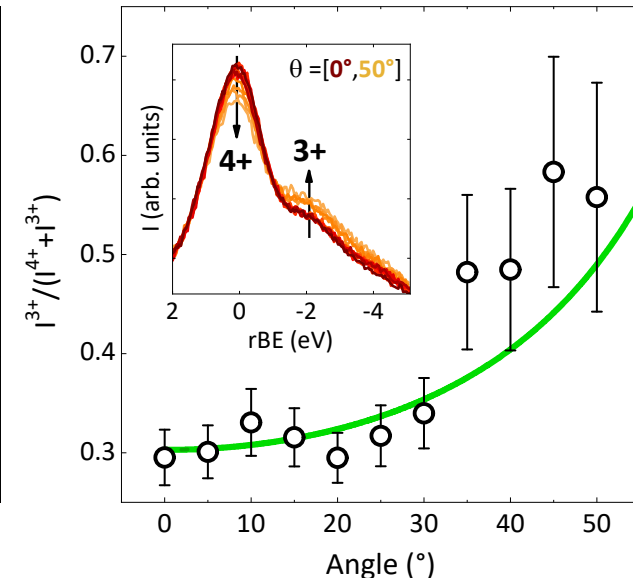
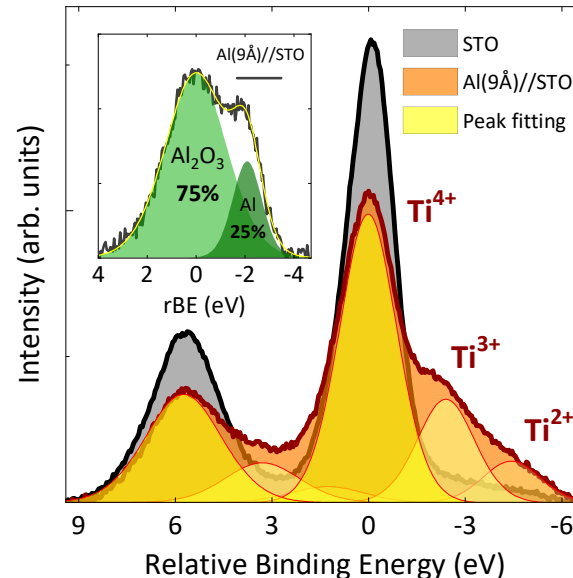
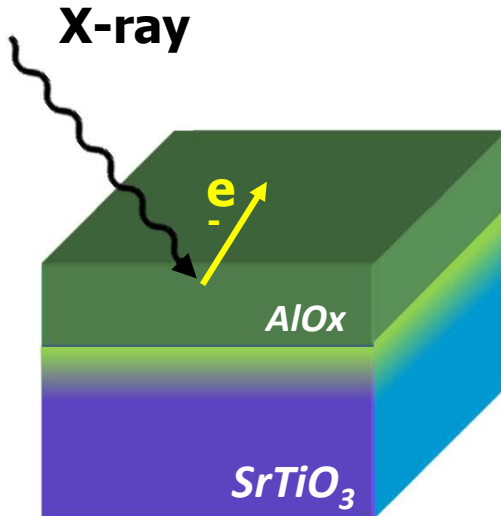
- Deposition of 9 Å of aluminum
- Aluminum pulls oxygen from the STO
- Oxygen vacancies are formed
- A 2DEG emerges at the interface

A 2DEG in Al/STO



- ➊ Deposition of 9 Å of aluminum
- ➋ Aluminum pulls oxygen from the STO
- ➌ Oxygen vacancies are formed
- ➍ A 2DEG emerges at the interface
- ➎ The deposited aluminum layer is completely oxidized

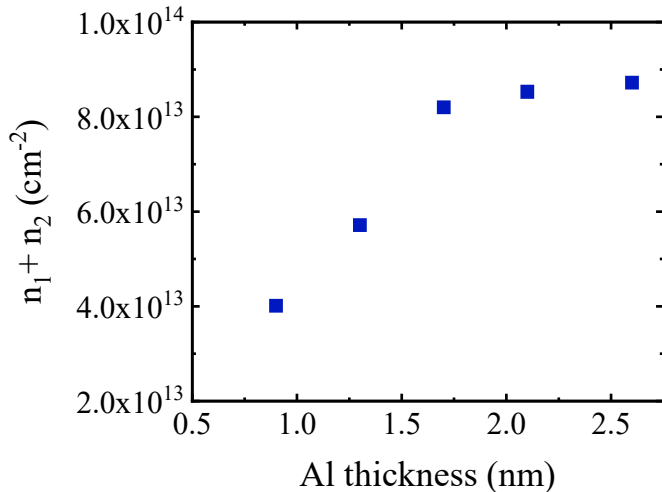
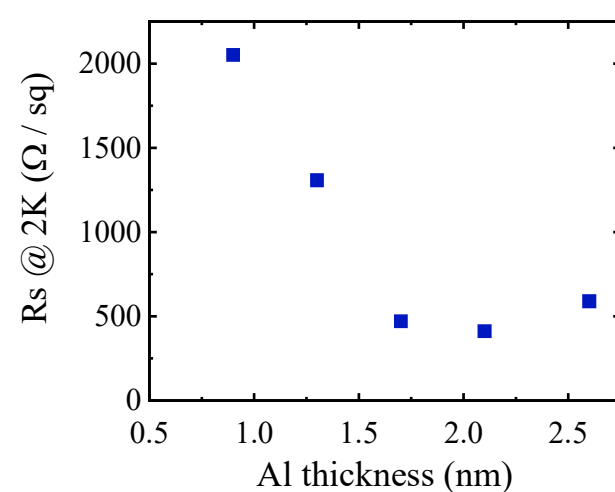
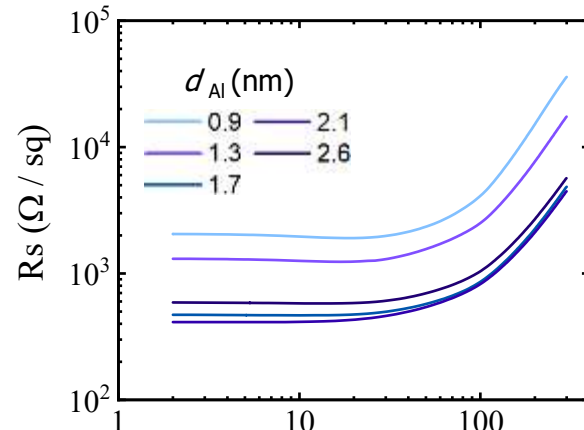
A 2DEG in Al/STO



○ Presence of 1 nm AlOx layer at interface with STO

○ Very little interdiffusion if any

Dependence of transport properties with Al thickness



- Conductivity and carrier density increase with Al thickness
- More oxygen vacancies, more carriers

Vicente-Arche, MB et al, PR Mater 5 064005 (2021)

First observation of 2DEG in Al/STO by Rödel et al, Adv. Mater. 28, 1976 (2016)

1. SrTiO₃-based 2DEGs

1.1 Physics of bulk SrTiO₃

1.2 LaAlO₃/SrTiO₃ 2DEGs

1.3 Other SrTiO₃ 2DEGs

1.4 Electronic structure of SrTiO₃ 2DEGs

1.5 Superconductivity in SrTiO₃ 2DEGs

1.5 Introducing ferroic orders into SrTiO₃ 2DEGs

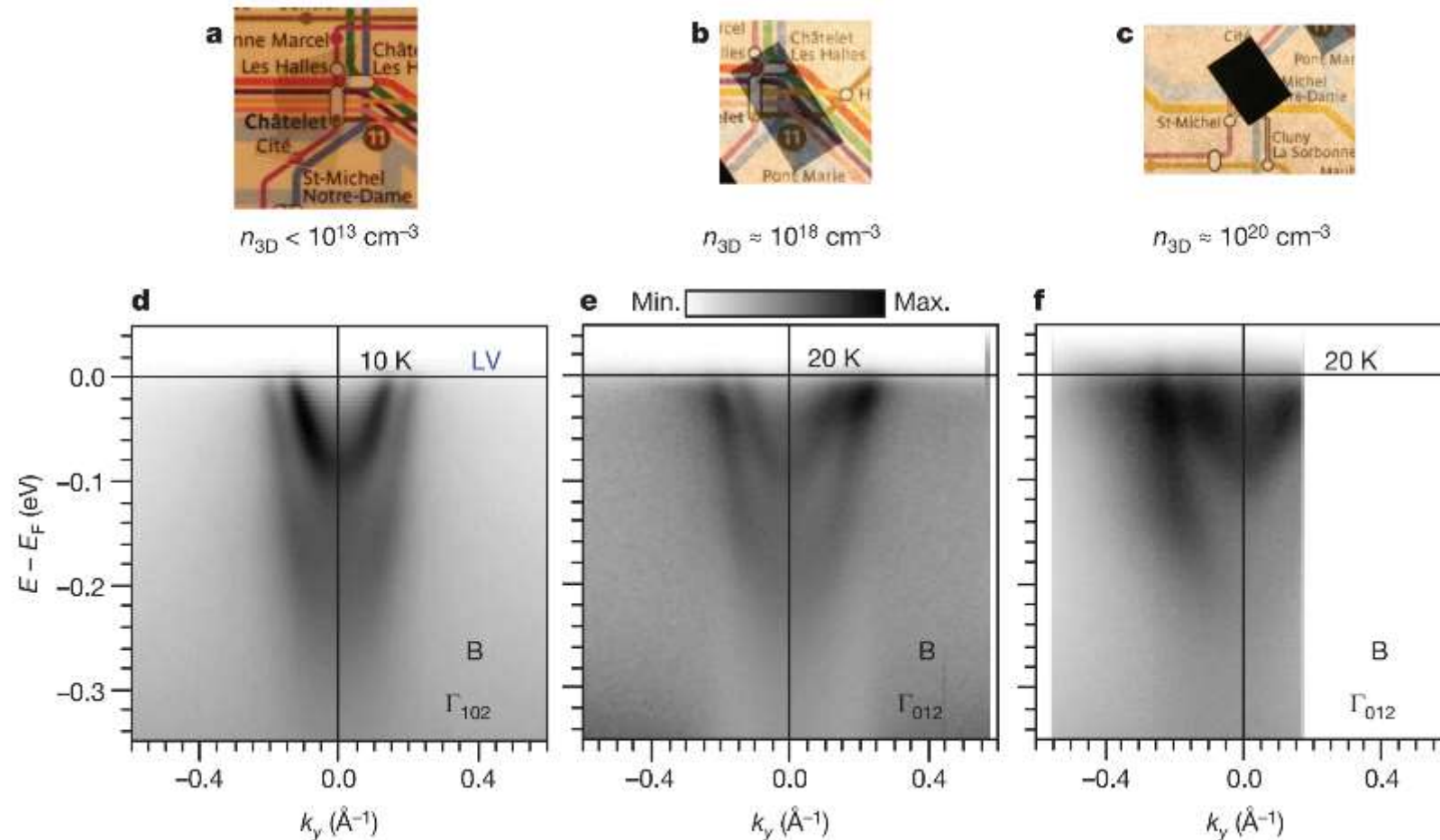
2. KTaO₃-based 2DEGs

2.1 Physics of bulk KTaO₃

2.2 KTaO₃ 2DEGs

2.3 Superconductivity in KTaO₃ 2DEGs

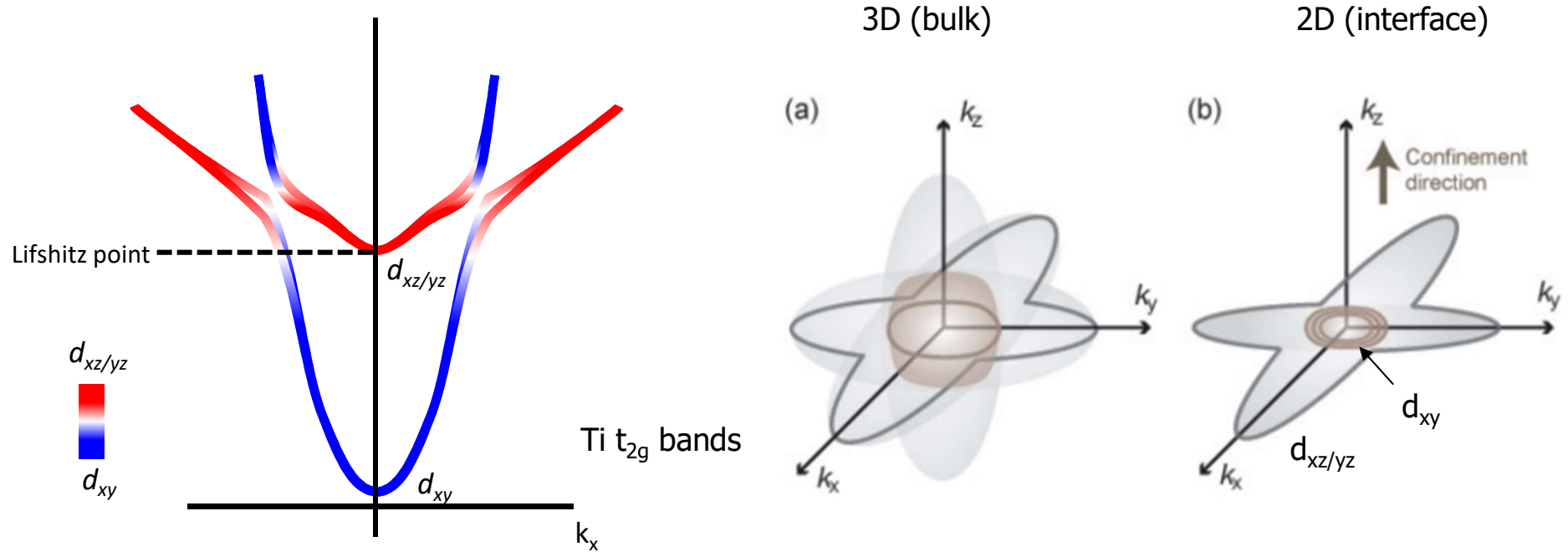
A 2DEG at the surface of STO



- Fracturing a STO crystal in vacuum creates a 2DEG at its surface
- 2DEG electronic structure very similar to that of the LAO/STO 2DEG

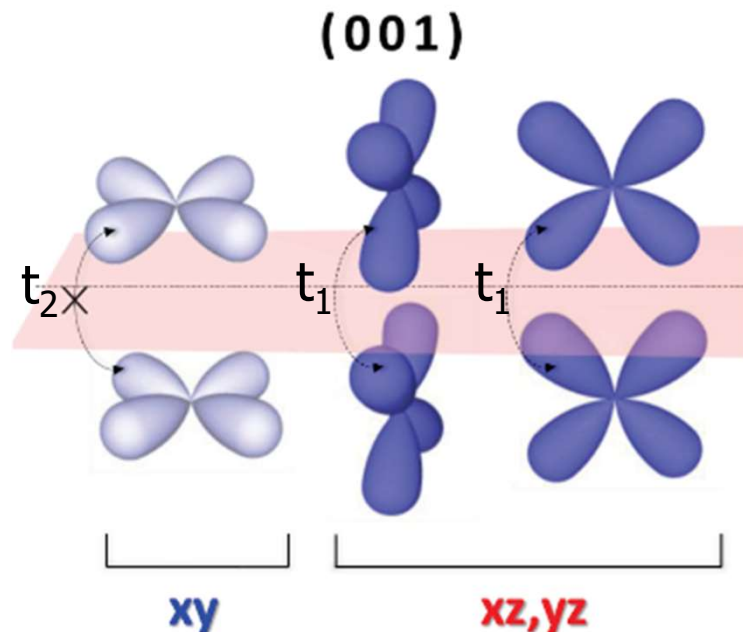
Santander, MB et al, Nature 469, 189 (2011)

Electronic structure of the 2DEG



- Compared to bulk STO, the degenerescence of the t_{2g} states is lifted (splitting is 50-100 meV)
- Low lying d_{xy} band with light mass
- Above Lifshitz point, onset of second band with $d_{xz/yz}$ character and heavier mass
- Avoided crossing due to orbital mixing and spin orbit coupling (more on this later)

Quantum confinement and band structure



Hopping terms : $t_1 \approx -300\text{meV}$ & $t_2 \approx -15\text{meV}$

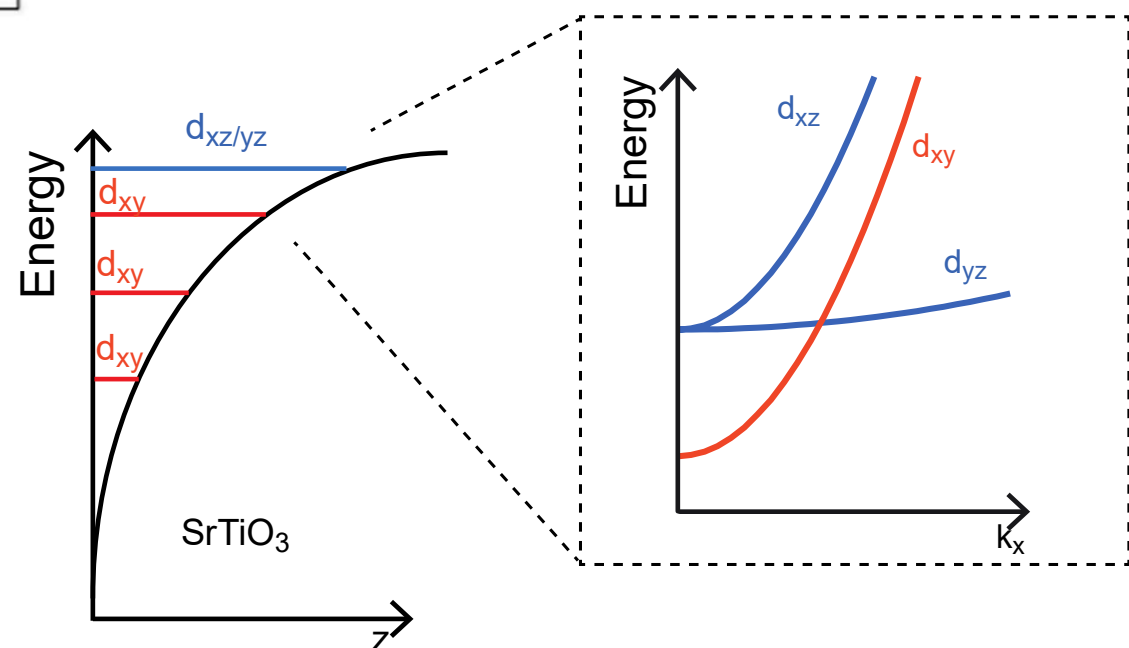
$$\begin{array}{ccc} \text{light} & & \text{heavy} \\ m_l = -\frac{\hbar^2}{2a^2t_1} \approx 0.7m_0 & & m_h = -\frac{\hbar^2}{2a^2t_2} \approx 14m_0 \end{array}$$

Interfacial quantum well

$$\text{Bands energy : } E \propto \frac{1}{m_{001}}$$

$$m_{001}^{xy} = 14m_0$$

$$m_{001}^{xz,yz} = 0.7m_0$$



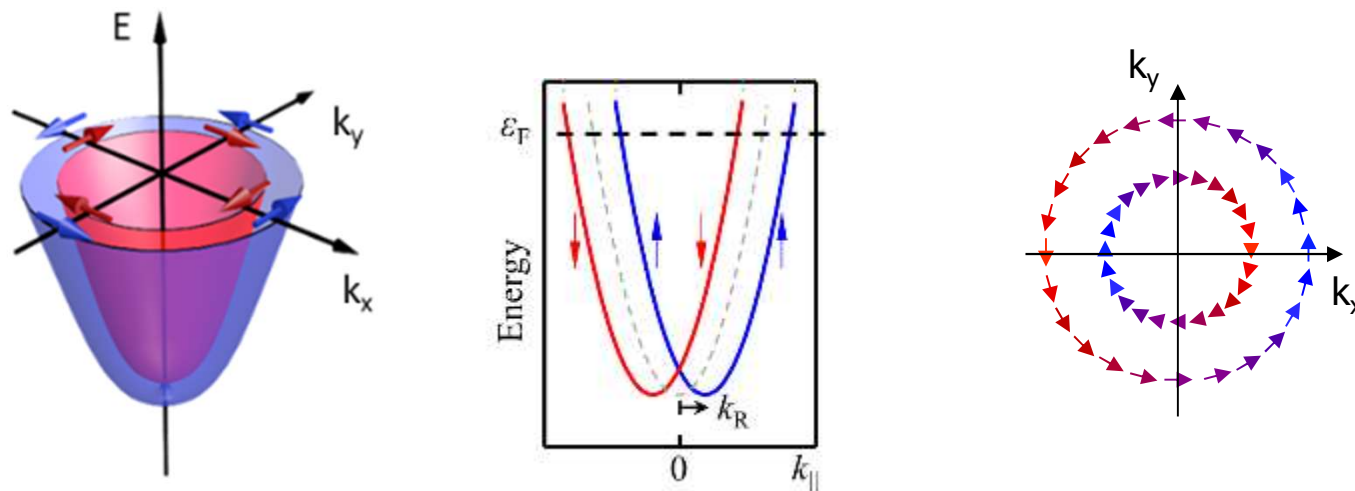
Spin/charge interconversion in Rashba systems

Rashba spin-orbit coupling

The **Rashba effect** – manifestation of spin-orbit interaction (SOI) in solids, more particularly in two-dimensional electron systems, where spin degeneracy is lifted due to a symmetry-breaking electric field normal to an heterointerface.

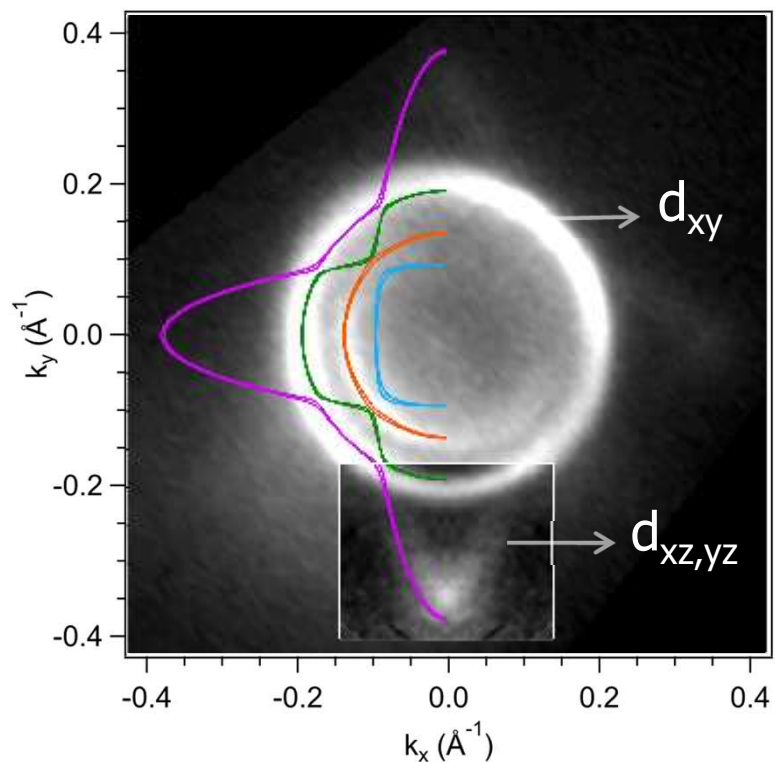
$$H_R = \frac{\alpha_R}{\hbar} (\vec{\sigma} \wedge \vec{p}) \bullet \vec{z}$$

Bychkov & Rashba, Sov. Phys. JETP Lett. 39, 78 (1984)
Manchon et al., Nature Mater. 14, 871 (2015)

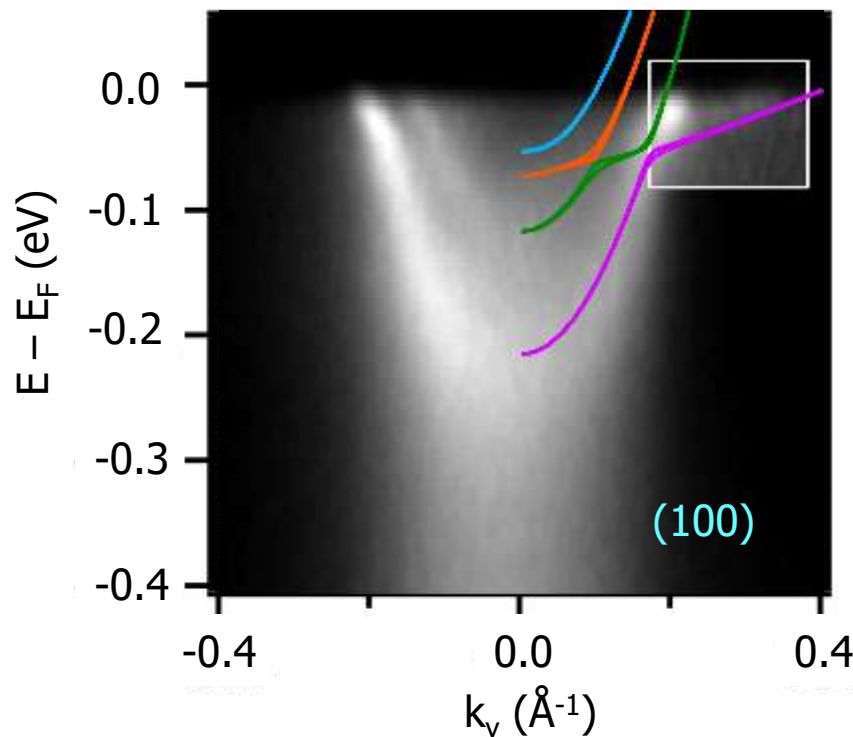
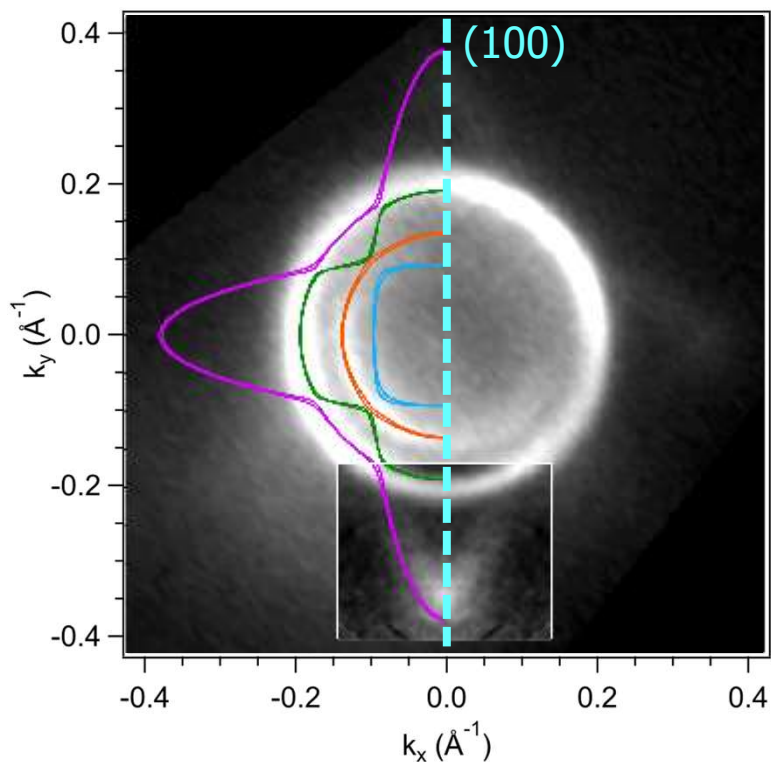


Strength of Rashba coupling is expressed by the Rashba coefficient α_R that is on the order of 20-50 meV.A in STO 2DEGs
(cf around 1 eV.A at surfaces of heavy metals)

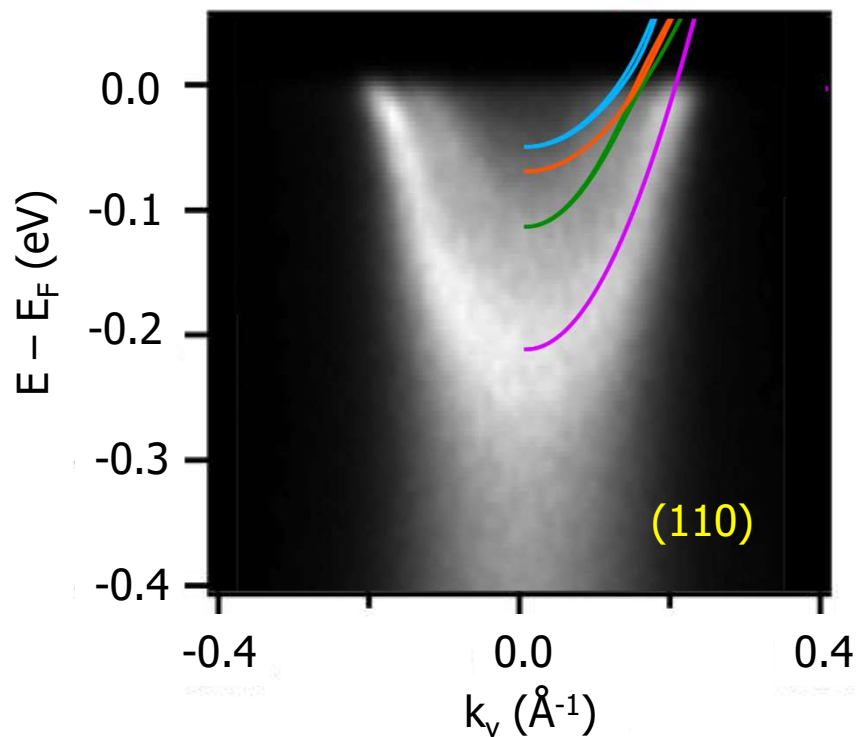
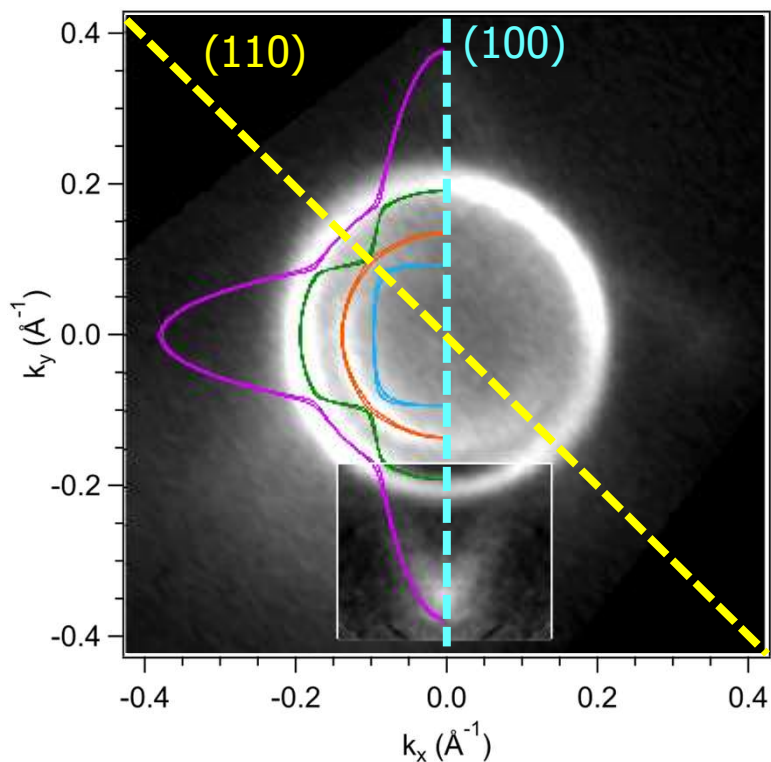
Electronic structure of STO 2DEGs



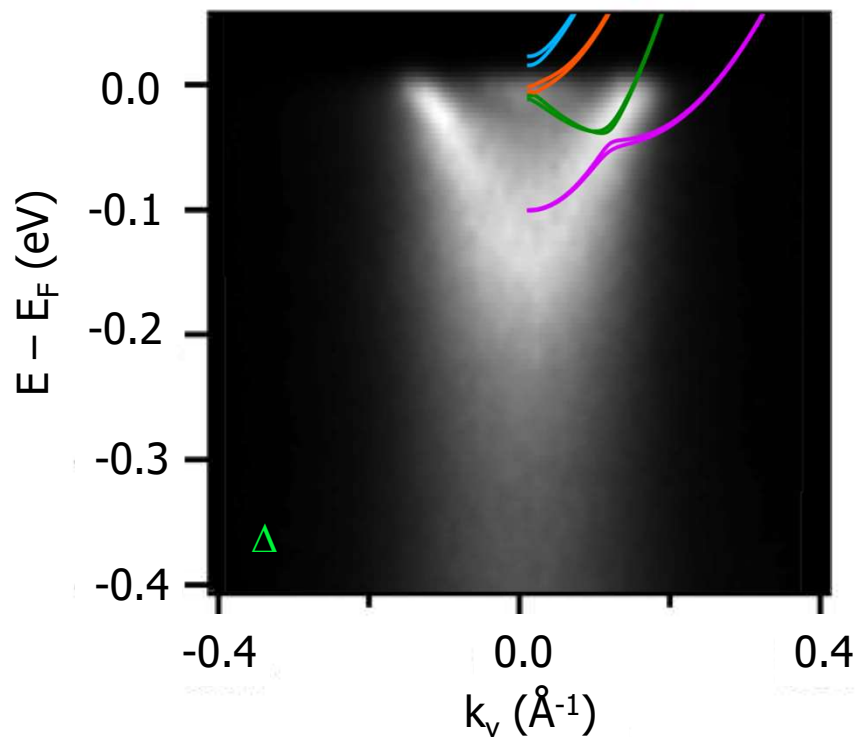
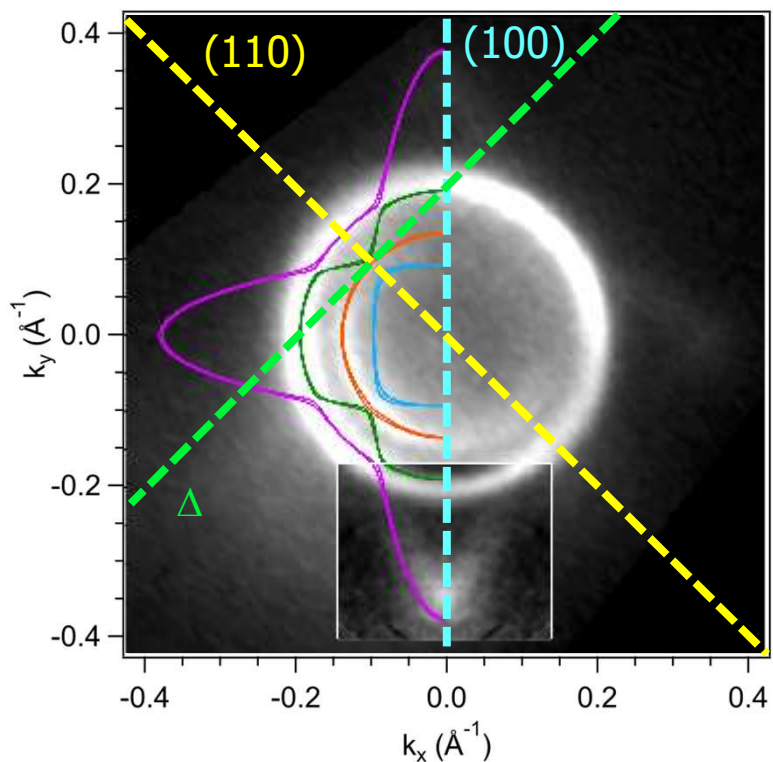
Electronic structure of STO 2DEGs



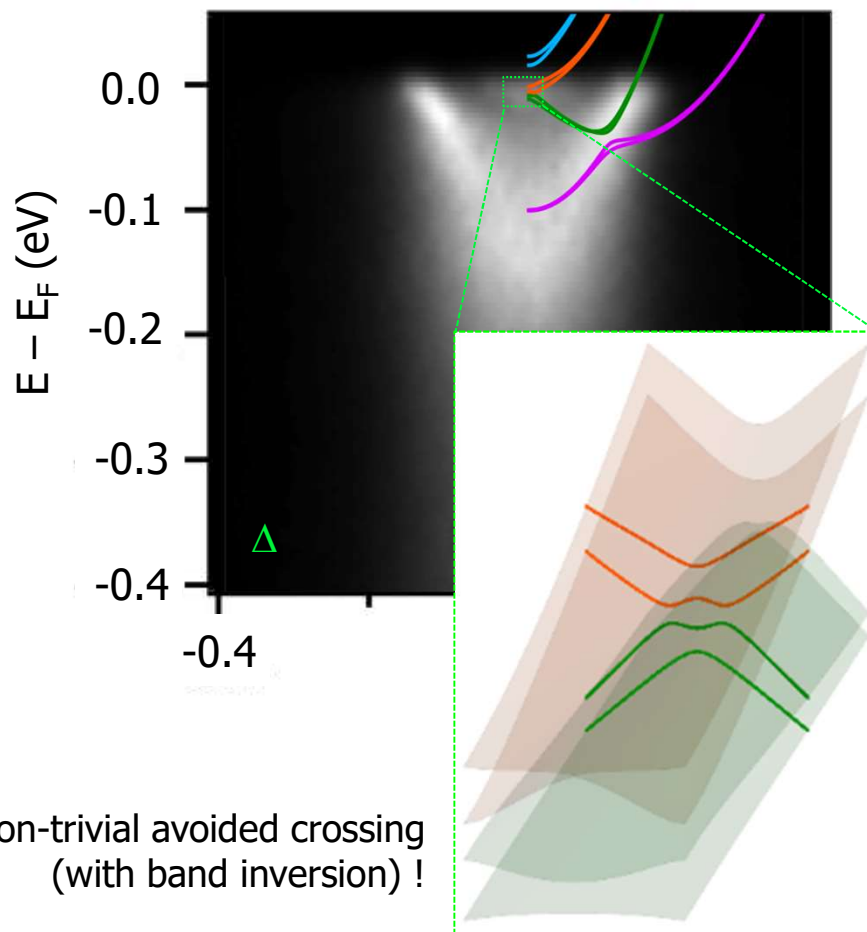
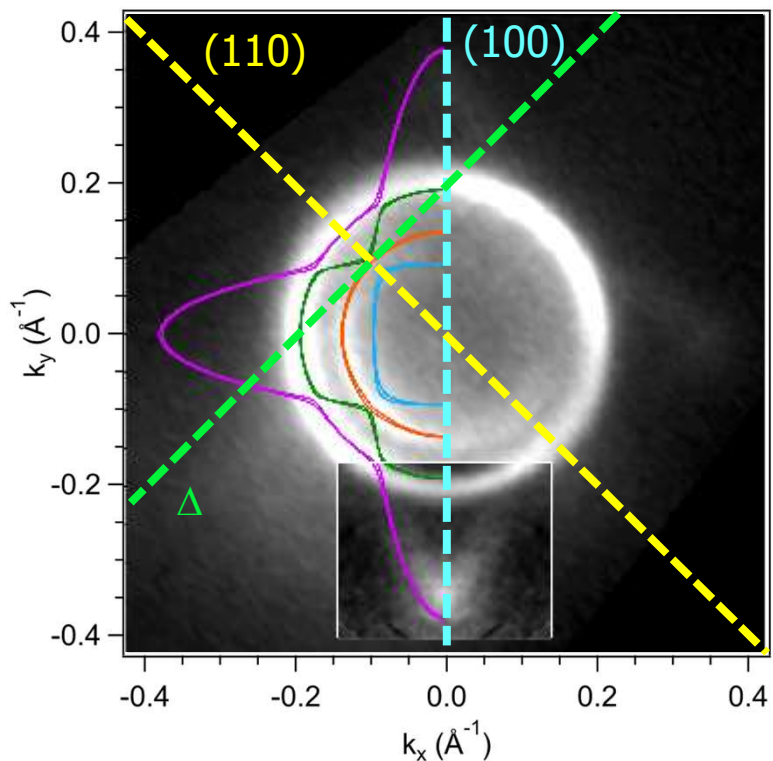
Electronic structure of STO 2DEGs



Electronic structure of STO 2DEGs



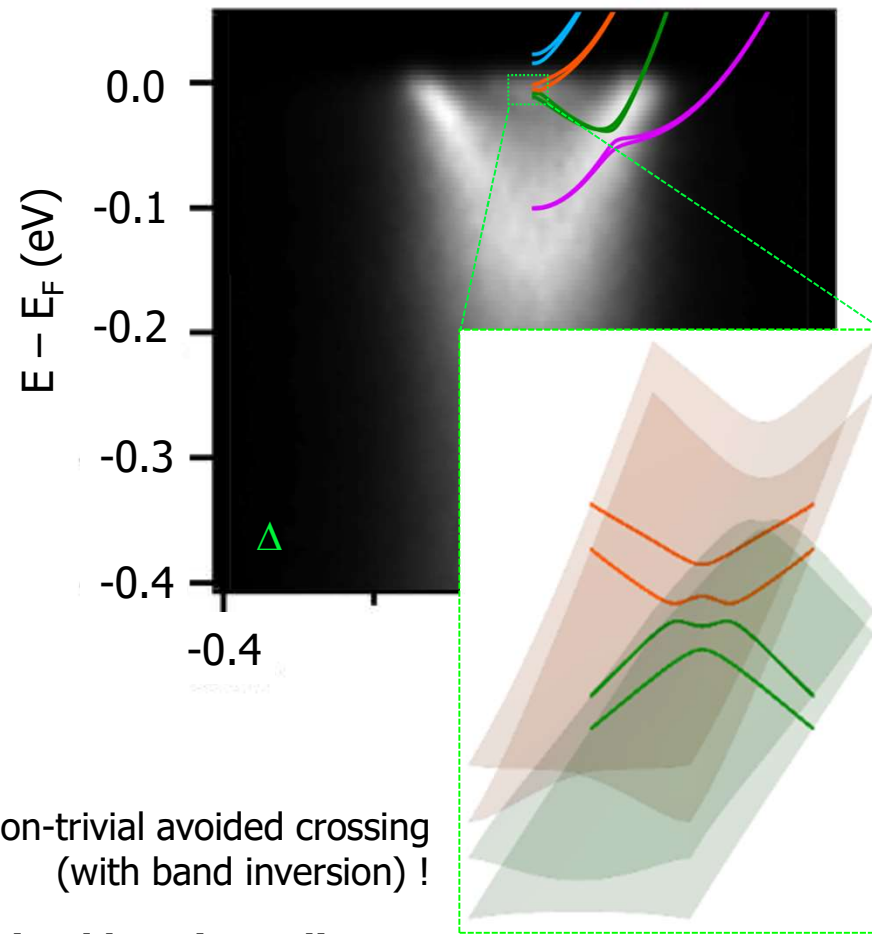
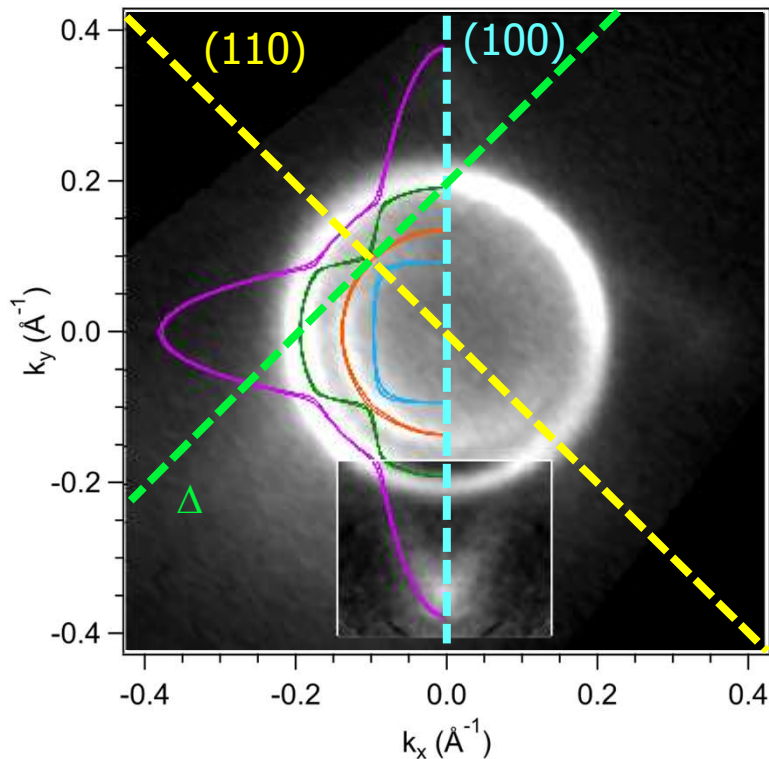
Electronic structure of STO 2DEGs



Topologically non-trivial avoided crossing
(with band inversion) !

M. Vivek et al, PRB 95, 165117 (2017)

Electronic structure of STO 2DEGs



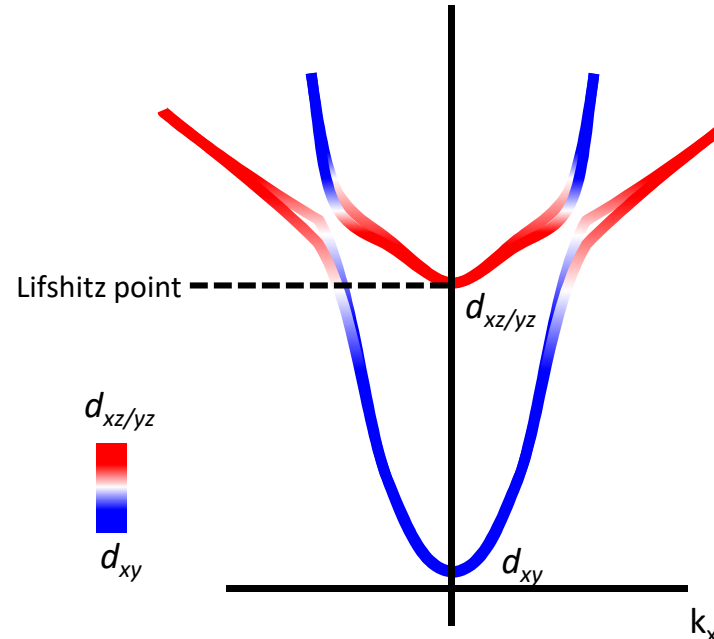
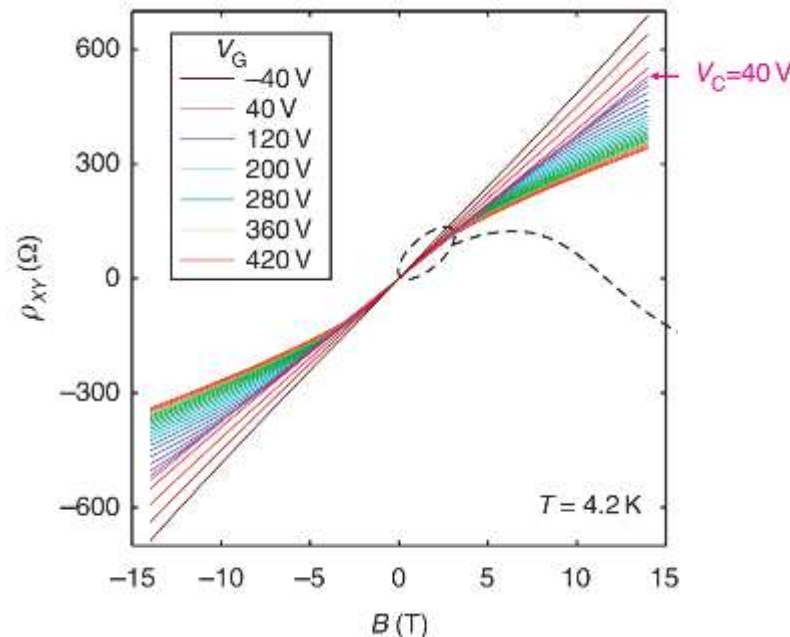
Topologically non-trivial avoided crossing
(with band inversion) !

Electronic structure of STO 2DEGs determined by 4 ingredients

1. Splitting of d_{xy} and $d_{xz/yz}$ bands by confinement potential
2. Sub-bands due to quantum confinement
3. Spin-orbit coupling
4. Orbital mixing

Vaz, MB et al, Nature Mater. 18, 1187 (2019)

Electrostatic gating



- At low carrier density (negative gate voltages), the Hall effect is linear : one type of carriers
- Upon adding carriers, the Hall effect becomes non-linear : two types of carriers
- Gate induced Lifshitz transition (at $1.5\text{--}2.5 \times 10^{13} \text{ cm}^{-2}$)

Joshua et al, Nature Comm. 3, 1129 (2012)

- 1. SrTiO₃-based 2DEGs**
 - 1.1 Physics of bulk SrTiO₃**
 - 1.2 LaAlO₃/SrTiO₃ 2DEGs**
 - 1.3 Other SrTiO₃ 2DEGs**
 - 1.4 Electronic structure of SrTiO₃ 2DEGs**
 - 1.5 Superconductivity in SrTiO₃ 2DEGs**
 - 1.5 Introducing ferroic orders into SrTiO₃ 2DEGs**
- 2. KTaO₃-based 2DEGs**
 - 2.1 Physics of bulk KTaO₃**
 - 2.2 KTaO₃ 2DEGs**
 - 2.3 Superconductivity in KTaO₃ 2DEGs**

Superconducting properties

Superconductivity in $\text{LaAlO}_3/\text{SrTiO}_3$

Reyren et al. Science 317, 1196 (2007)

Superconductivity in $\text{LaTiO}_3/\text{SrTiO}_3$

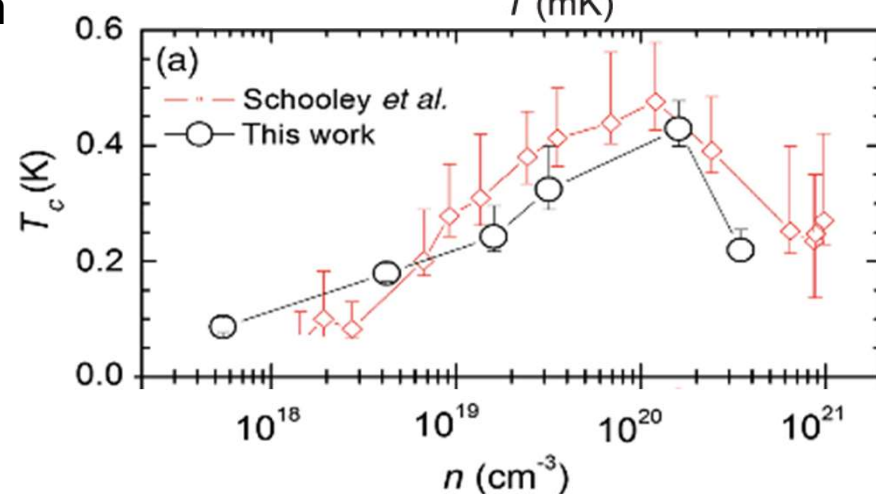
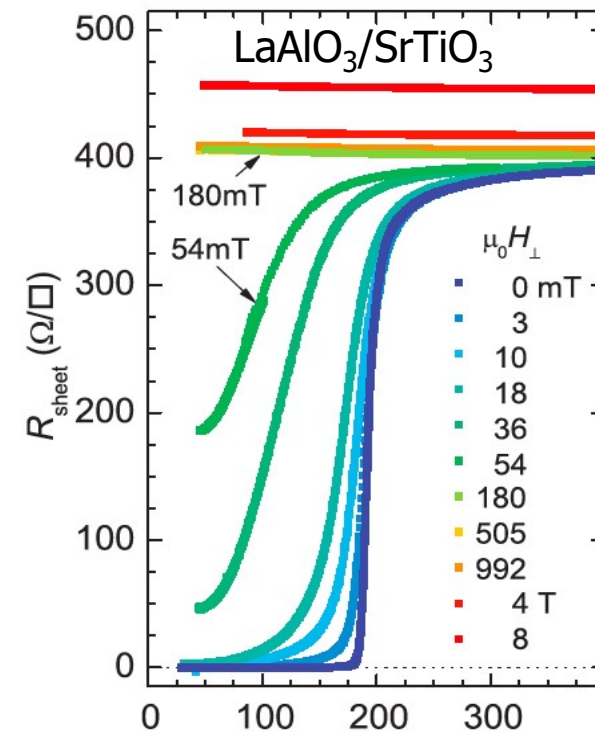
Biscaras et al. Nat. Commun. 1, 89 (2010)

Critical magnetic field

$$\left. \begin{aligned} H_{\perp}(T) &= \frac{\phi_0}{2\pi\xi_{\parallel}(T)} \\ H_{\parallel}(T) &= \frac{\sqrt{3}\phi_0}{\pi d \xi_{\parallel}(T)} \end{aligned} \right\} \quad \begin{aligned} \xi_{\parallel}(T=0) &\approx 40 - 50 \text{ nm} \\ \text{thickness } d &< 12 \text{ nm} \end{aligned}$$

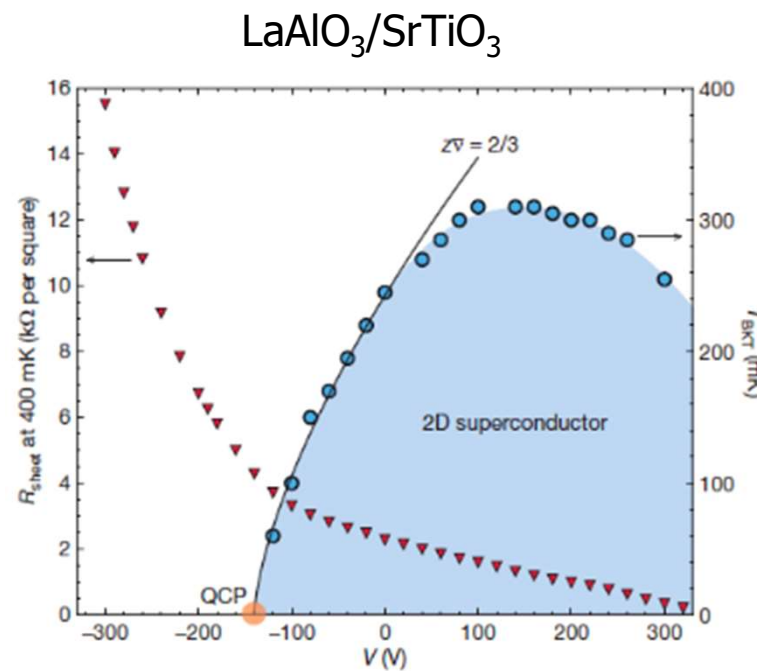
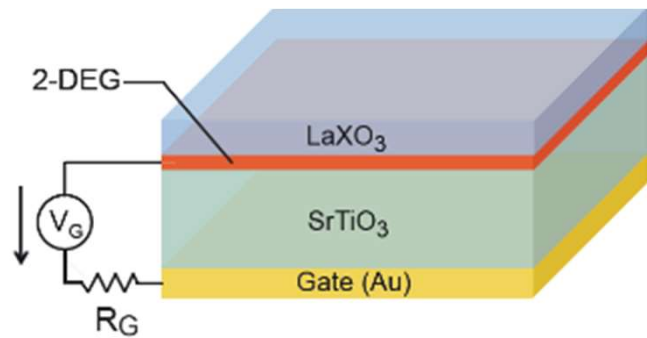
- Superconducting 2-DEG
- T_c similar to doped bulk SrTiO_3

Lin et al. PRX (2013)

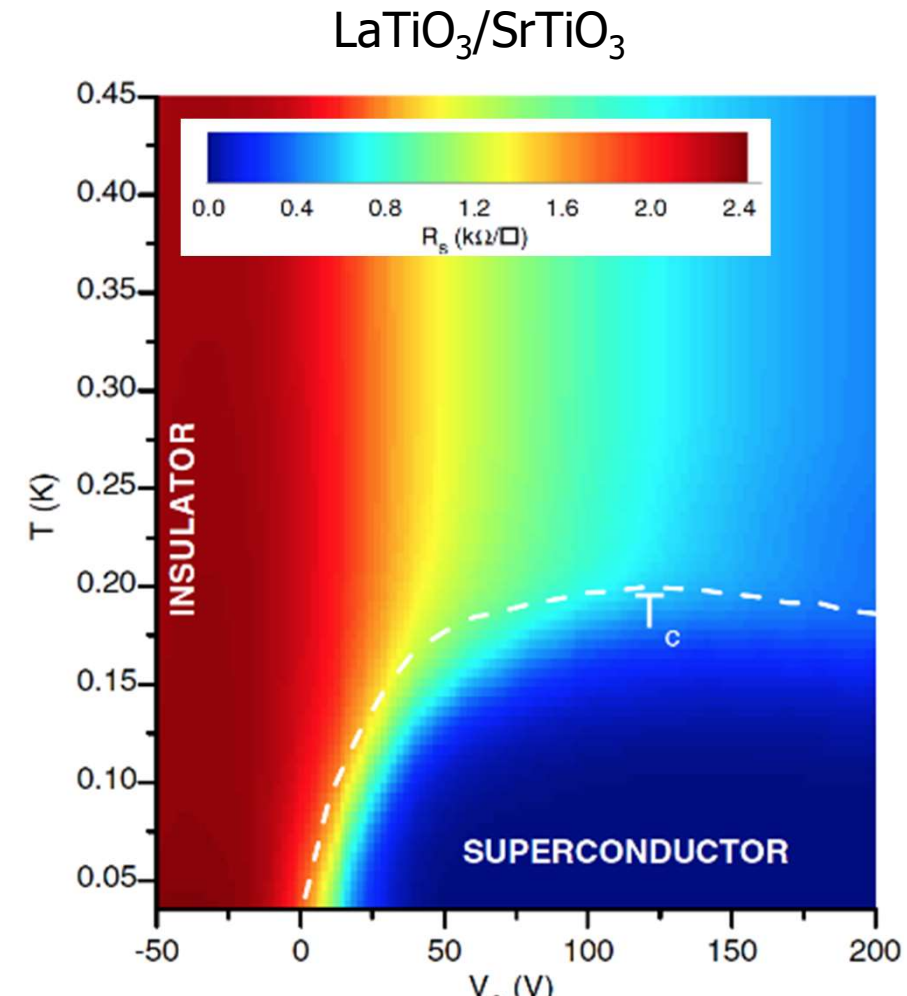


Gate dependence

Back-gating



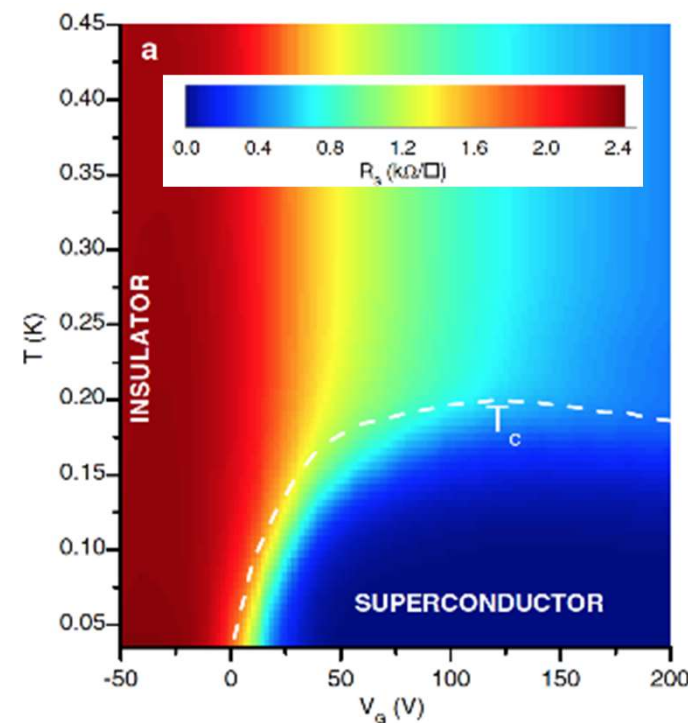
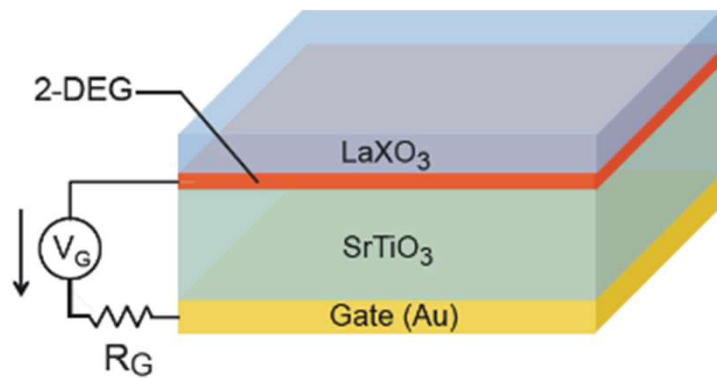
A. Caviglia et al Nature (2008)



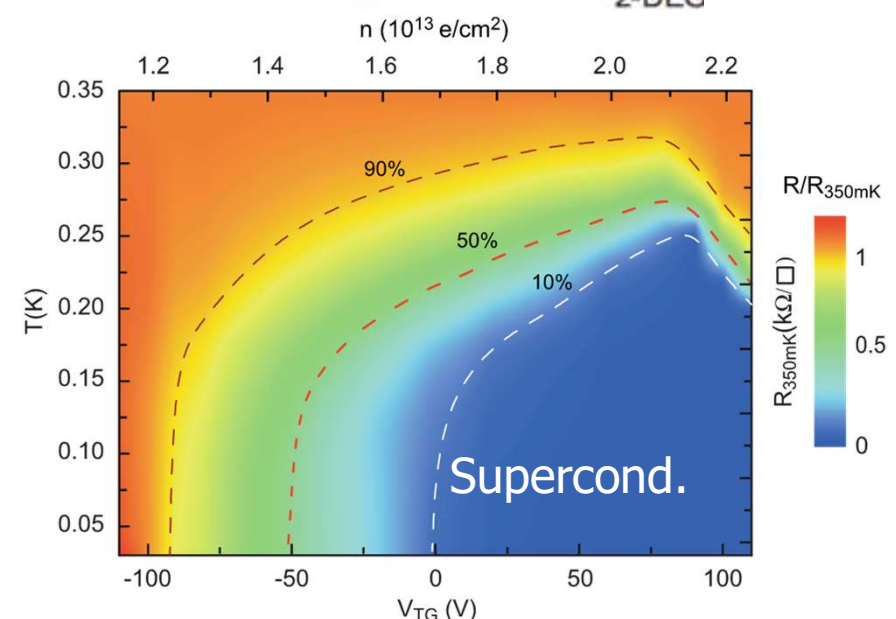
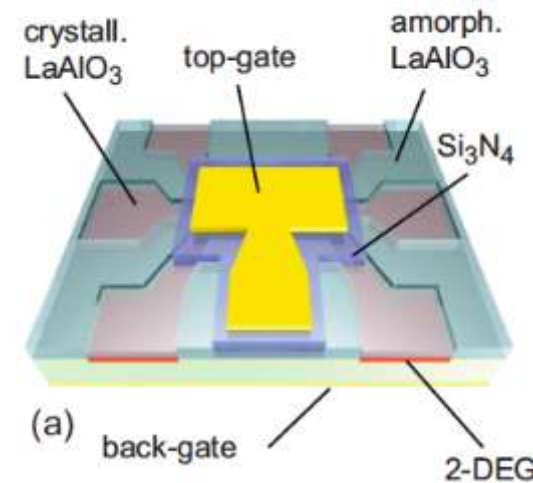
J. Biscaras et al Phys. Rev. Lett. 108, 247004 (2012)

Field effect devices

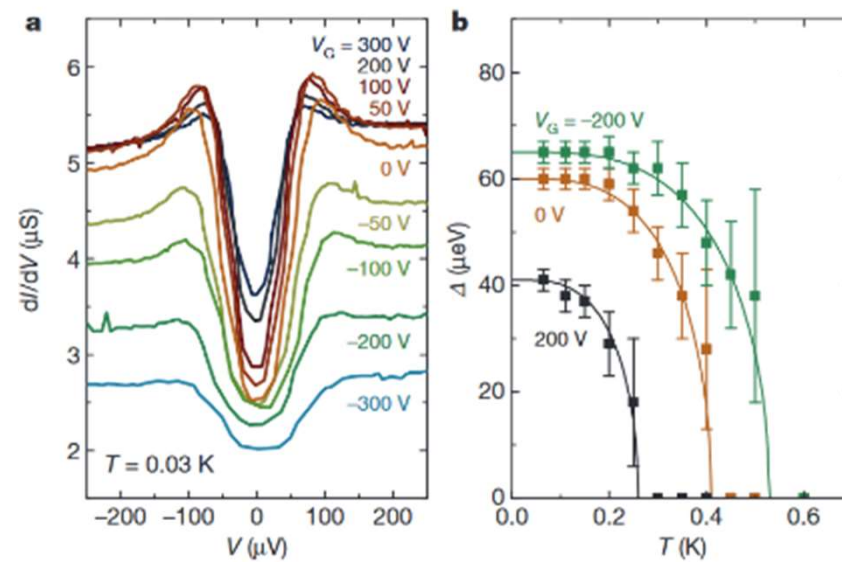
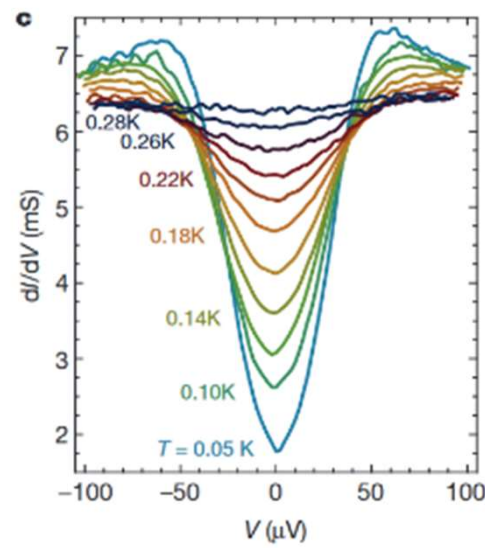
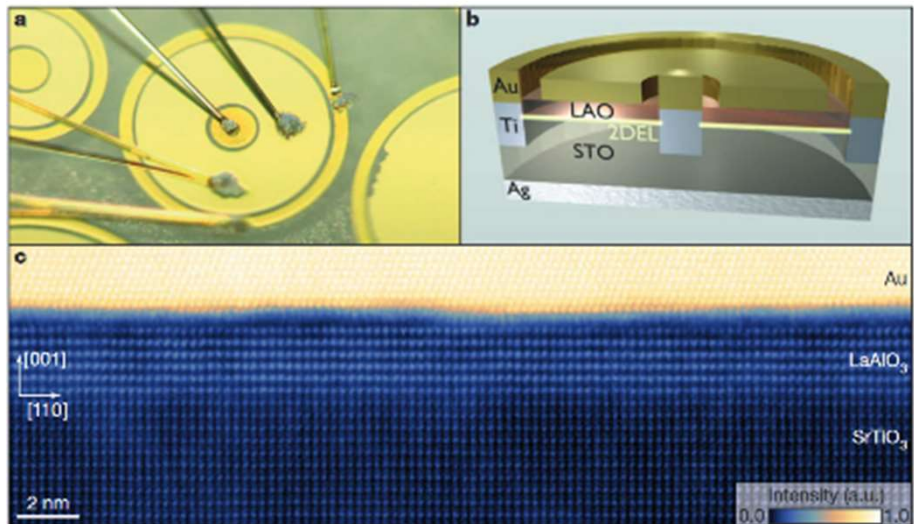
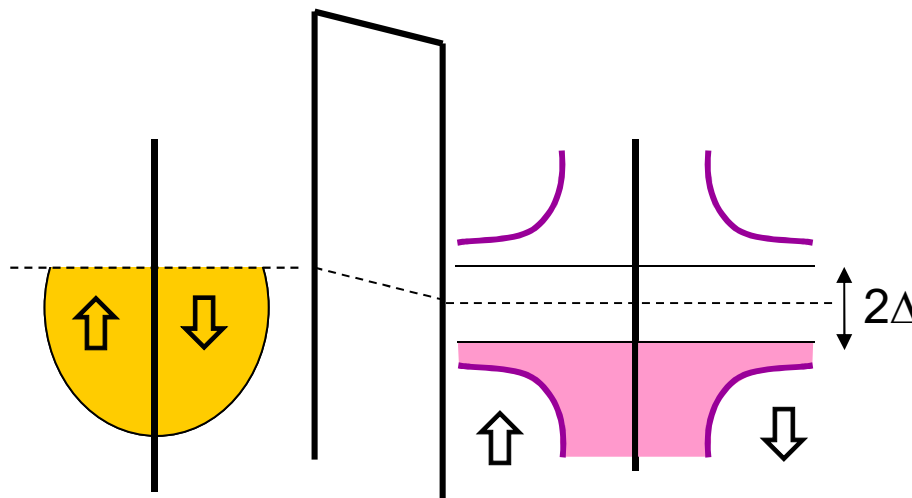
Back-gating



Top-gating



Tunneling experiments



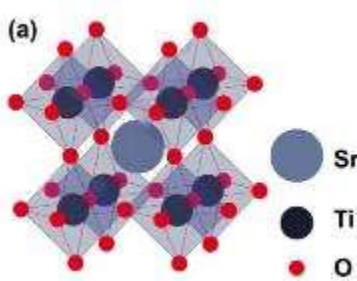
- Determination of the superconducting gap and its evolution with T and gate V

Richter et al, Nature 502, 528 (2013)

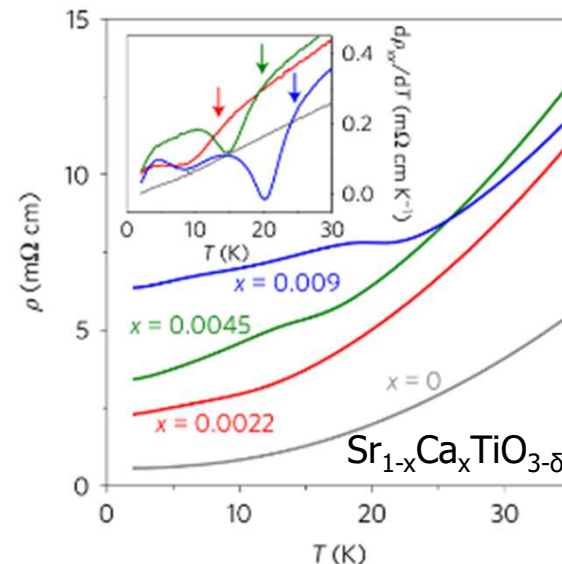
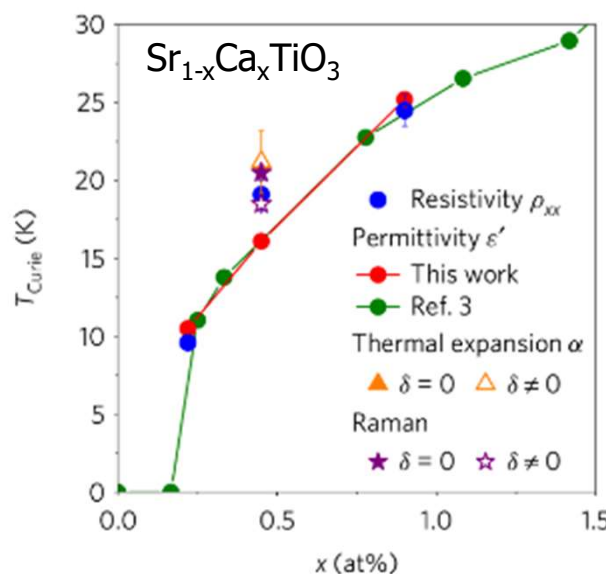
- 1. SrTiO₃-based 2DEGs**
 - 1.1 Physics of bulk SrTiO₃**
 - 1.2 LaAlO₃/SrTiO₃ 2DEGs**
 - 1.3 Other SrTiO₃ 2DEGs**
 - 1.4 Electronic structure of SrTiO₃ 2DEGs**
 - 1.5 Superconductivity in SrTiO₃ 2DEGs**
 - 1.5 Introducing ferroic orders into SrTiO₃ 2DEGs**
- 2. KTaO₃-based 2DEGs**
 - 2.1 Physics of bulk KTaO₃**
 - 2.2 KTaO₃ 2DEGs**
 - 2.3 Superconductivity in KTaO₃ 2DEGs**

Ferroelectricity in SrTiO_3 by Ca substitution

Structure and dipolar behaviour of SrTiO_3



- POSSIBILITY to induce ferroelectricity behavior in SrTiO_3 by ionic substitution:
 - Fraction x (at%) of Sr ions replaced by Ba, Pb or **Ca**
 - For $\text{Sr}_{1-x}\text{Ca}_x\text{TiO}_3$, ferroelectric state present already at $x = 0.25\%$
 - T_C increases with x



- Oxygen vacancies
- Bulk conductivity
- Ionic substitution
- Ferroelectric signature (structural transition)

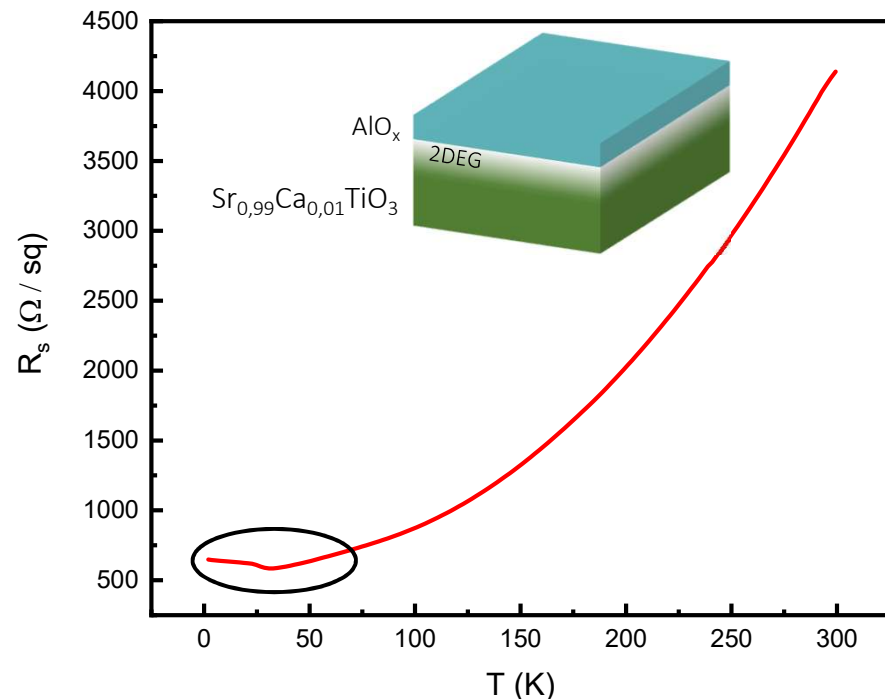
Bednorz, J. G. & Müller, K. A., Phys. Rev. Lett. 52, 2289–2292 (1984)

Rischau, C. W. et al., Nature Phys 13, 643–648 (2017)

Mitsui, et al. Phys. Rev. 124, 1354–1359 (1961)

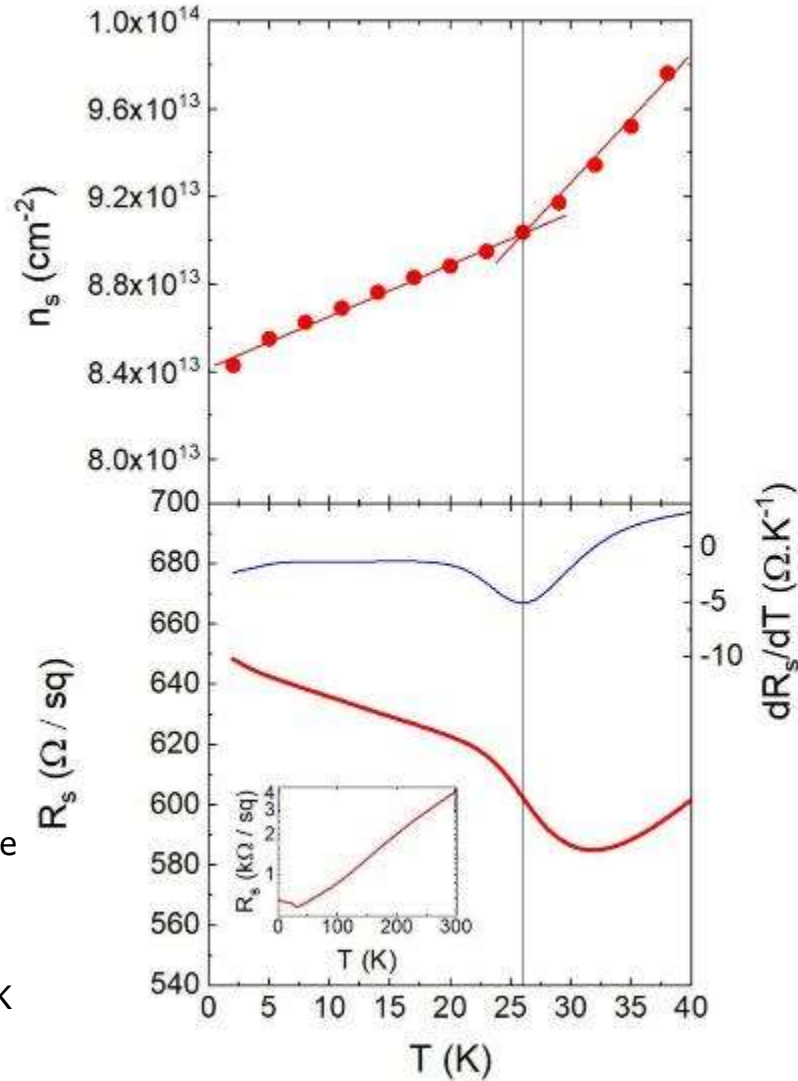
2DEG fabrication and transport with Al/Sr_{0,99}Ca_{0,01}TiO₃

Sheet resistance vs. temperature



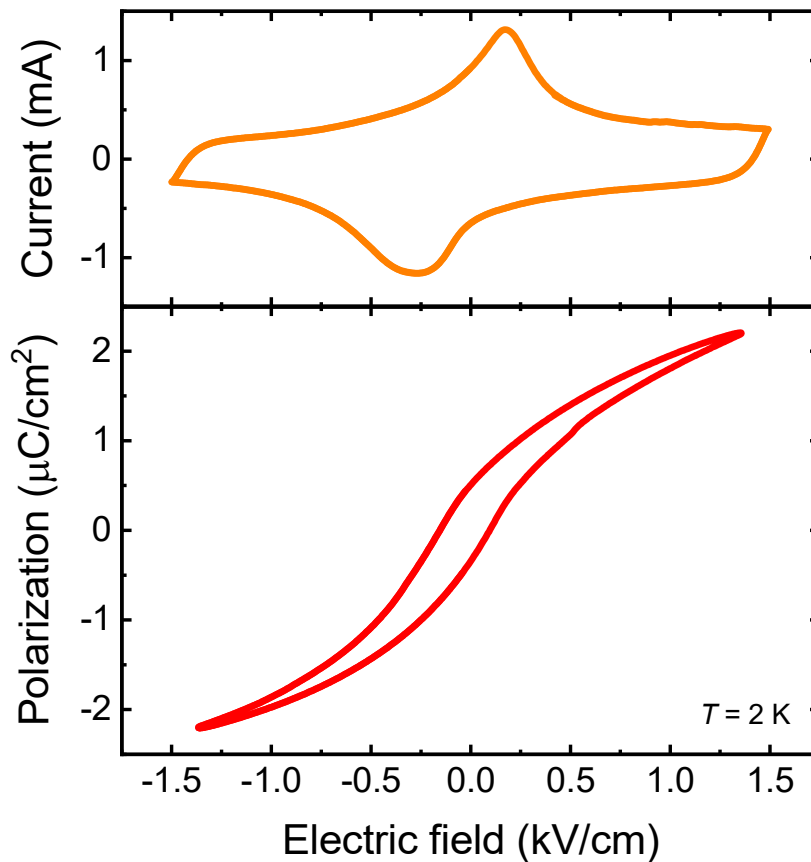
- With 1,84 nm of Al sputtered, metallic behaviour is found at the Al// $\text{Sr}_{1-x}\text{Ca}_x\text{TiO}_3$ interface as in Al//SrTiO₃ 2DEGs
- A «kink» in the sheet resistance temperature dependence is visible around 30 K
- Hall effect measurements show a change in carrier density evolution vs. temperature which coincides with $R_s(T)$ «kink» at 26 K

Carrier density and sheet resistance vs. temperature



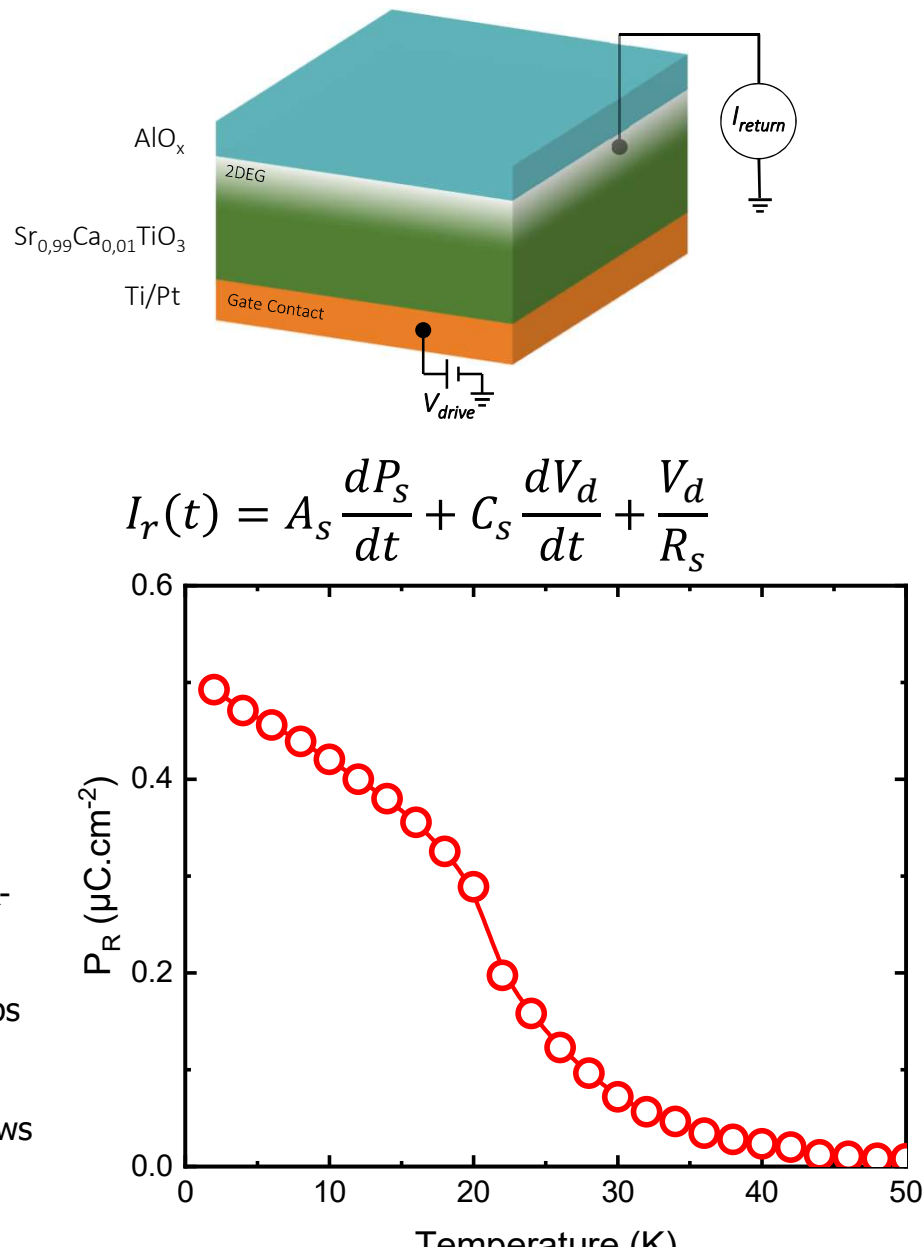
J. Bréhin, MB et al., Phys. Rev. Mat. 4, 041002(R) (2020)

Ferroelectricity in Al/Sr_{0.99}Ca_{0.01}TiO₃: polarization loops

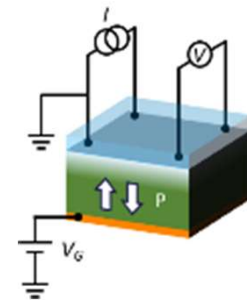
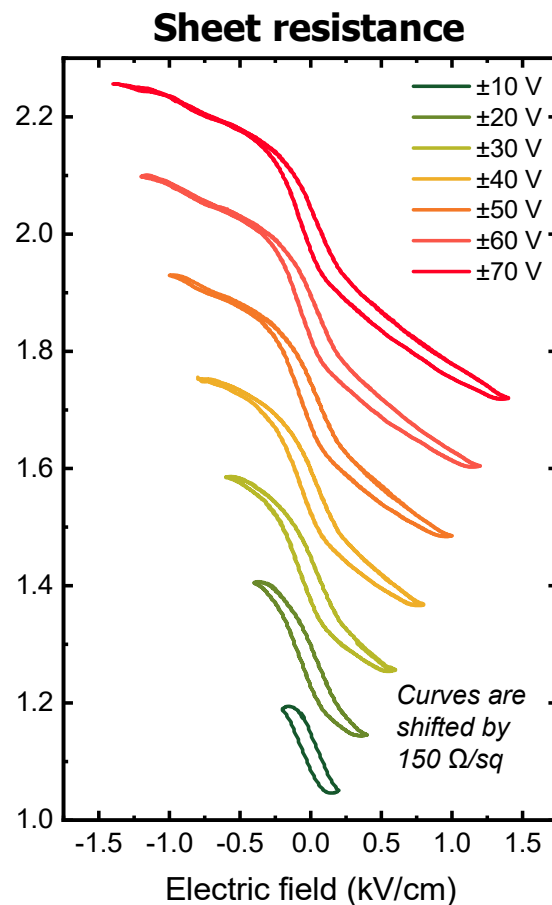
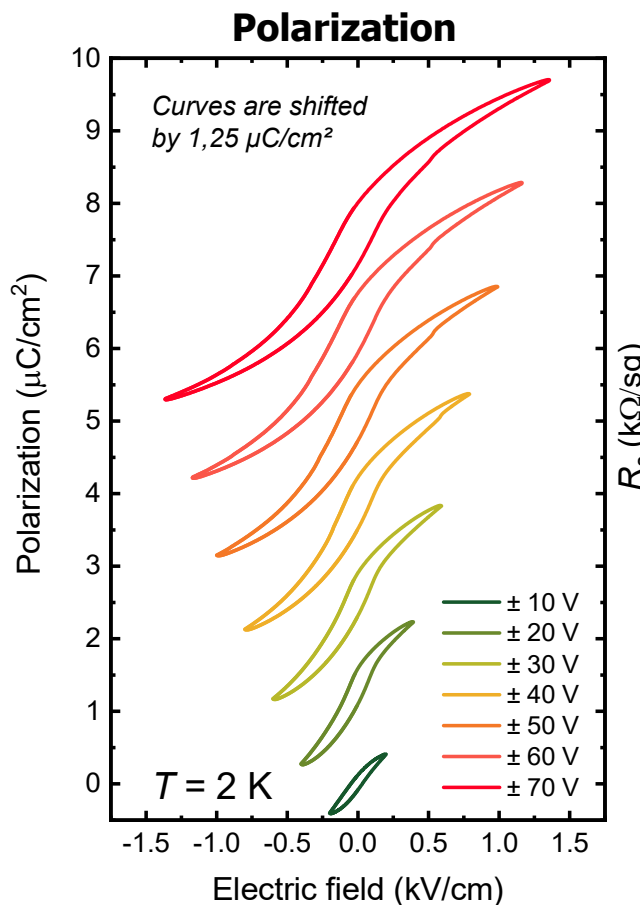
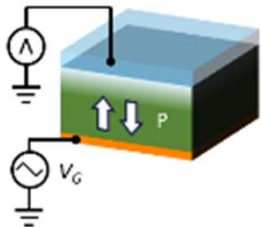


- Hysteresis cycles with 2DEG as top-contact and Ti/Pt back-gate
- Hysteretic behaviour of the polarisation versus E-field loops
- Switching current peaks are clearly visible
→ Sample shows ferroelectricity
- Temperature dependence of the remnant polarization shows again the FE ↔ PE transition around 25 K

J. Bréhin, MB et al., Phys. Rev. Mat. 4, 041002(R) (2020)



Ferroelectric behaviour of a 2DEG based on Al/Sr_{0.99}Ca_{0.01}TiO₃

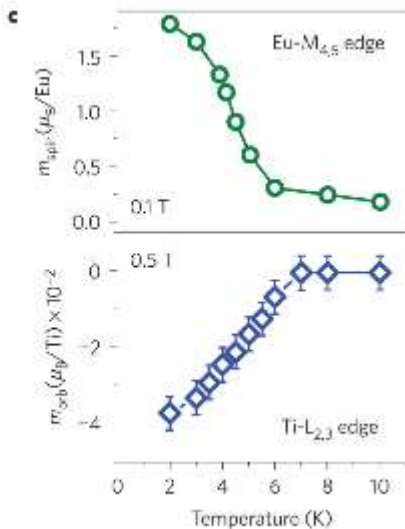
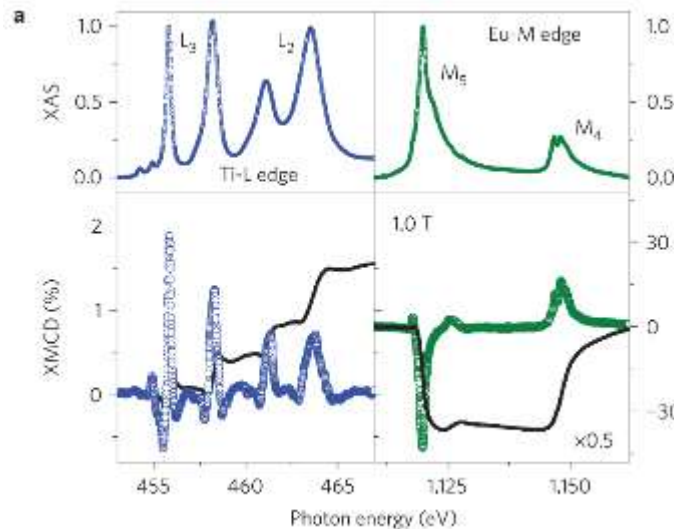
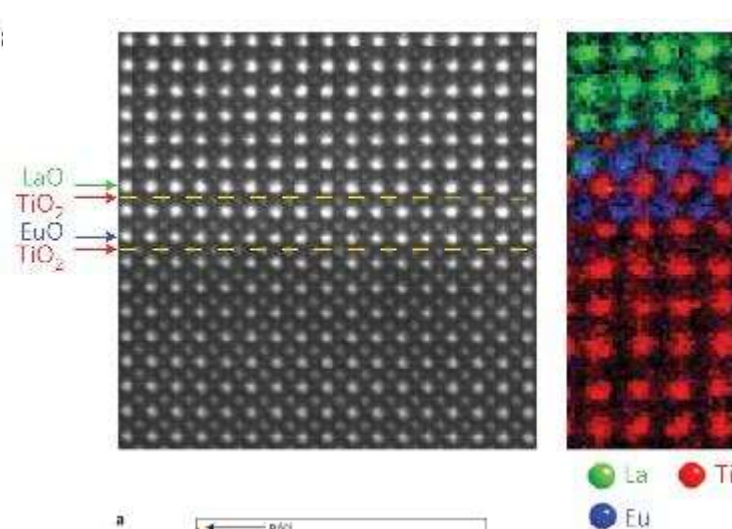


- Cycling of the **sheet resistance** and **polarization** w.r.t. electric-field both show **hysteresis** and **match**
- Carrier density is modulated at remanence by $\Delta n_s = 5,68 \cdot 10^{12} \text{ cm}^{-2}$, i.e. $\pm 3,35\%$ of the total carrier density in initial state

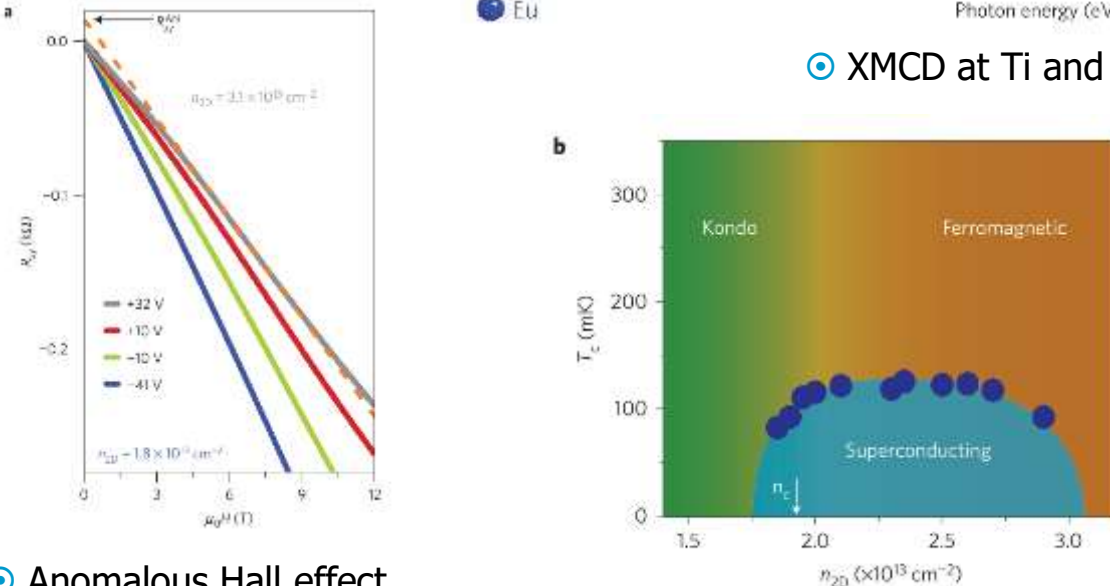
J. Bréhin, MB et al., Phys. Rev. Mat. 4, 041002(R) (2020)

Engineering a magnetic 2DEG

Insert a monolayer of EuTiO_3 between LAO and STO



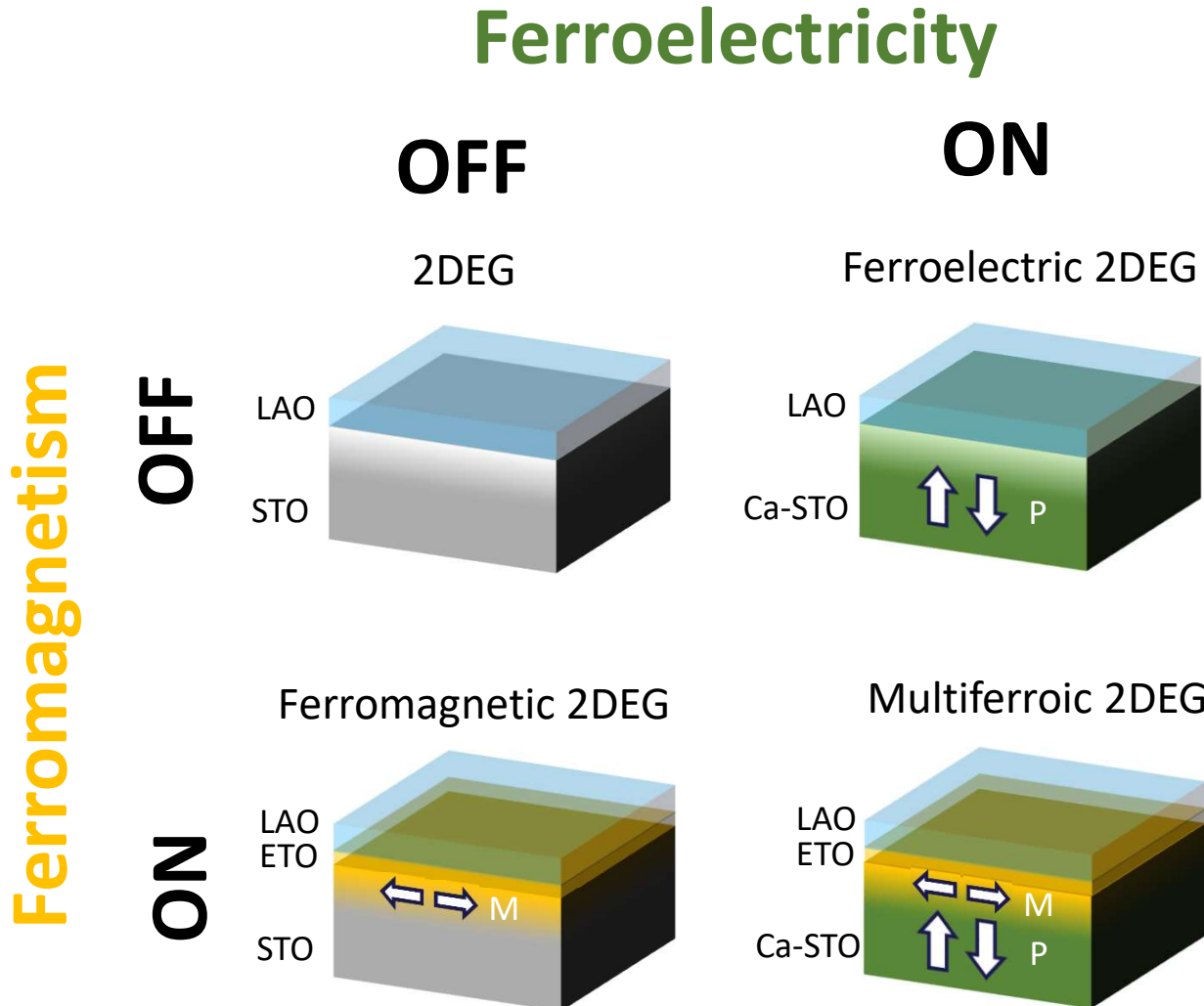
XMCD at Ti and Eu edges



Anomalous Hall effect

Coexistence of ferromagnetism and superconductivity, tunable by gate voltage

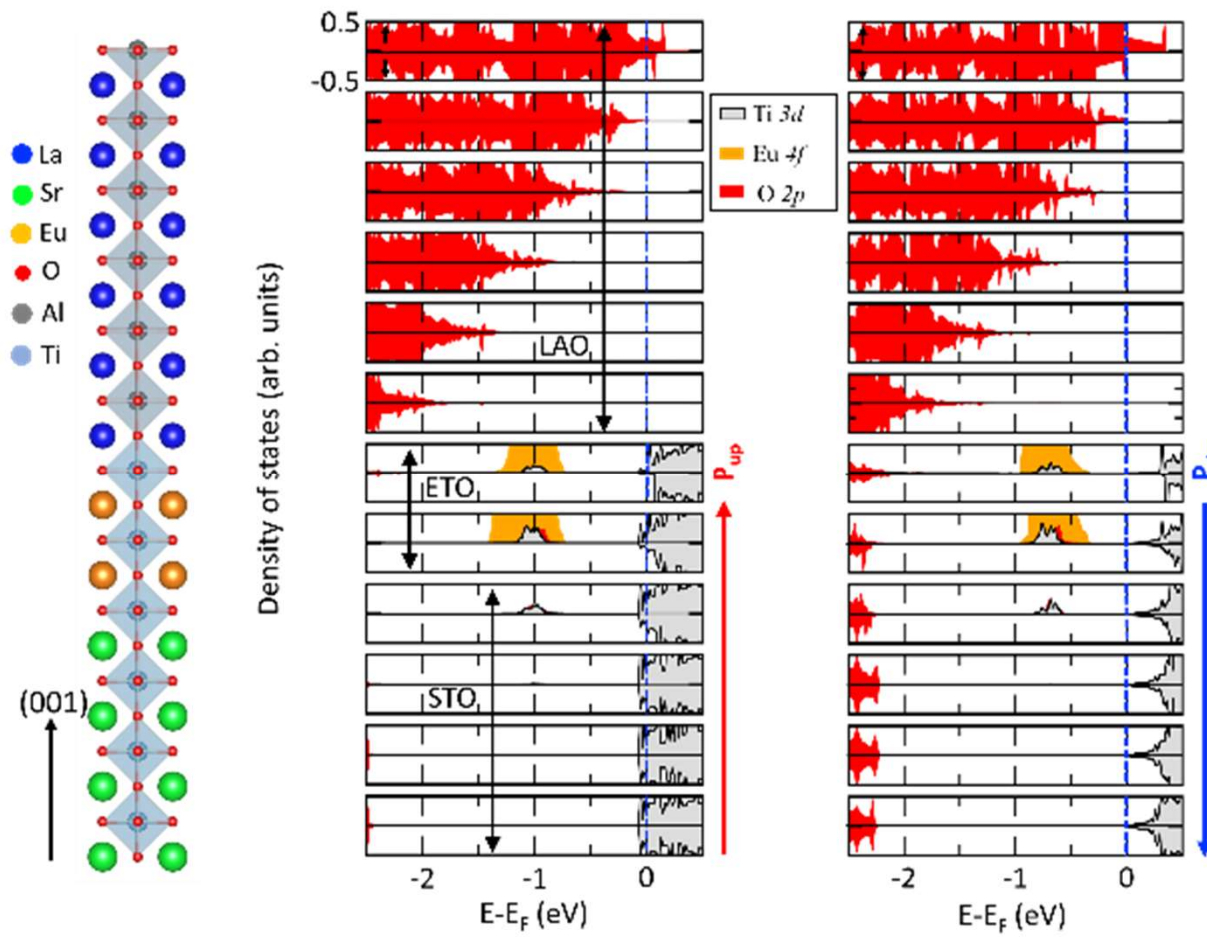
Stornaiuolo et al, Nature Mater 15, 278 (2016)



ETO: EuTiO_3 (AF isolator in bulk C.L. Chien et al, PRB 10, 3913 (1974) but becomes FM when electron-doped T. Katsufuji et al, Phys. Rev. B. 60, R15021 (1999))

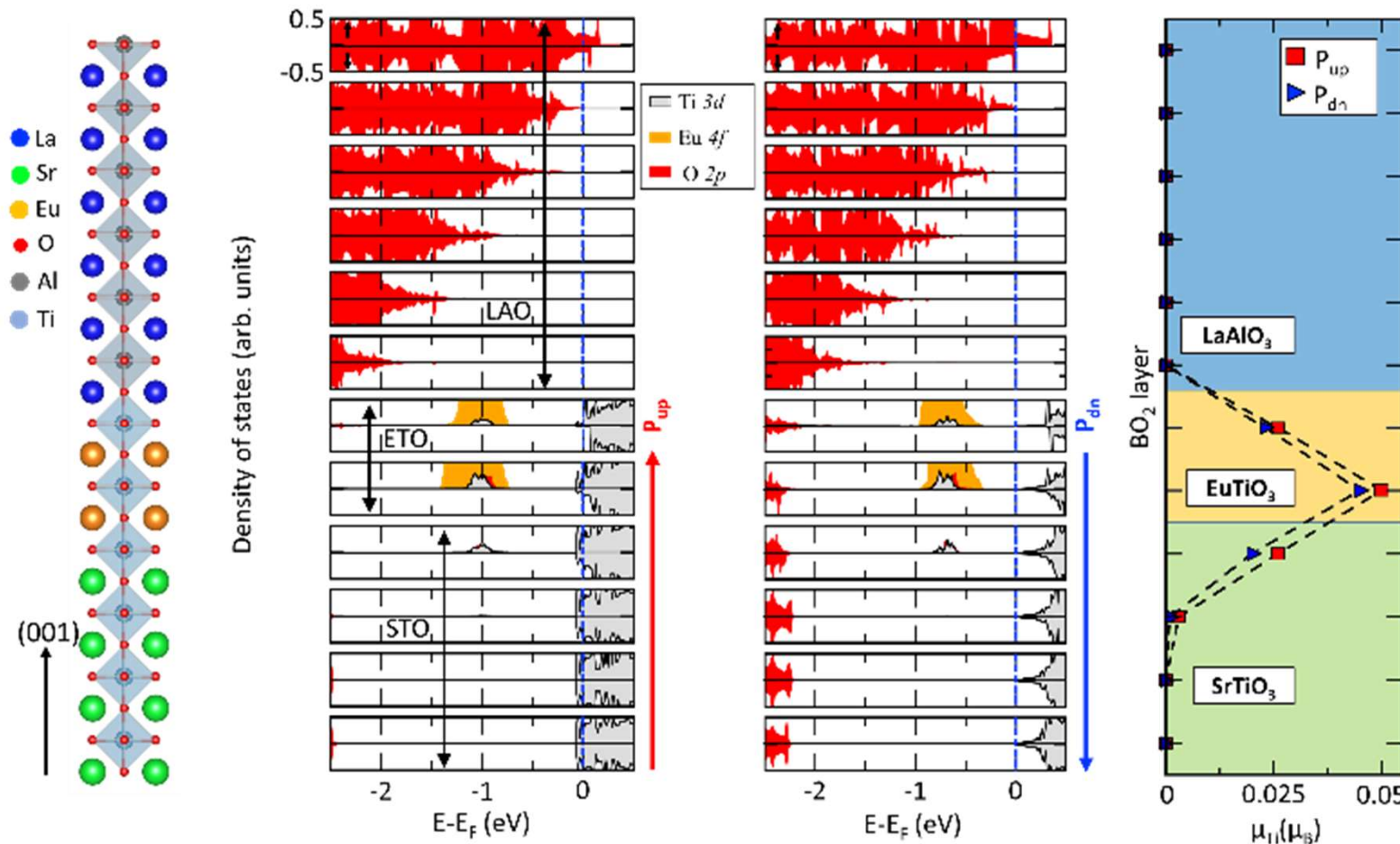
Cf previous work on LAO/ETO//STO 2DEGs by D. Stroniuolo et al, Nature Mater. 15, 278 (2016)

DFT calculations



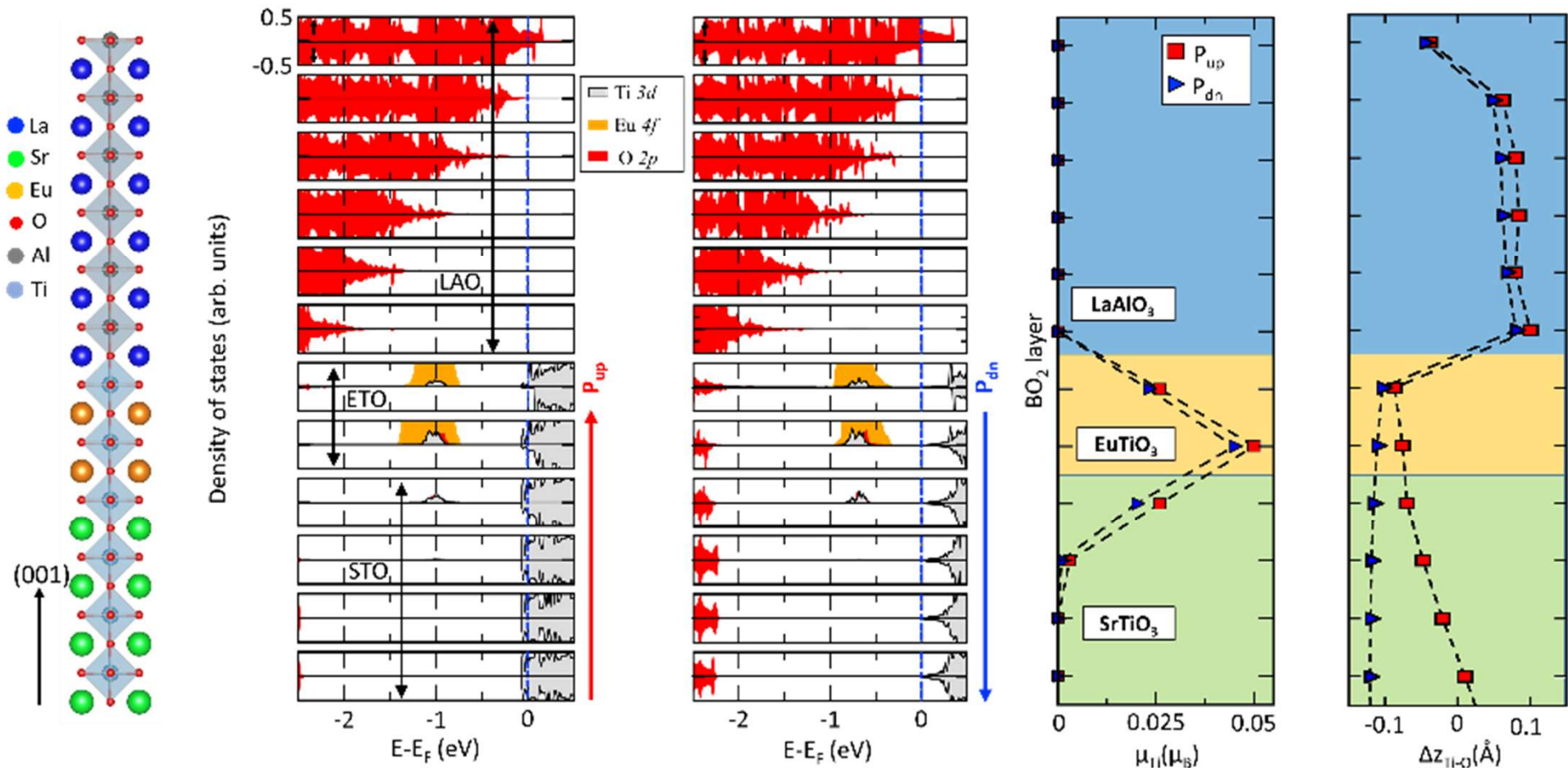
- Ferroelectricity induced by introducing 1.6% compressive strain
- 2DEG forms and DOS at E_F depends on P direction

DFT calculations



- Ferroelectricity induced by introducing 1.6% compressive strain
- 2DEG forms and DOS at E_F depends on P direction
- Magnetic moment present in 2DEG region and depends on P direction : **magnetoelectric coupling**

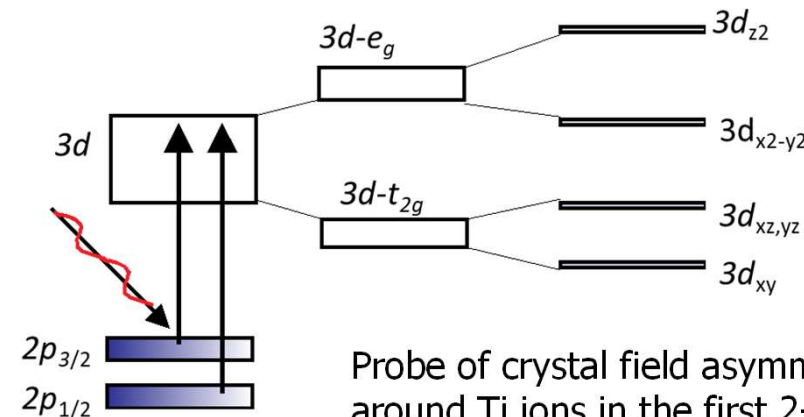
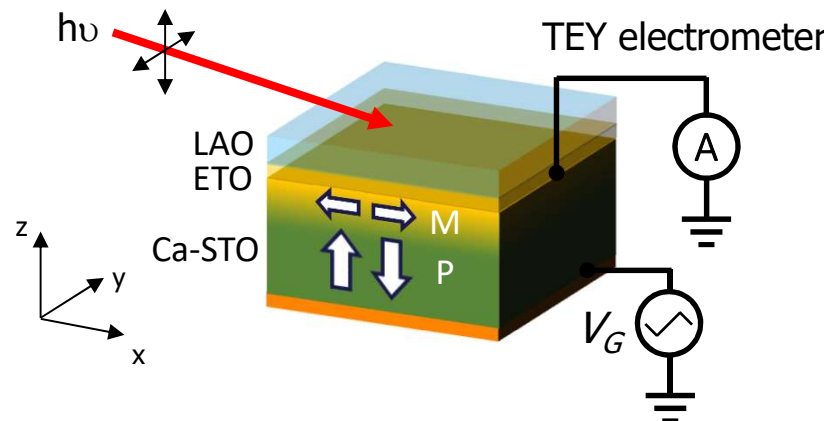
DFT calculations



- Ferroelectricity induced by introducing 1.6% compressive strain
- 2DEG forms and DOS at E_F depends on P direction
- Magnetic moment present in 2DEG region and depends on P direction : **magnetoelectric coupling**
- Polar displacements present in STO away from and in the 2DEG region : **2DEG is ferroelectric**

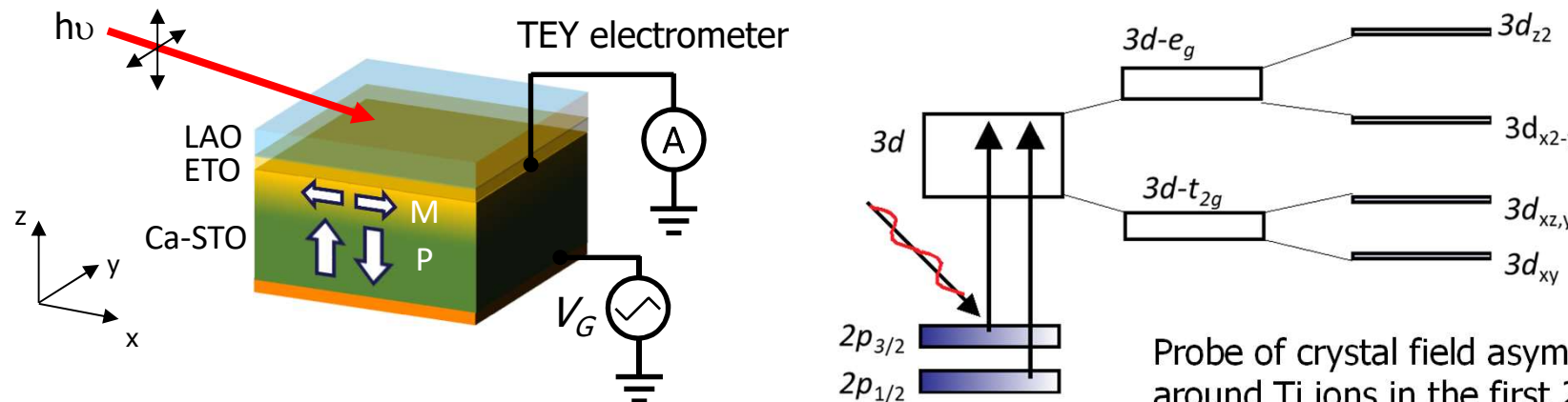
J. Bréhin, MB et al, Nature Phys. 19, 823 (2023)

X-ray linear dichroism: probing the presence of electric dipoles in the 2DEG

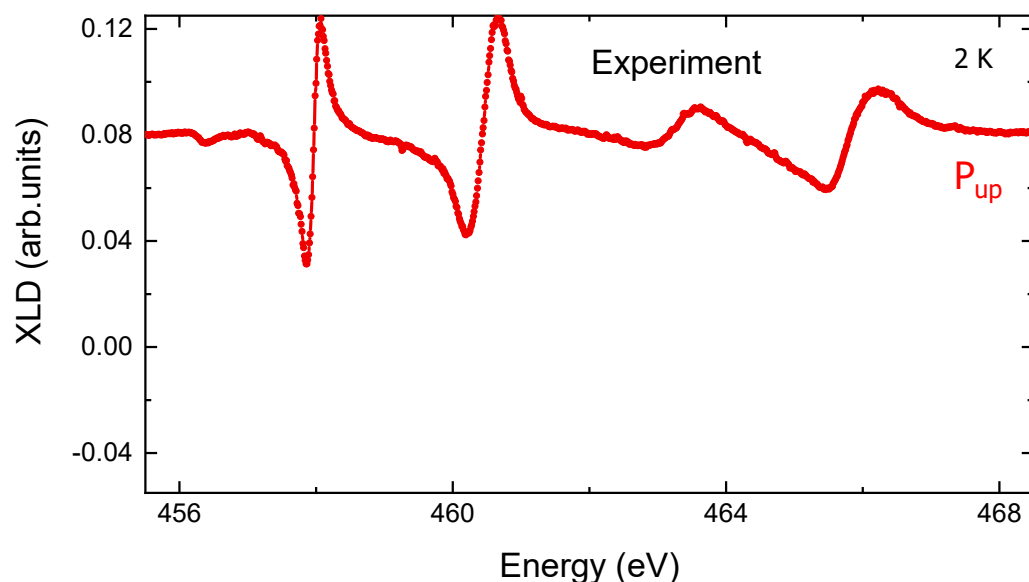


Probe of crystal field asymmetry
around Ti ions in the first 2-3 nm of the
sample (i.e. only in the 2DEG region)

X-ray linear dichroism: probing the presence of electric dipoles in the 2DEG

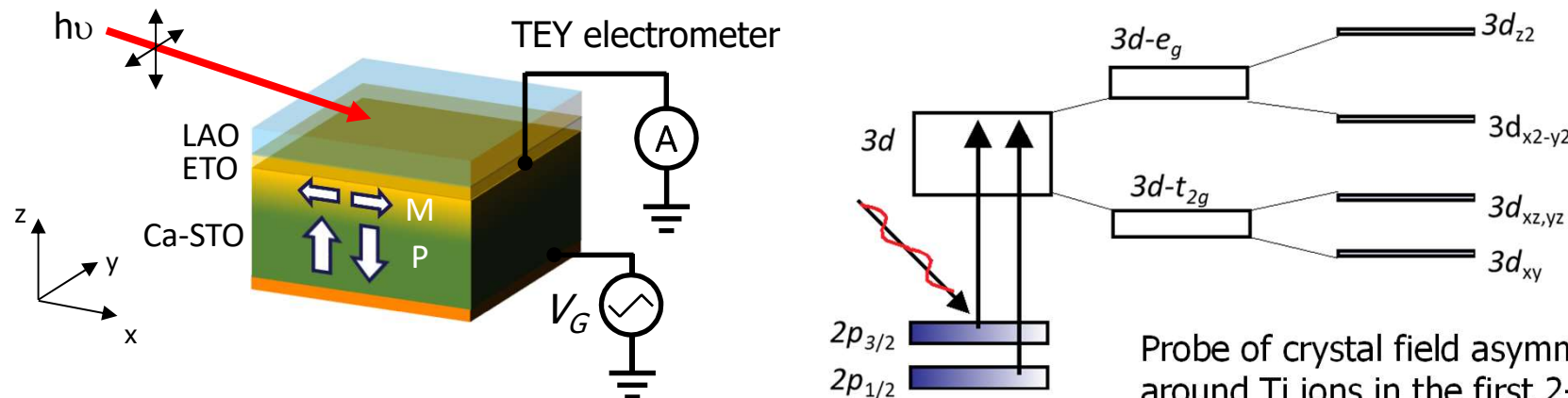


Probe of crystal field asymmetry around Ti ions in the first 2-3 nm of the sample (i.e. only in the 2DEG region)

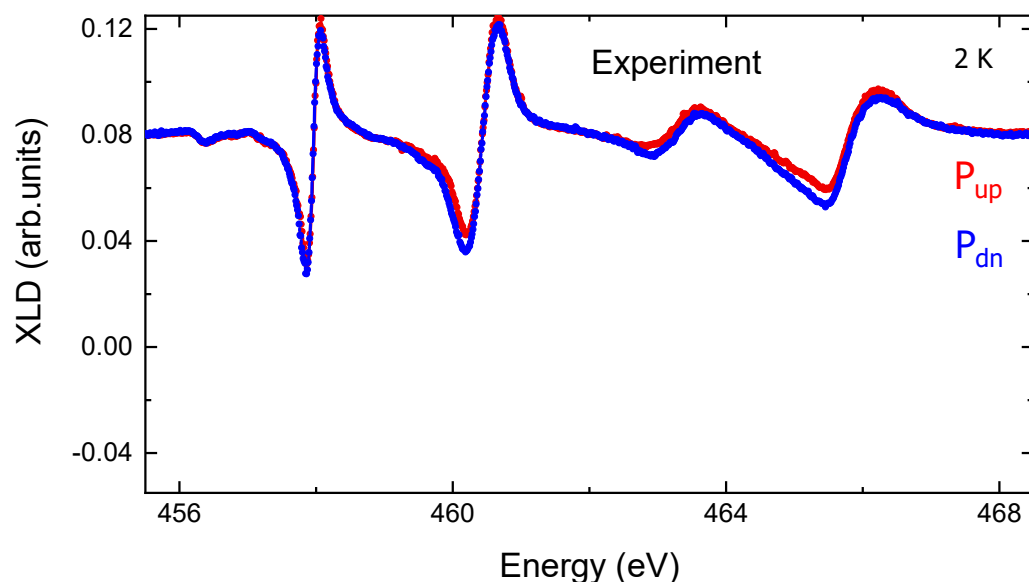


- Strong XLD expected from off-centered Ti ions with respect to oxygen ions in the 2DEG → electric dipole

X-ray linear dichroism: probing the presence of electric dipoles in the 2DEG

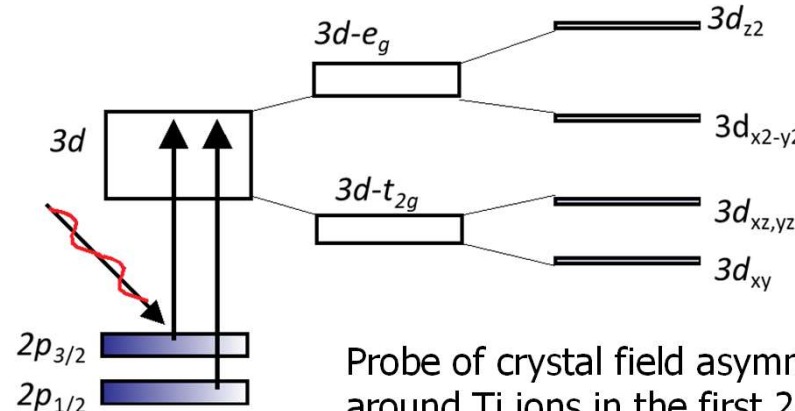
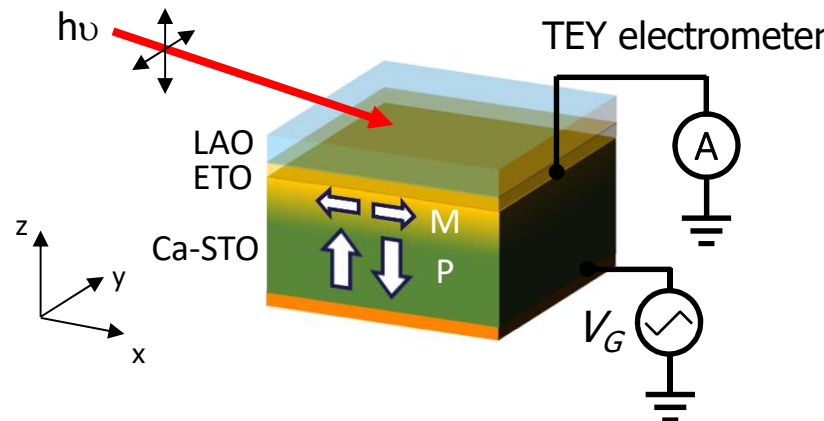


Probe of crystal field asymmetry around Ti ions in the first 2-3 nm of the sample (i.e. only in the 2DEG region)

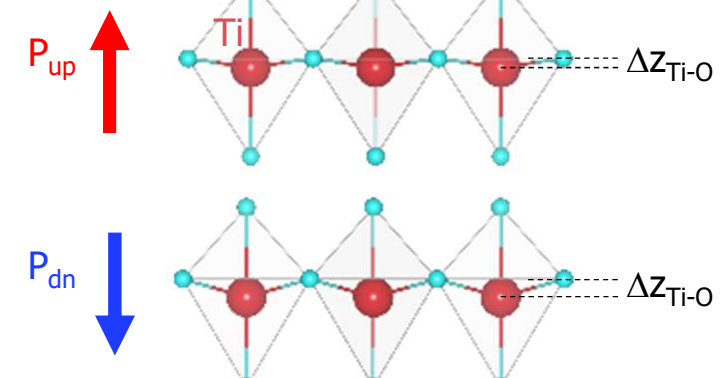
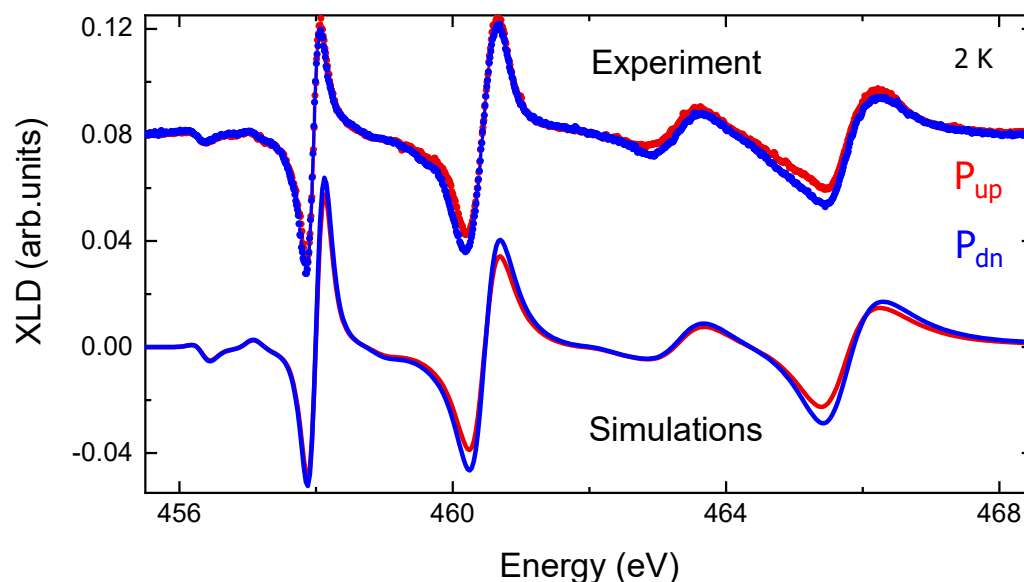


- Strong XLD expected from off-centered Ti ions with respect to oxygen ions in the 2DEG → electric dipole
- XLD depends on P direction → different electric dipole amplitude for different P state

X-ray linear dichroism: probing the presence of electric dipoles in the 2DEG

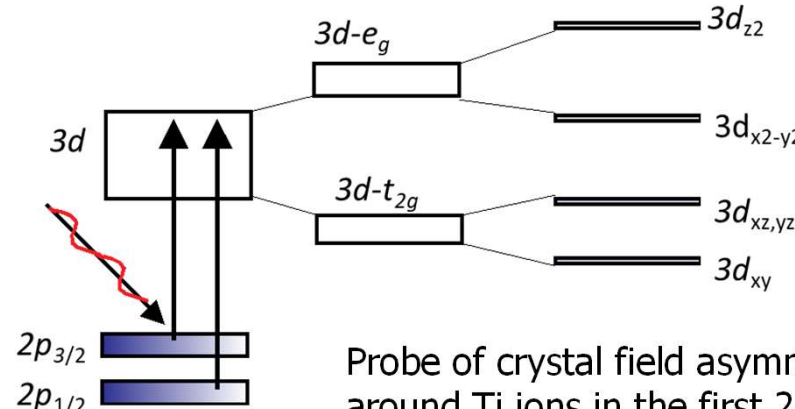
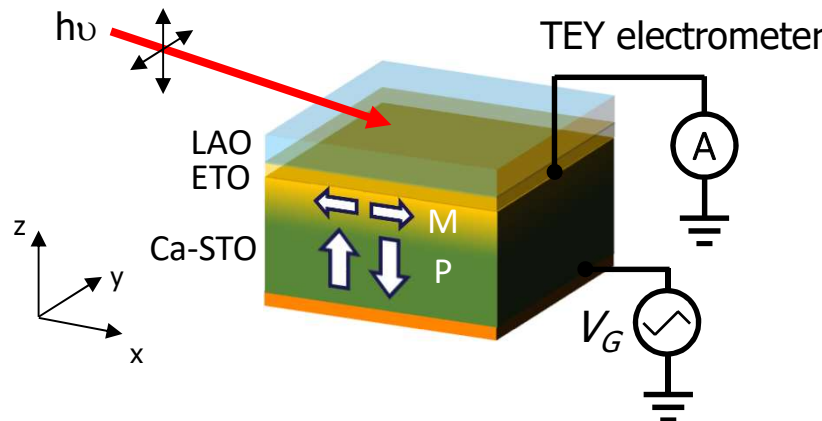


Probe of crystal field asymmetry around Ti ions in the first 2-3 nm of the sample (i.e. only in the 2DEG region)

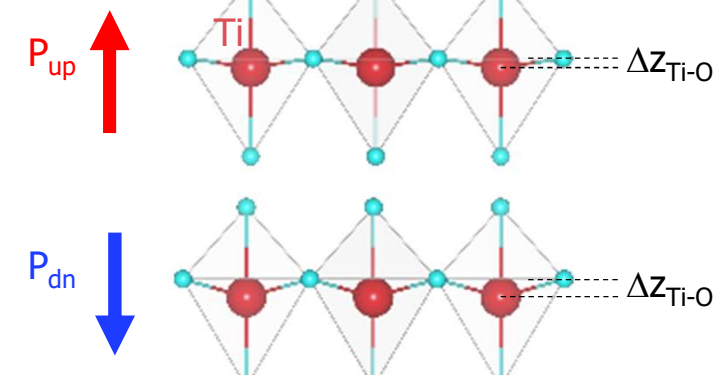
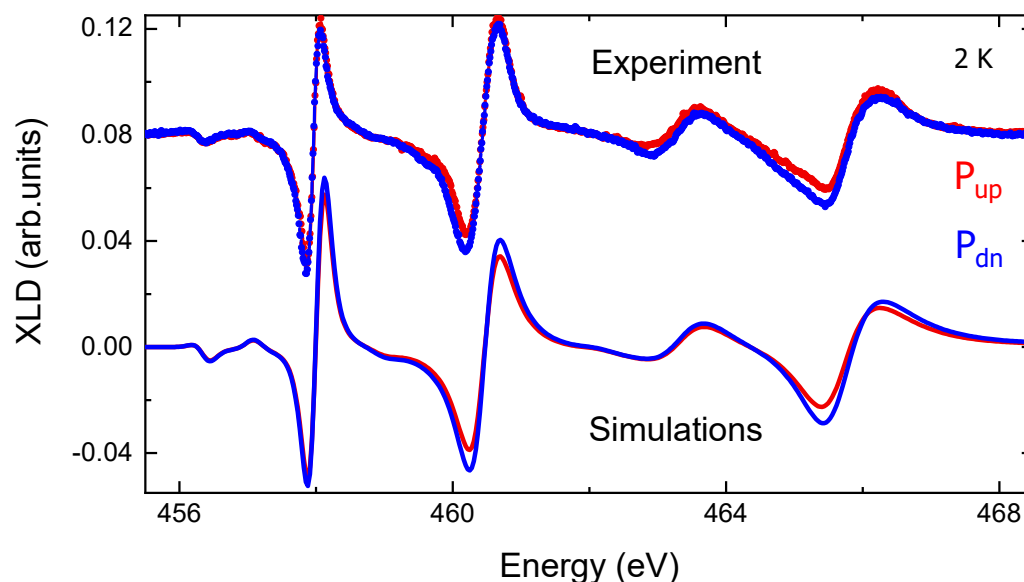


- Strong XLD expected from off-centered Ti ions with respect to oxygen ions in the 2DEG → electric dipole
- XLD depends on P direction → different electric dipole amplitude for different P state
- Multiplet simulations reproducing data indicate larger electric dipole in P_{dn} than P_{up} , consistent with DFT

X-ray linear dichroism: probing the presence of electric dipoles in the 2DEG



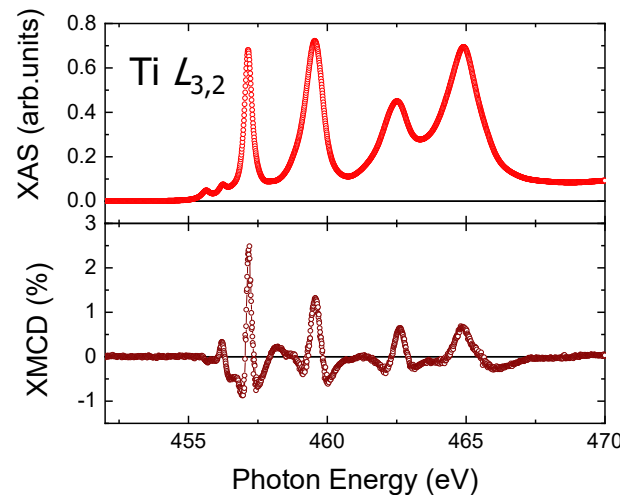
Probe of crystal field asymmetry around Ti ions in the first 2-3 nm of the sample (i.e. only in the 2DEG region)



- Strong XLD expected from off-centered Ti ions with respect to oxygen ions in the 2DEG → electric dipole
- XLD depends on P direction → different electric dipole amplitude for different P state
- Multiplet simulations reproducing data indicate larger electric dipole in P_{dn} than P_{up} , consistent with DFT
- Switchable dipoles in the 2DEG region → **the 2DEG is ferroelectric**

X-ray magnetic circular dichroism: probing magnetism in the 2DEG

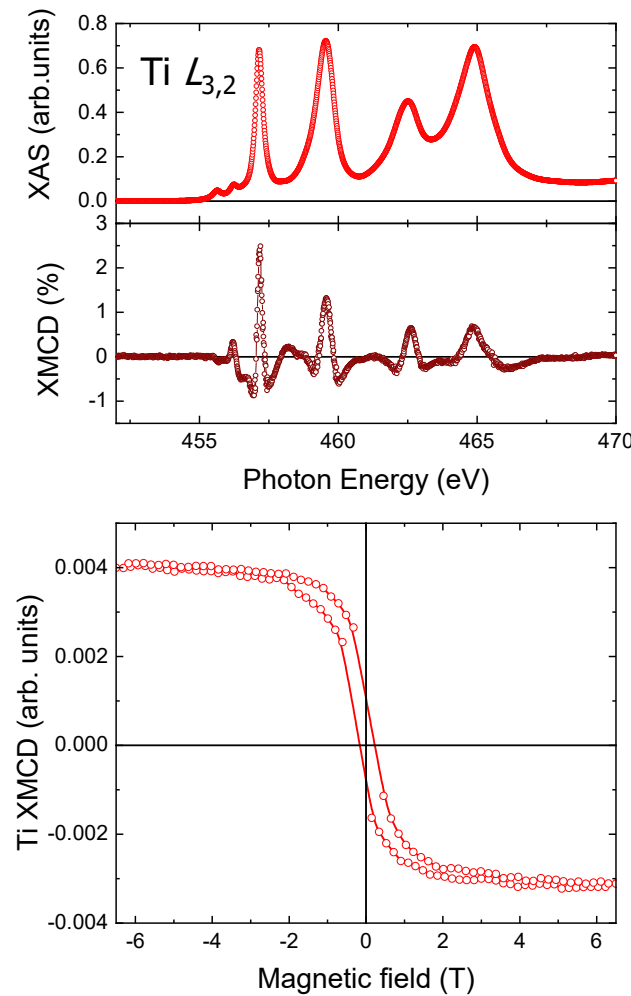
TEY mode
B in plane
T=2 K



- XAS at Ti $L_{3,2}$ edge typical of Ti^{4+} with a small fraction of Ti^{3+} (few %), expected for STO 2DEGs.
- Clear XMCD (2%) observed at Ti $L_{3,2}$ edge → magnetic moments in the 2DEG

X-ray magnetic circular dichroism: probing magnetism in the 2DEG

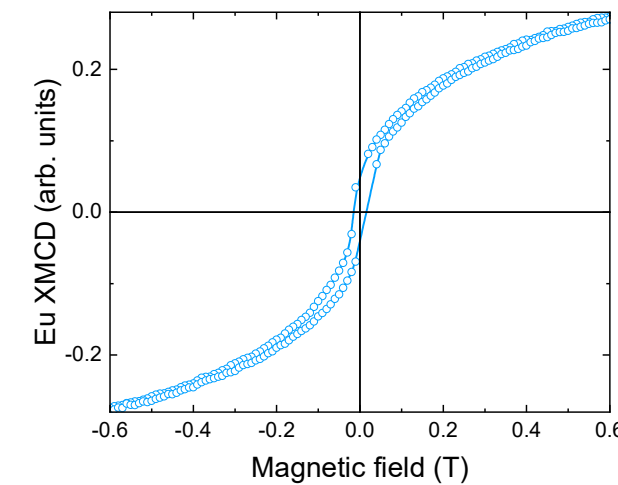
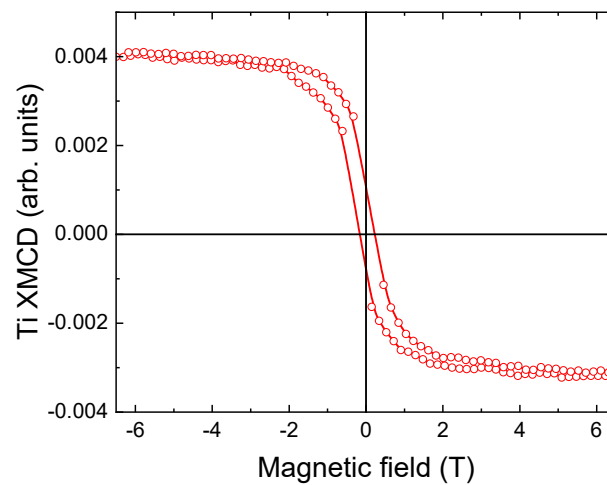
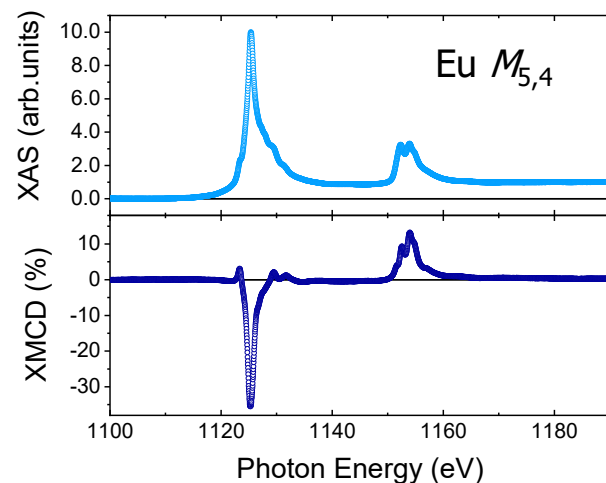
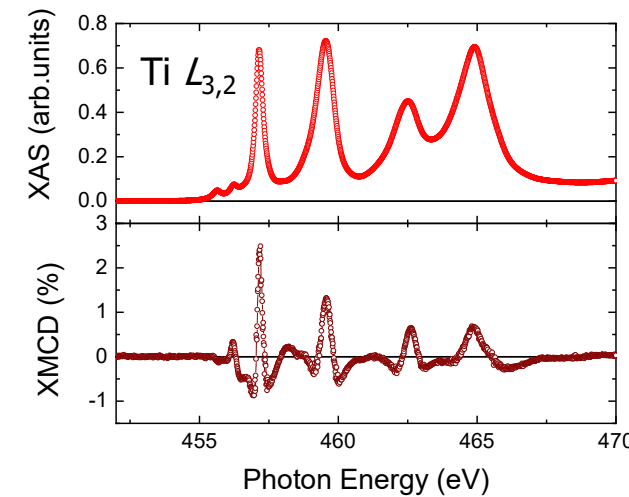
TEY mode
B in plane
T=2 K



- XAS at $\text{Ti } L_{3,2}$ edge typical of Ti^{4+} with a small fraction of Ti^{3+} (few %), expected for STO 2DEGs.
- Clear XMCD (2%) observed at $\text{Ti } L_{3,2}$ edge → magnetic moments in the 2DEG
- Hysteresis with in plane B → ferromagnetic order with in-plane easy axis

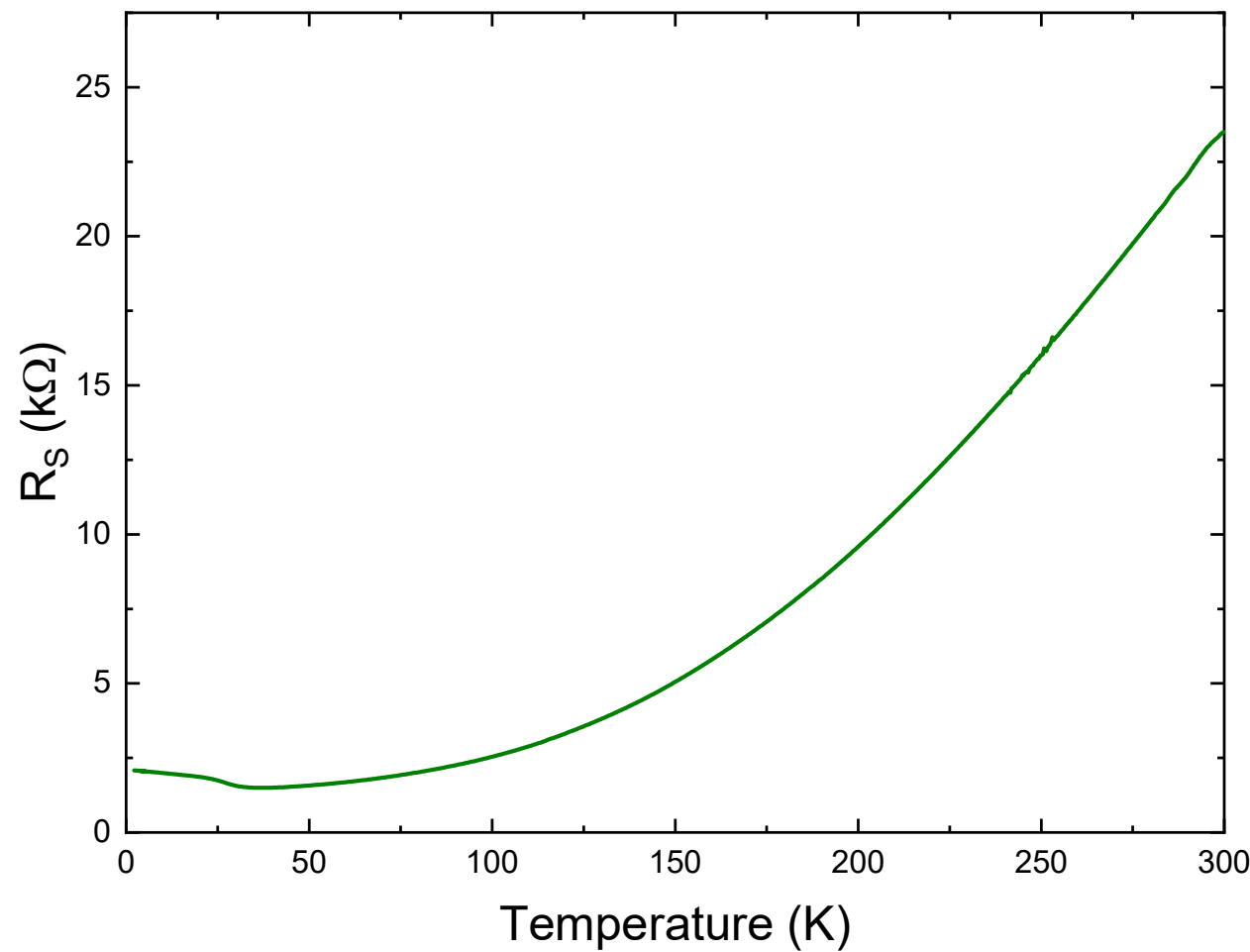
X-ray magnetic circular dichroism: probing magnetism in the 2DEG

TEY mode
B in plane
T=2 K



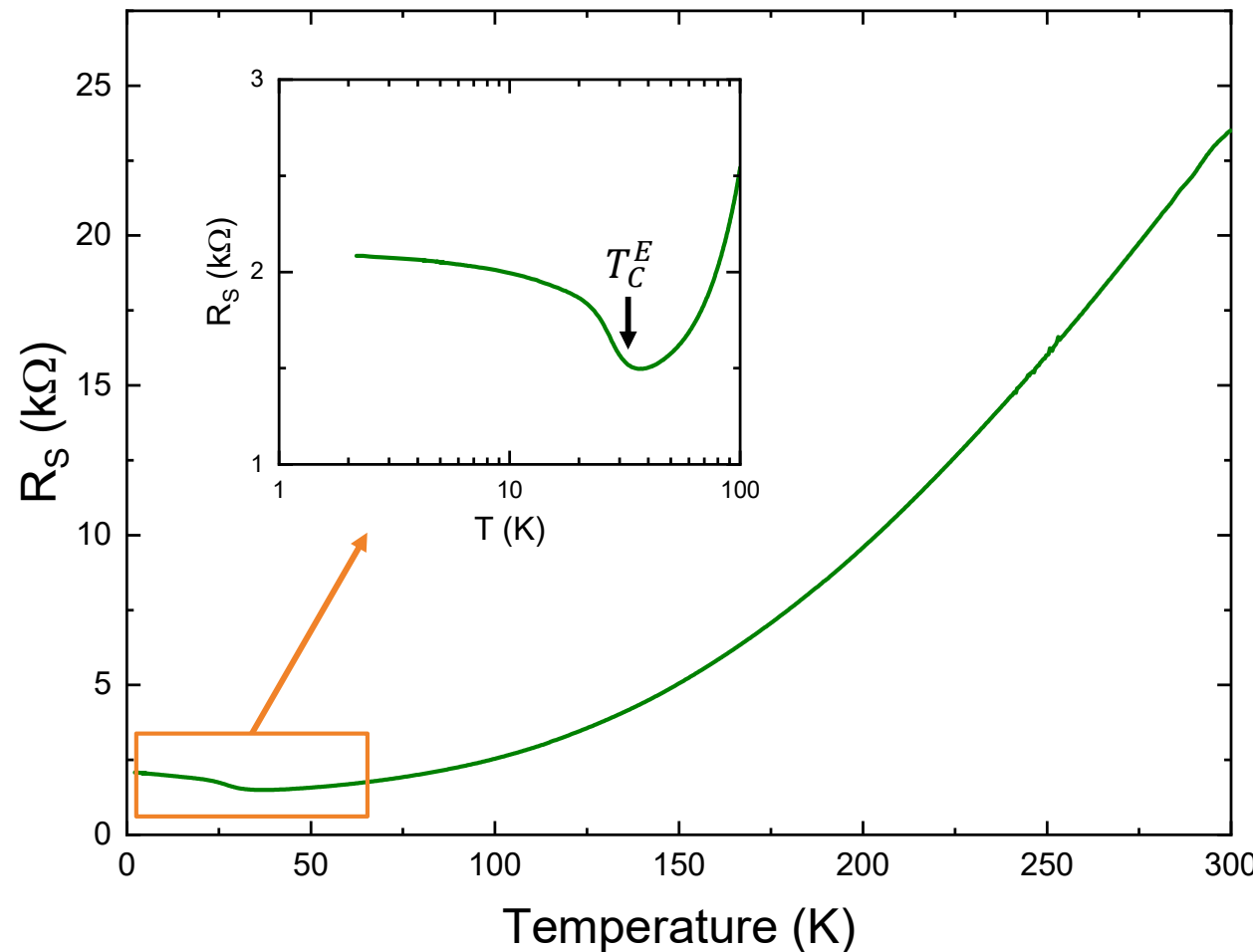
- XAS at $\text{Ti } L_{3,2}$ edge typical of Ti^{4+} with a small fraction of Ti^{3+} (few %), expected for STO 2DEGs.
- Clear XMCD (2%) observed at $\text{Ti } L_{3,2}$ edge → magnetic moments in the 2DEG
- Hysteresis with in plane B → ferromagnetic order with in-plane easy axis
- XMCD also observed at $\text{Eu } M_{5,4}$ edge
- **the 2DEG is magnetic**

Coupling between conductivity and ferroelectricity



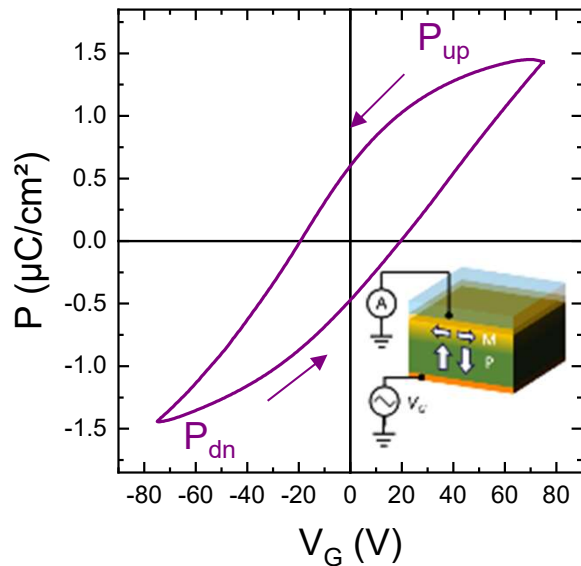
- ➊ R vs T evidences **metallic behaviour** typical of STO 2DEGs

Coupling between conductivity and ferroelectricity



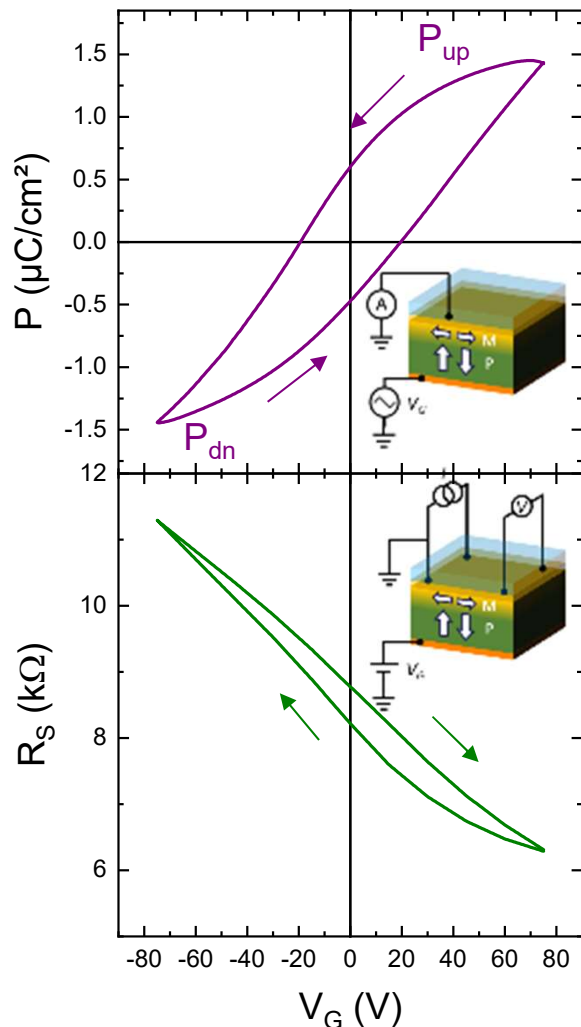
- R vs T evidences **metallic behaviour** typical of STO 2DEGs
- Kink at low temperature at ~ 30 K signalling transition to ferroelectric state
(also seen in Al/Ca-STO 2DEGs and in e-doped Ca-STO bulk)

Coupling between conductivity and ferroelectricity



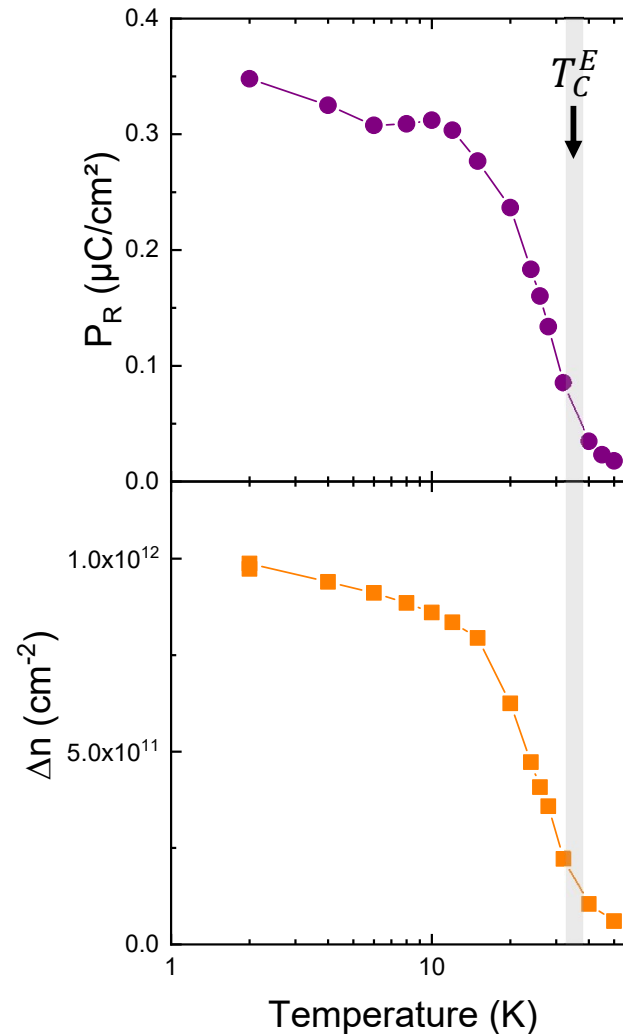
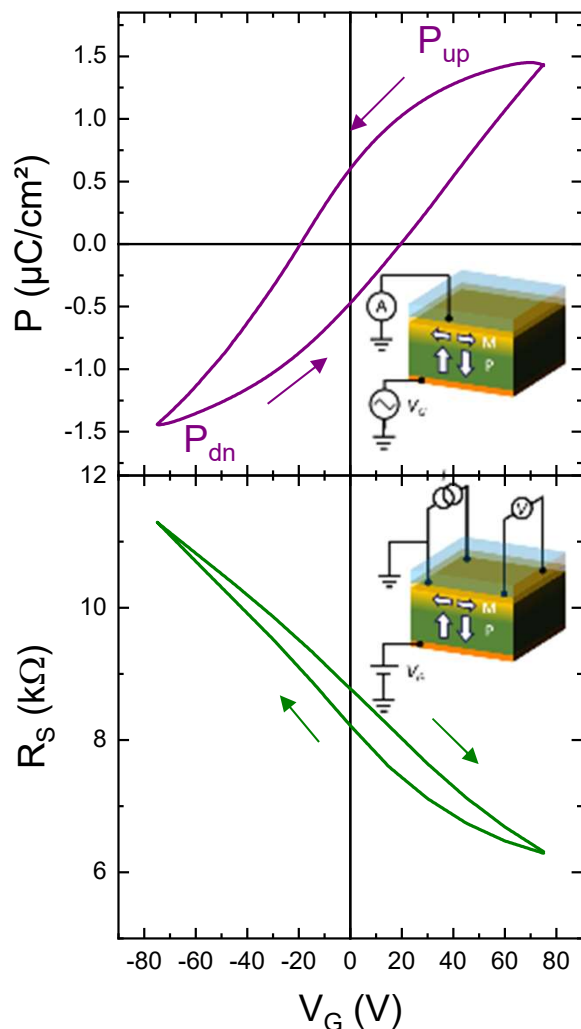
- P vs V_G loops evidence **ferroelectric behaviour**

Coupling between conductivity and ferroelectricity



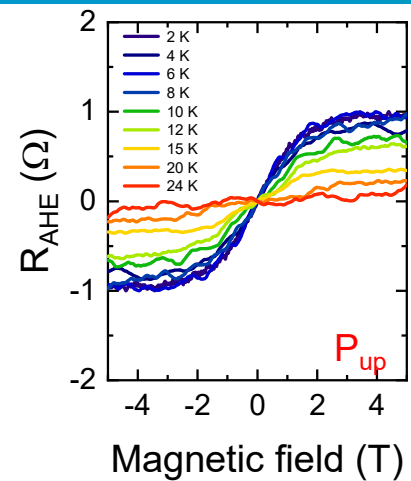
- P vs V_G loops evidence **ferroelectric behaviour**
- R_S vs V_G show reproducible hysteresis loops, absent in LAO/STO → **coupling between transport and FE**

Coupling between conductivity and ferroelectricity



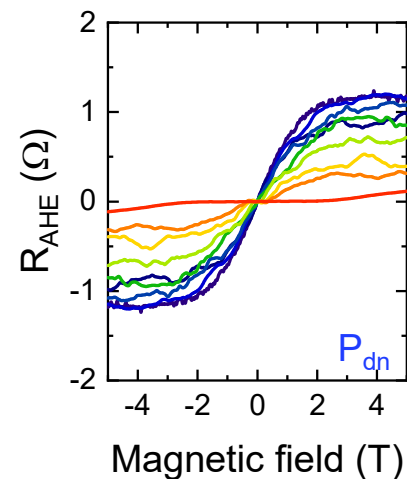
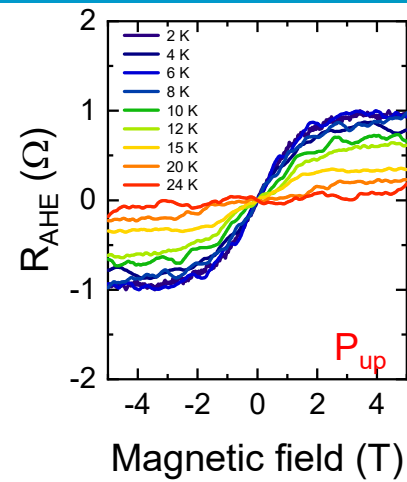
- P vs V_G loops evidence **ferroelectric behaviour**
- R_s vs V_G show reproducible hysteresis loops, absent in LAO/STO → **coupling between transport and FE**
- Ferroelectric T_C is ~ 30 K, as expected
- Carrier density at electrical remanence is modulated up to T_C^E

Coupling between conductivity, magnetism and ferroelectricity



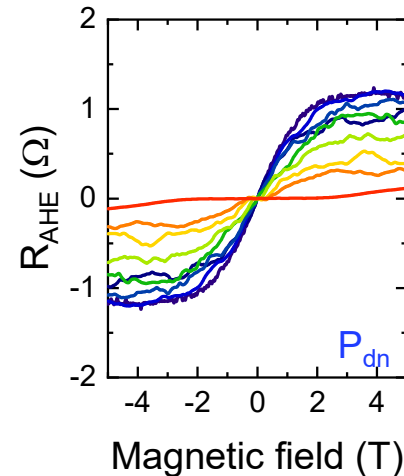
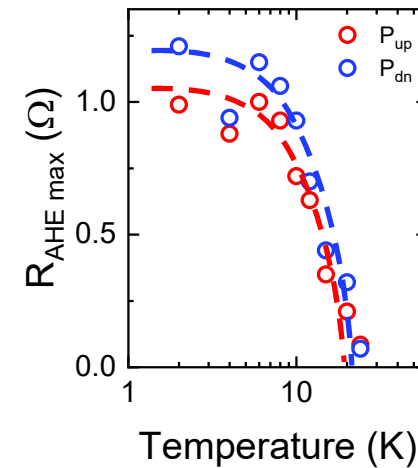
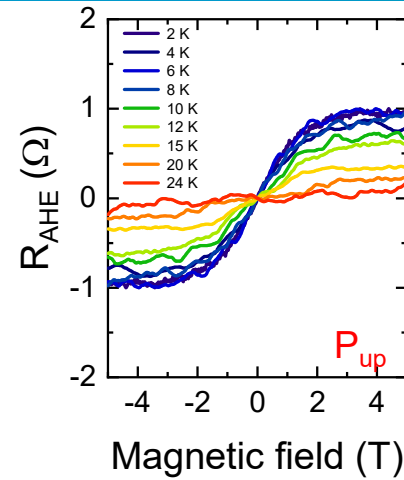
- Anomalous Hall effect is observed at low T

Coupling between conductivity, magnetism and ferroelectricity



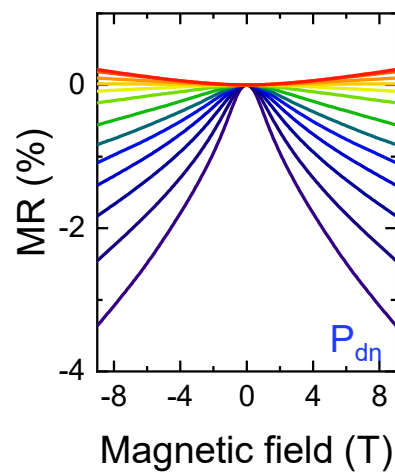
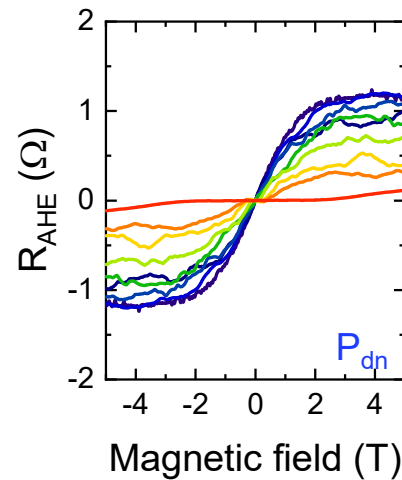
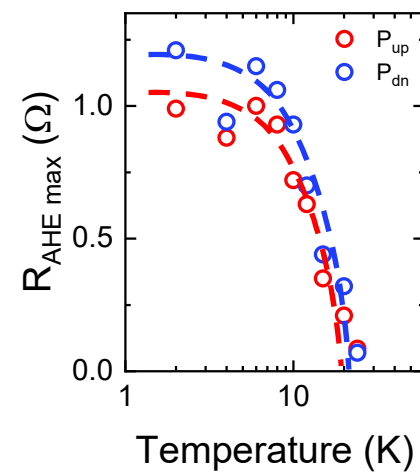
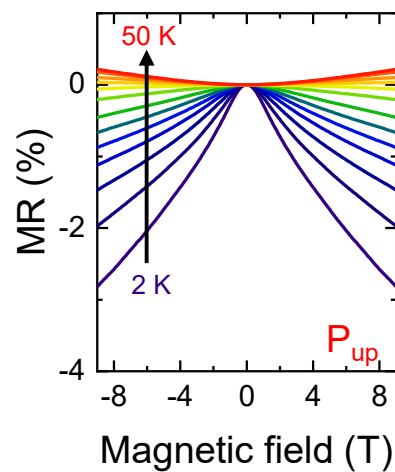
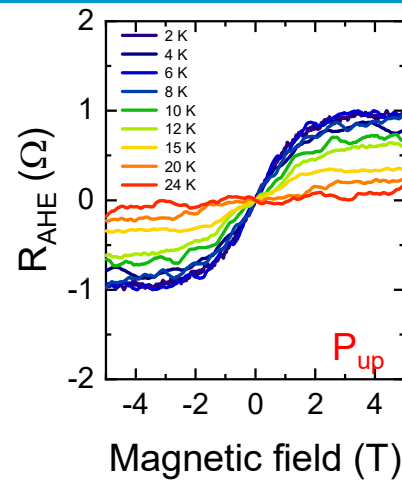
- Ⓐ Anomalous Hall effect is observed at low T
- Ⓐ AHE amplitude depends on remanent polarization state (~20% change) → **magnetoelectric coupling**

Coupling between conductivity, magnetism and ferroelectricity



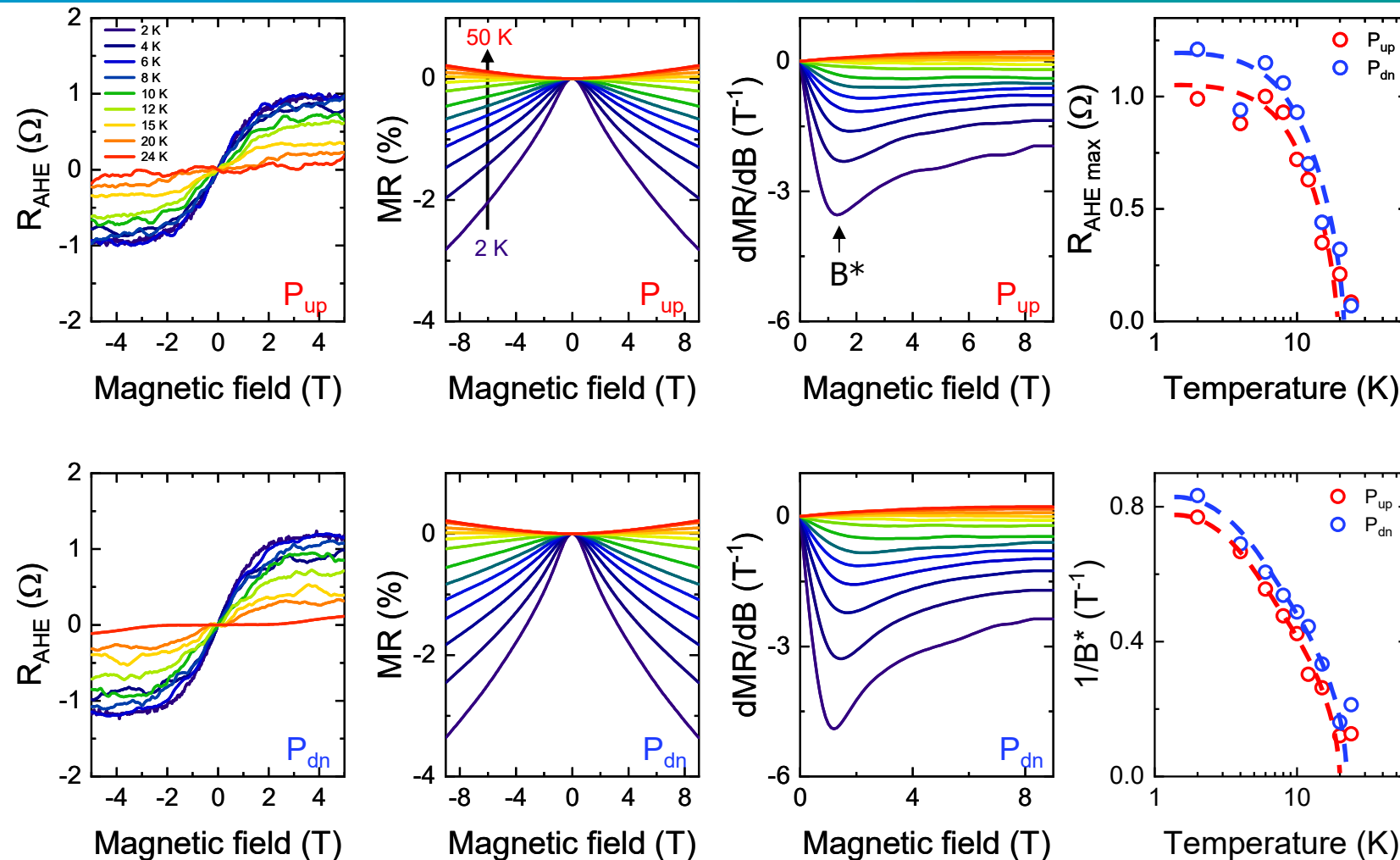
- Ⓐ Anomalous Hall effect is observed at low T
- Ⓐ AHE amplitude depends on remanent polarization state (~20% change) → **magnetoelectric coupling**
- Ⓐ Temperature dependence suggests magnetic $T_C \sim 20\text{K}$

Coupling between conductivity, magnetism and ferroelectricity



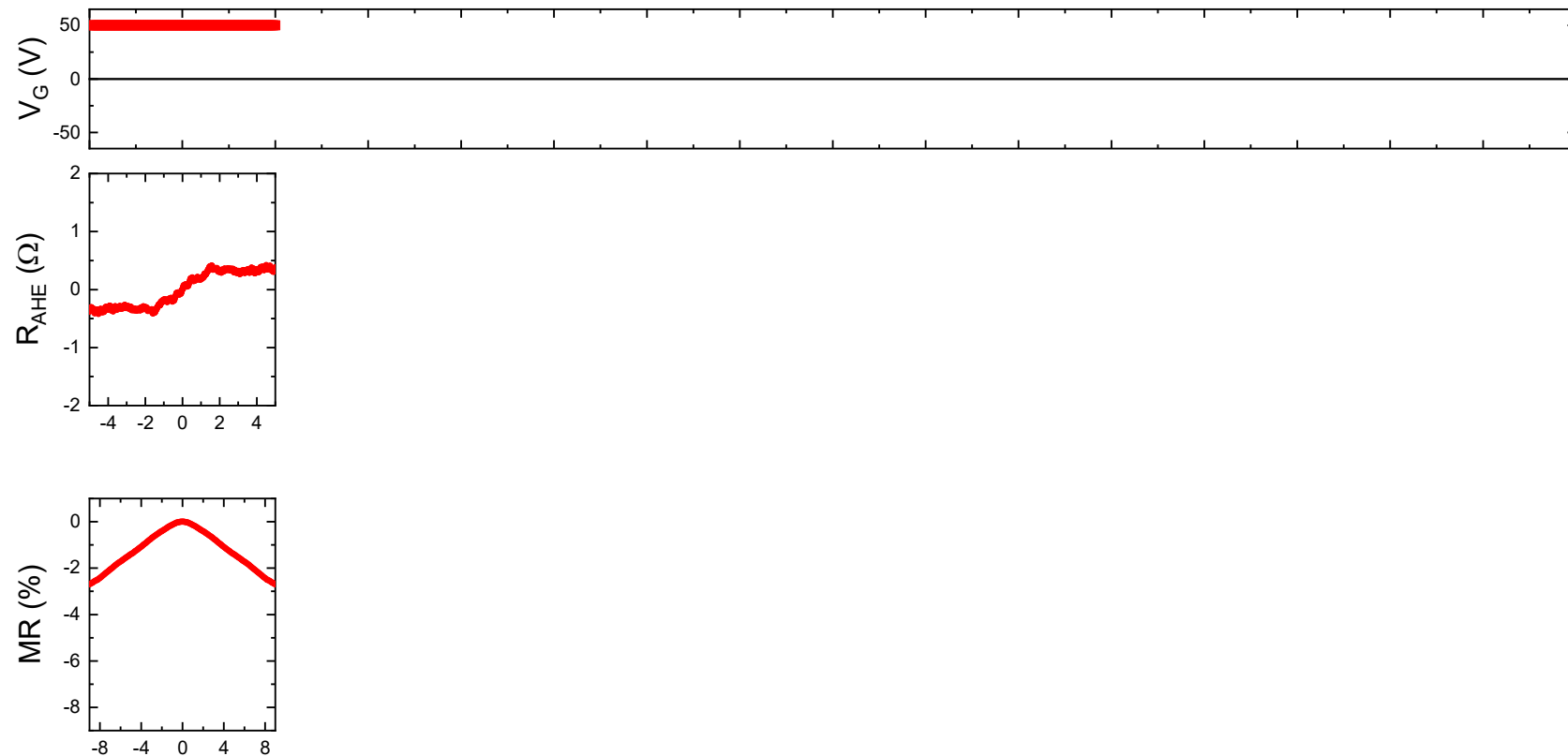
- ➊ Anomalous Hall effect is observed at low T
- ➋ AHE amplitude depends on remanent polarization state (~20% change) → **magnetoelectric coupling**
- ➌ Temperature dependence suggests magnetic $T_C \sim 20\text{K}$
- ➍ MR is parabolic at high T (Lorentz MR) but negative at low T → spin disordered state

Coupling between conductivity, magnetism and ferroelectricity

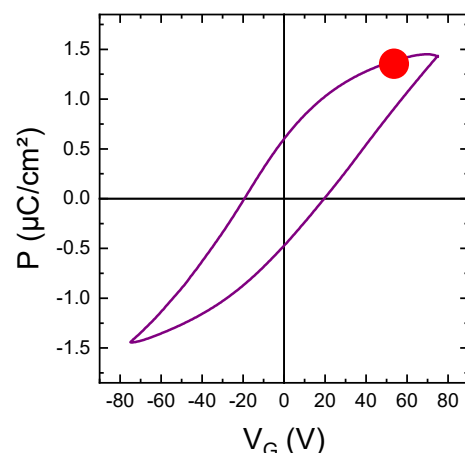


- Ⓐ Anomalous Hall effect is observed at low T
- Ⓐ AHE amplitude depends on remanent polarization state ($\sim 20\%$ change) → **magnetoelectric coupling**
- Ⓐ Temperature dependence suggests magnetic $T_C \sim 20\text{K}$
- Ⓐ MR is parabolic at high T (Lorentz MR) but negative at low T → spin disordered state
- Ⓐ Inflection point in MR derivative also suggests magnetic T_C near 20 K

Cyclability and reproducibility of the magnetoelectric coupling

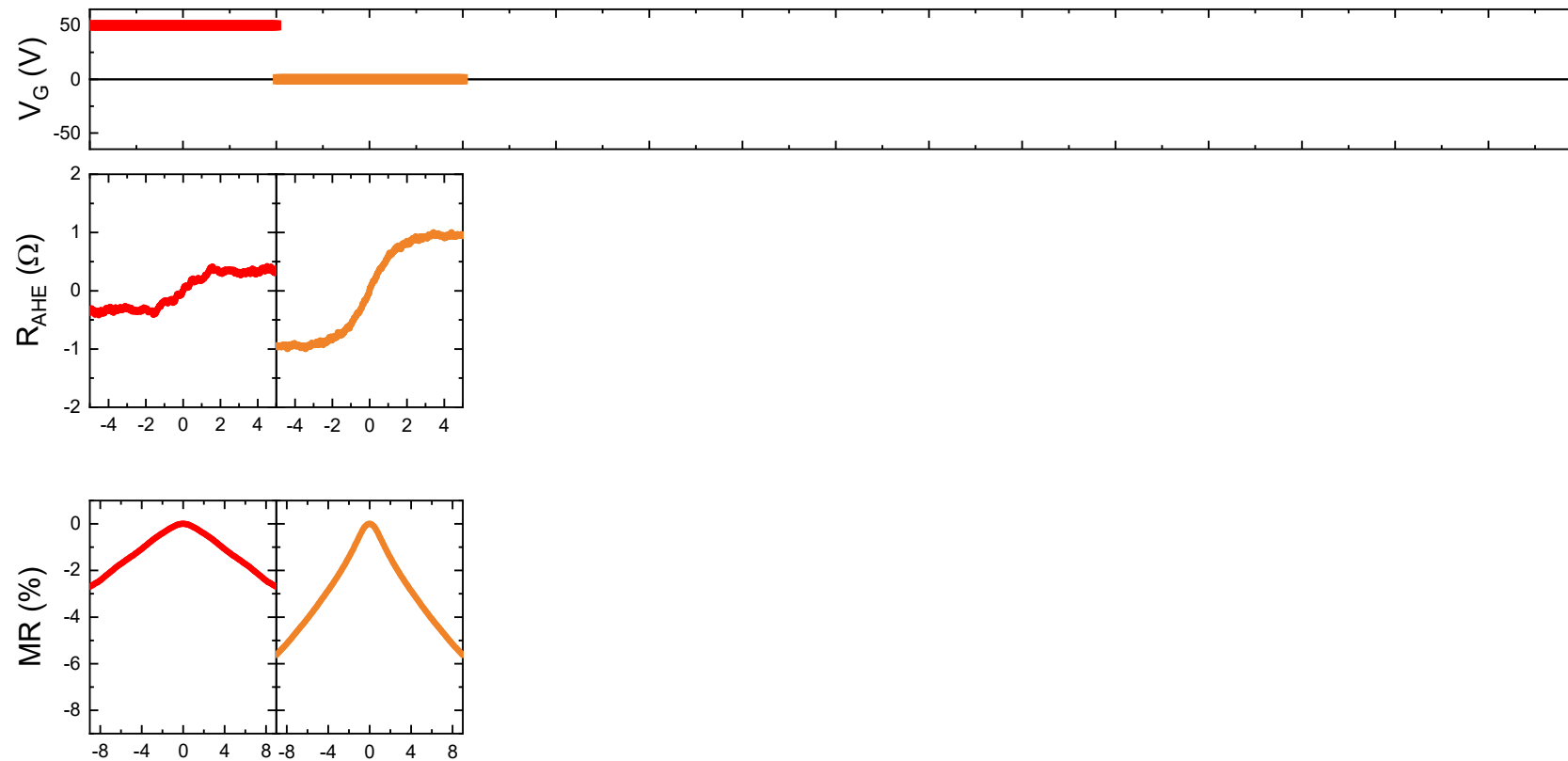


- ◎ We apply various voltages to set P in the « saturated » up

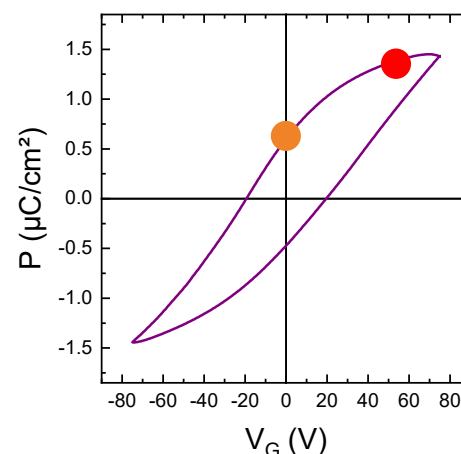


J. Bréhin, MB et al, Nature Phys. 19, 823 (2023)

Cyclability and reproducibility of the magnetoelectric coupling

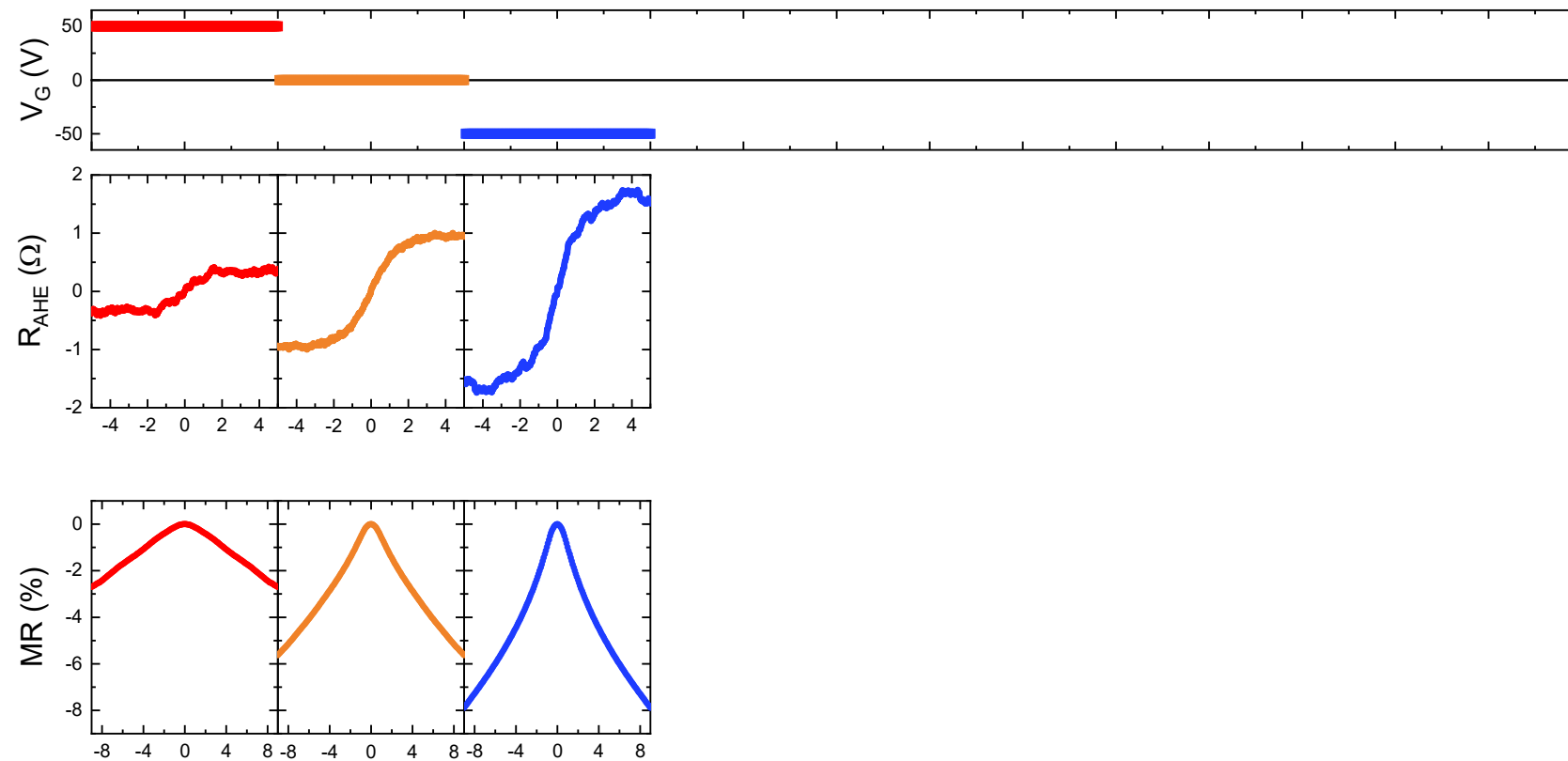


- We apply various voltages to set P in the « saturated » up, remanent up

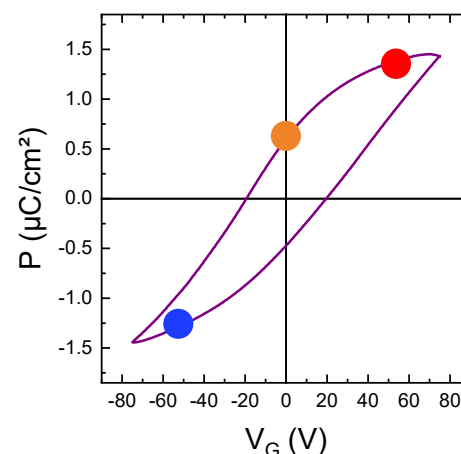


J. Bréhin, MB et al, Nature Phys. 19, 823 (2023)

Cyclability and reproducibility of the magnetoelectric coupling

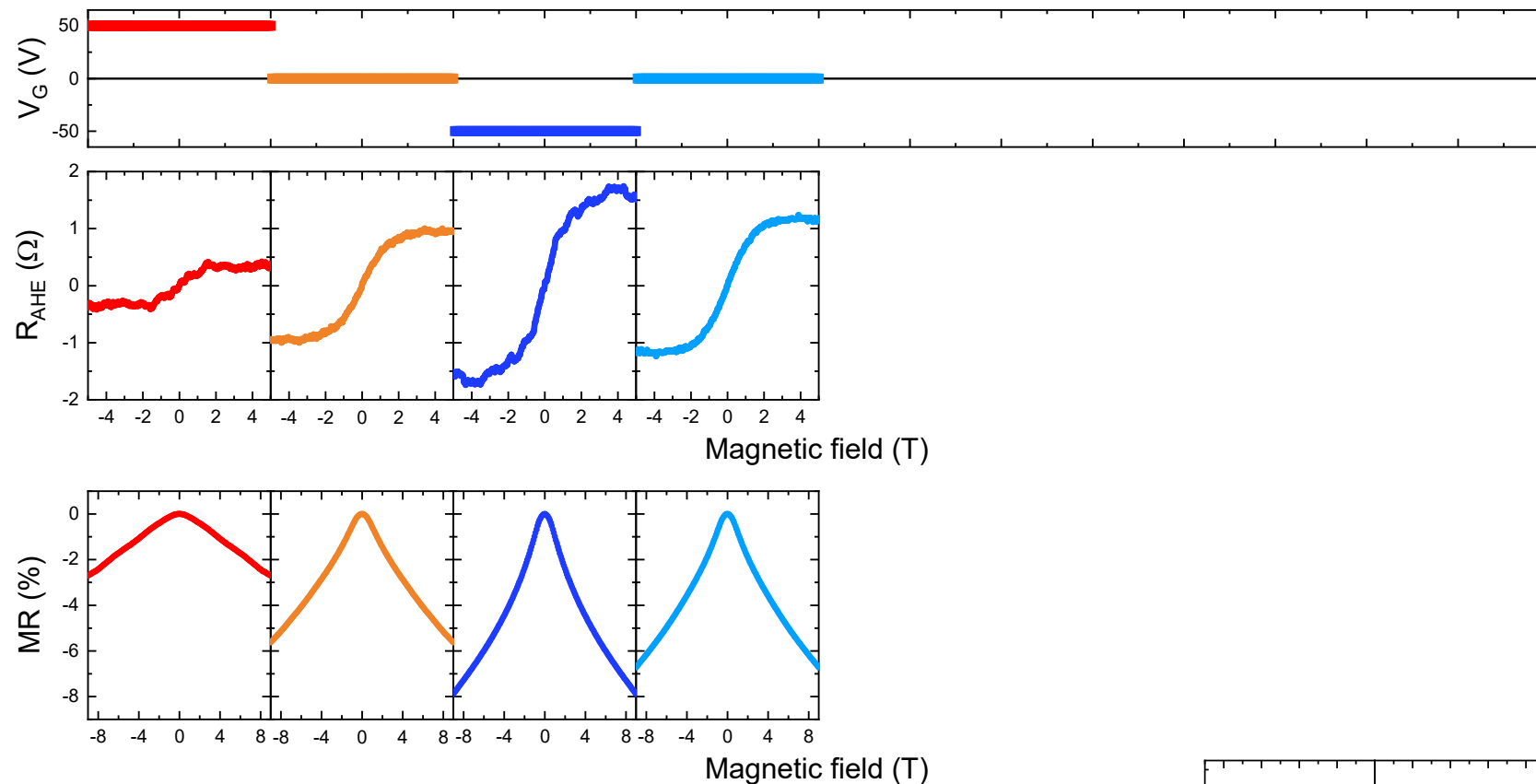


- We apply various voltages to set P in the « saturated » up, remanent up, « saturated » down

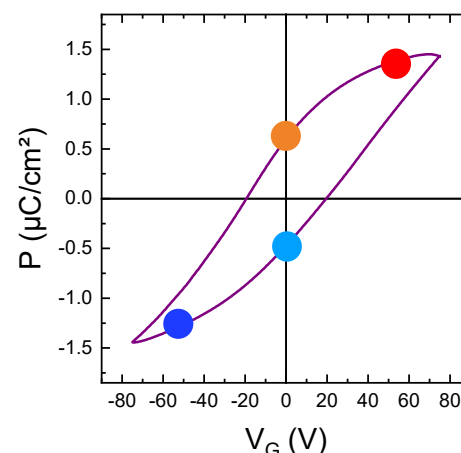


J. Bréhin, MB et al, Nature Phys. 19, 823 (2023)

Cyclability and reproducibility of the magnetoelectric coupling

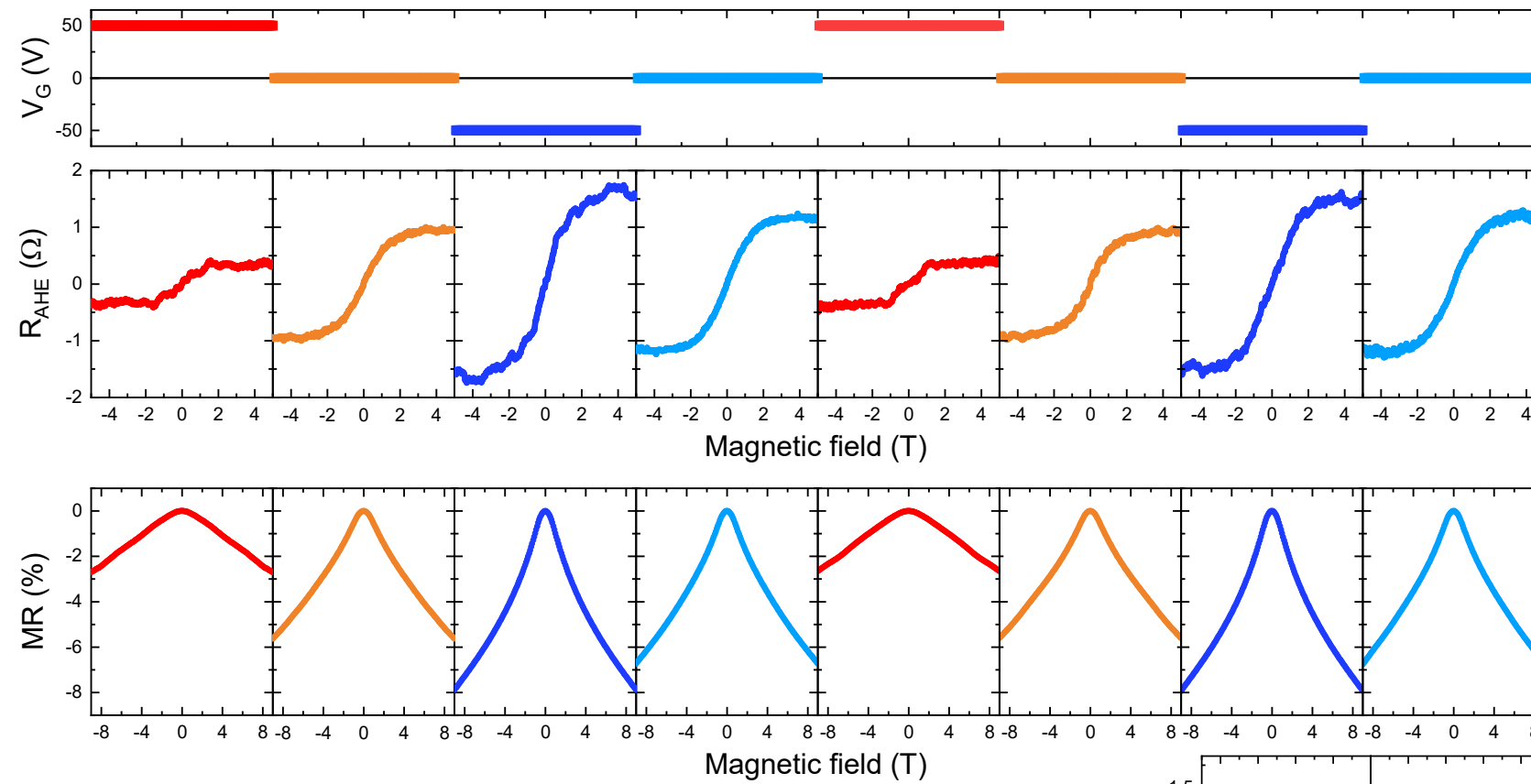


- We apply various voltages to set P in the « saturated » up, remanent up, « saturated » down and remanent down states
- Both the AHE and the MR are modulated by the polarization state at finite voltage and at remanence



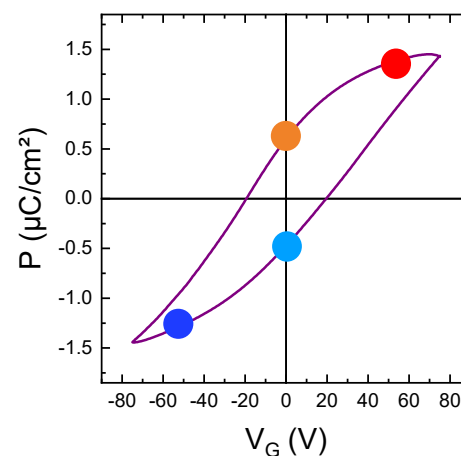
J. Bréhin, MB et al, Nature Phys. 19, 823 (2023)

Cyclability and reproducibility of the magnetoelectric coupling

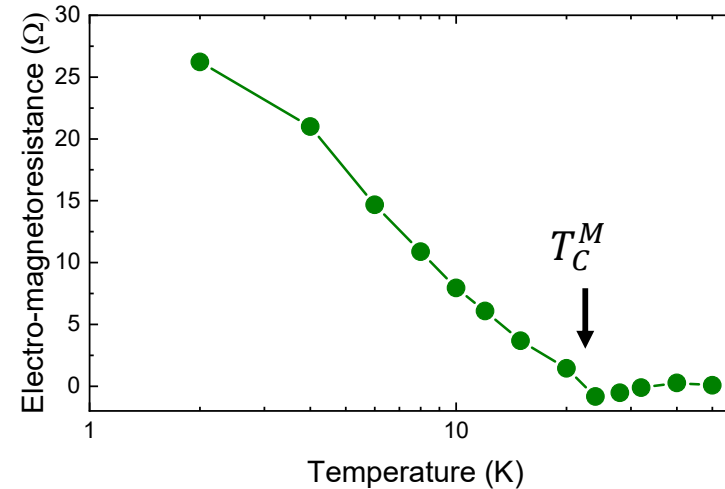
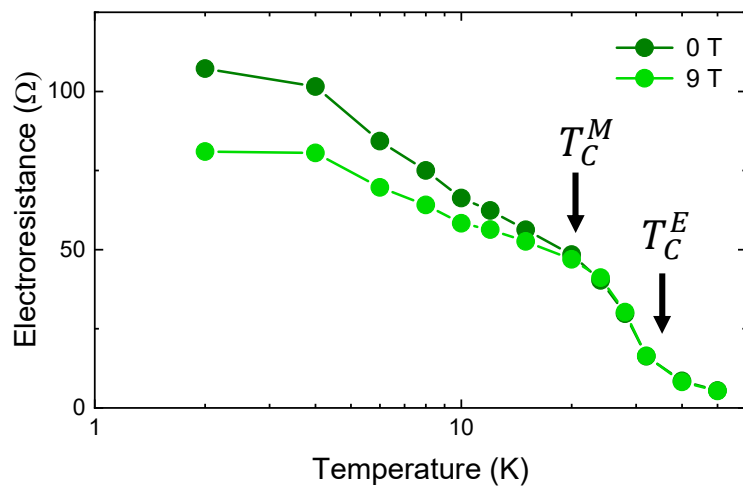


- We apply various voltages to set P in the « saturated » up, orange up, « saturated » down and remanent down states
- Both the AHE and the MR are modulated by the polarization state at finite voltage and at remanence
- The AHE and MR variations can be cycled by electric field
→ **reproducible magnetoelectric coupling**

J. Bréhin, MB et al, Nature Phys. 19, 823 (2023)



Temperature dependence



- Electroresistance depends on temperature and magnetic field
- Electroresistance vanishes at T_C^E as expected
- Difference in electroresistance with and without magnetic field defines an **electromagnetoresistance effect**
- Electro-magnetoresistance vanishes when the first ordering temperature is reached (here T_C^M)

J. Bréhin, MB et al, Nature Phys. 19, 823 (2023)

1. SrTiO₃-based 2DEGs

1.1 Physics of bulk SrTiO₃

1.2 LaAlO₃/SrTiO₃ 2DEGs

1.3 Other SrTiO₃ 2DEGs

1.4 Electronic structure of SrTiO₃ 2DEGs

1.5 Superconductivity in SrTiO₃ 2DEGs

1.5 Introducing ferroic orders into SrTiO₃ 2DEGs

2. KTaO₃-based 2DEGs

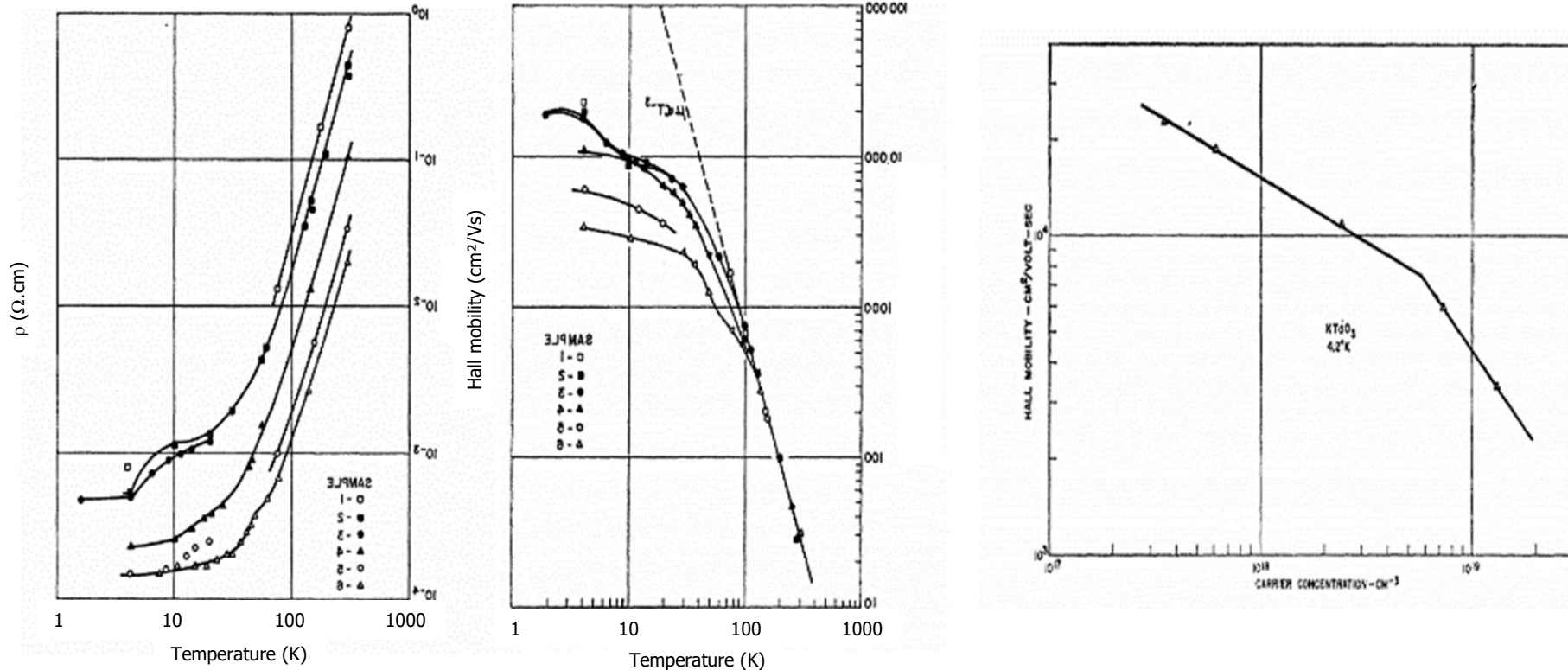
2.1 Physics of bulk KTaO₃

2.2 KTaO₃ 2DEGs

2.3 Superconductivity in KTaO₃ 2DEGs

Properties of bulk KTaO₃

Transport properties of electron doped KTaO₃



- Like STO, bulk KTO can be made metallic upon minute n-type doping
- n-type KTO can show mobilities up to 20000 cm²/Vs, higher than bulk STO
- Main difference : **Ta is heavier than Ti**
→ Spin-orbit coupling in KTO than in STO

Wemple PR 137, A1565 (1965)

1. SrTiO₃-based 2DEGs

1.1 Physics of bulk SrTiO₃

1.2 LaAlO₃/SrTiO₃ 2DEGs

1.3 Other SrTiO₃ 2DEGs

1.4 Electronic structure of SrTiO₃ 2DEGs

1.5 Superconductivity in SrTiO₃ 2DEGs

1.5 Introducing ferroic orders into SrTiO₃ 2DEGs

2. KTaO₃-based 2DEGs

2.1 Physics of bulk KTaO₃

2.2 KTaO₃ 2DEGs

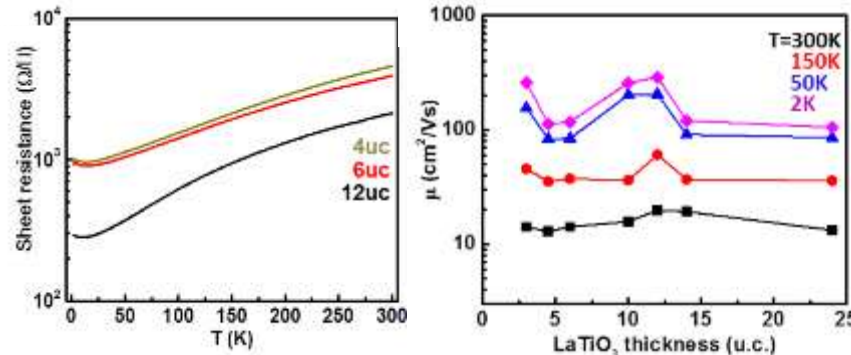
2.3 Superconductivity in KTaO₃ 2DEGs

KTaO₃ 2DEGs

APL MATERIALS 3, 036104 (2015)

LaTiO₃/KTaO₃ interfaces: A new two-dimensional electron gas system

K. Zou,¹ Sohrab Ismail-Beigi,¹ Kim Kisslinger,² Xuan Shen,^{2,3} Dong Su,² F. J. Walker,¹ and C. H. Ahn¹



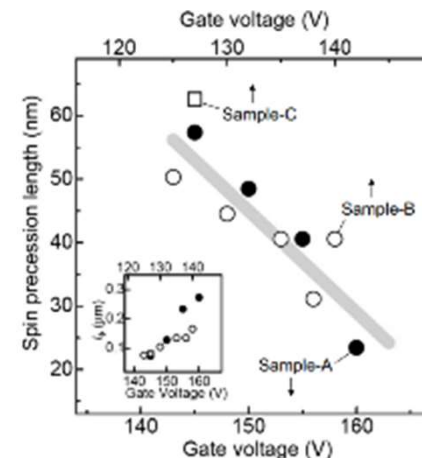
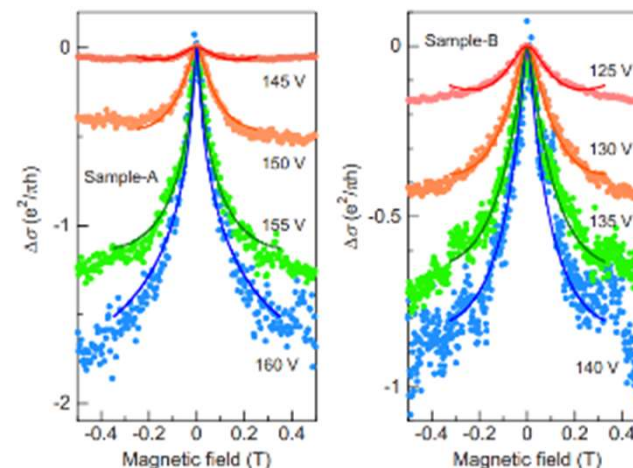
- 2DEGs can be generated in KTO by depositing various overlayers such as LaTiO₃ or LaAlO₃
- Weak antilocalization data in electrolyte-gated KTO suggests Rashba SOC higher than in STO 2DEGs

See recent review: Gupta et al, Adv. Mater. 2106481 (2022)

PHYSICAL REVIEW B 80, 121308(R) (2009)

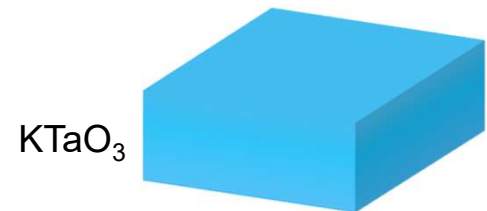
Electric field tuning of spin-orbit coupling in KTaO₃ field-effect transistors

H. Nakamura and T. Kimura
Division of Materials Physics, Graduate School of Engineering Science, Osaka University, Toyonaka, Osaka 560-8531, Japan

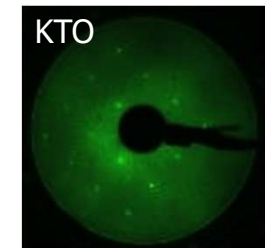
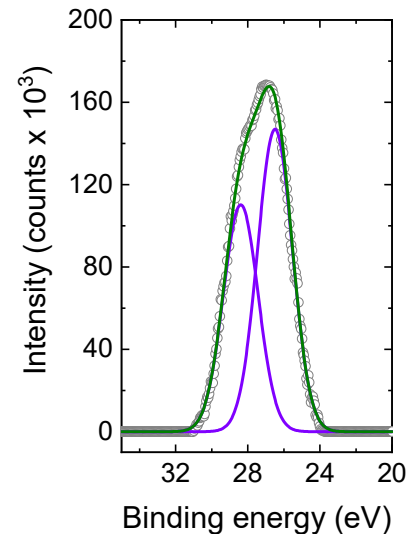


$$\alpha_R \approx 70 \text{ meV}\text{\AA}$$

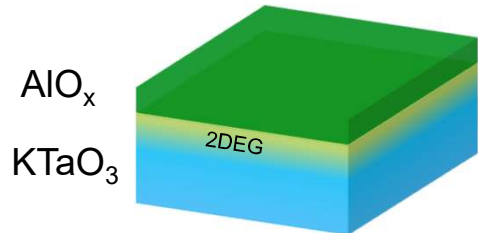
Generation of KTaO_3 2DEGs by Al sputtering at room temperature



(001) KTO substrates from Surface Net

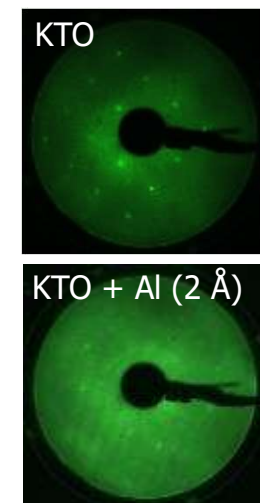
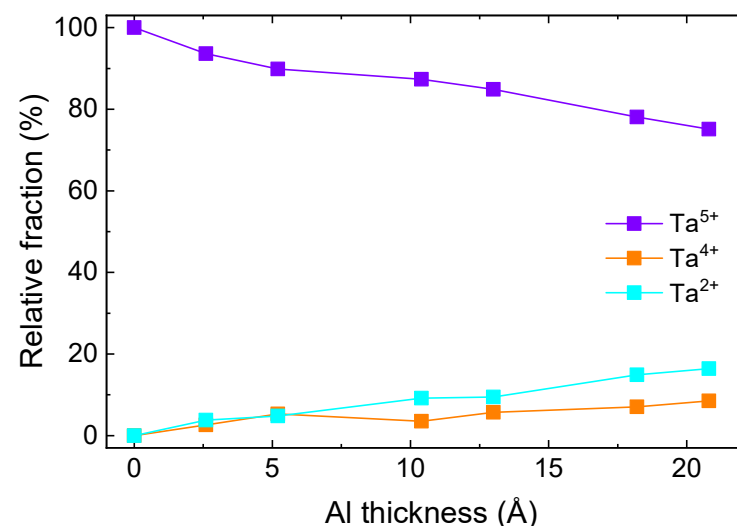
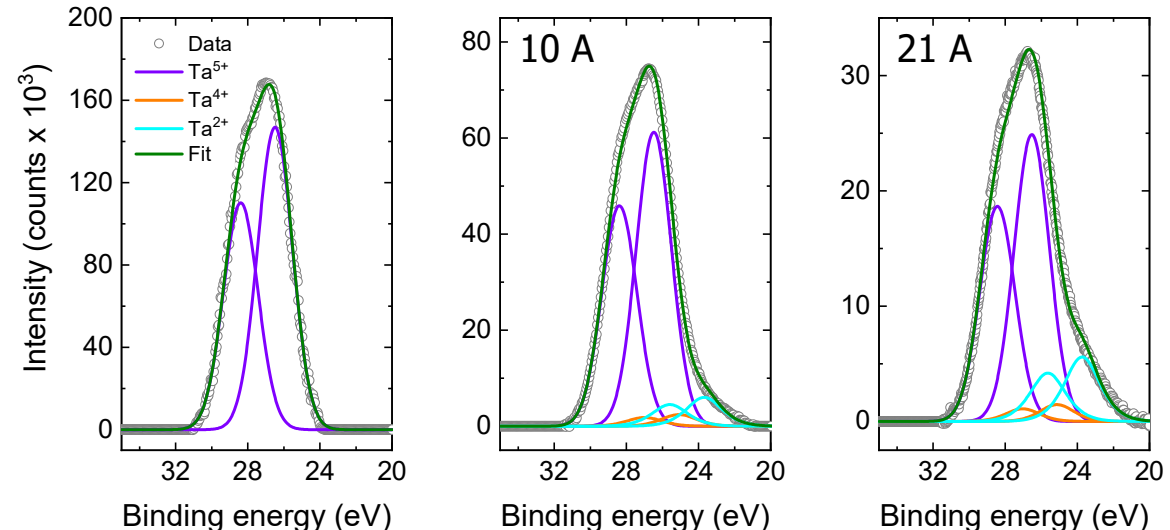
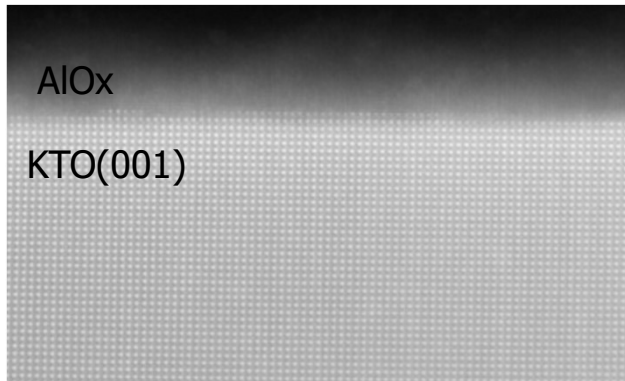


Generation of KTaO_3 2DEGs by Al sputtering at room temperature



(001) KTO substrates from Surface Net

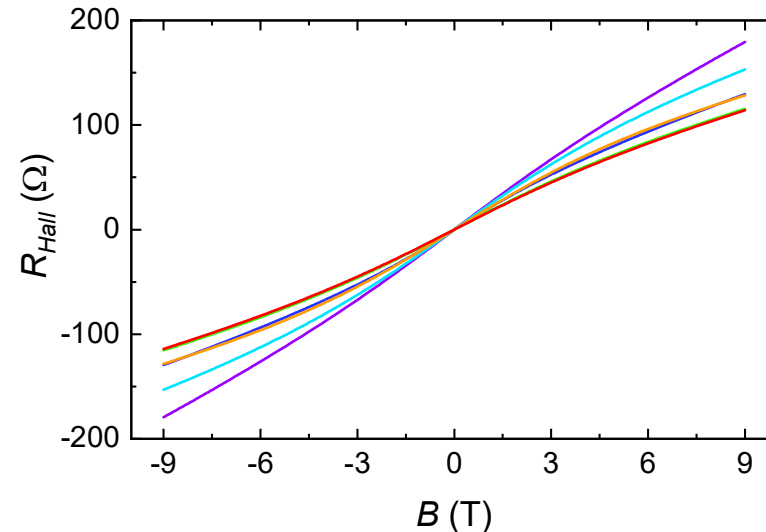
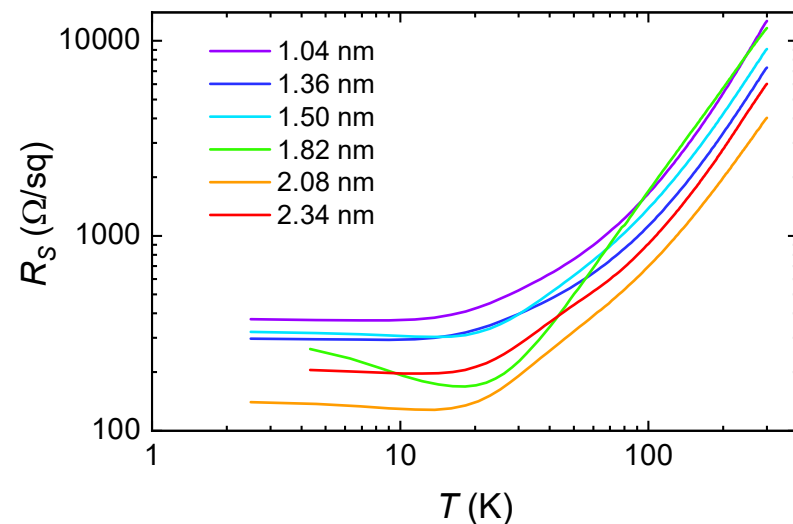
Growth of a few Å of Al by dc sputtering at room temperature



- As in STO/Al, redox reaction at KTO/Al interface : **2DEG formation**
- Proportion of reduced Ta increases with Al thickness
- Al/KTO interface looks clean in TEM

L.M. Vicente-Arche, MB et al,
Adv. Mater. 28, 202102 (2021)

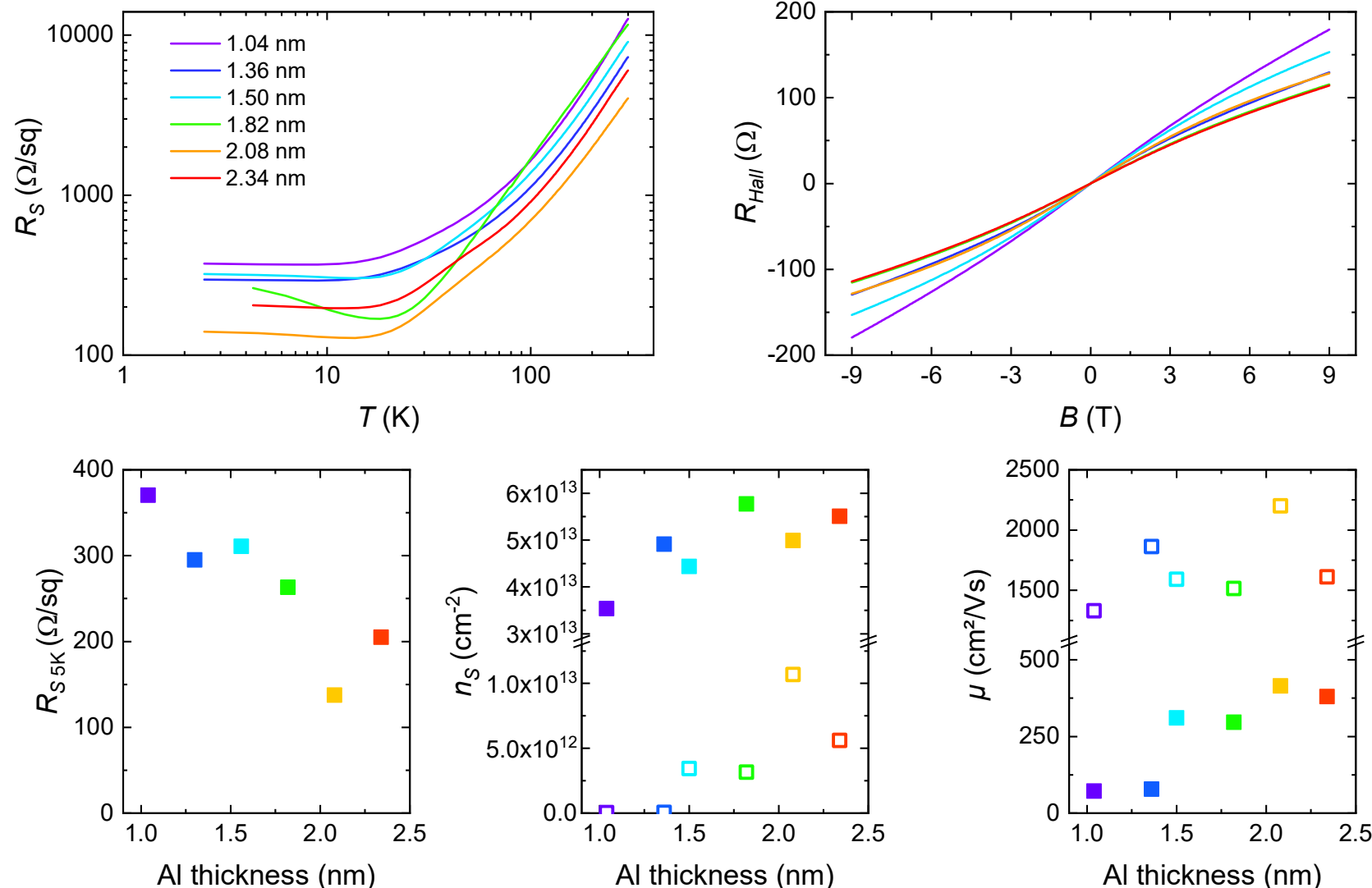
Transport properties of KTO/Al 2DEGs



- ⦿ Metallic behavior observed with high electron mobility at low T

L.M. Vicente-Arche, MB et al,
Adv. Mater. 28, 202102 (2021)

Transport properties of KTO/Al 2DEGs

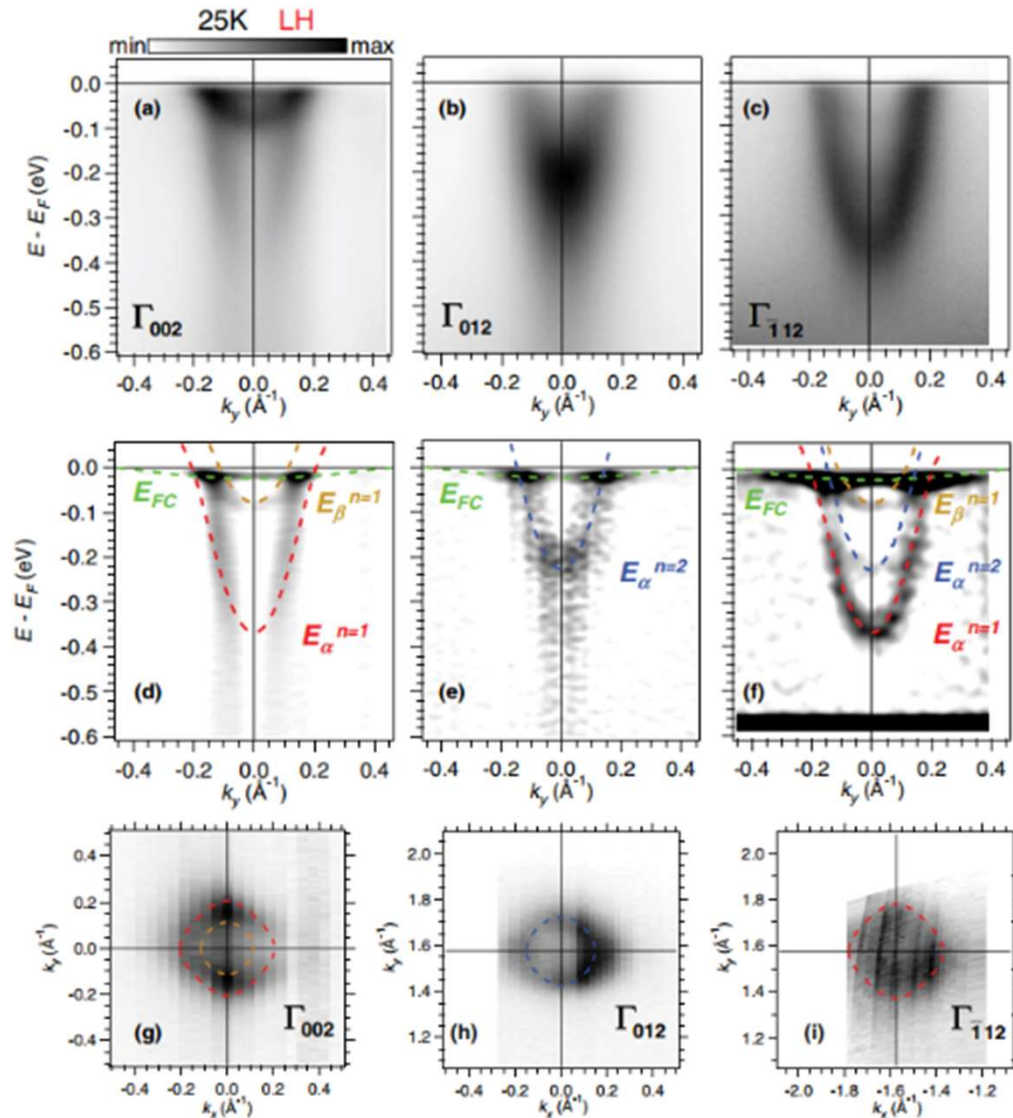


- Metallic behavior observed with high electron mobility at low T
- Carrier density and conductivity increase with Al thickness

L.M. Vicente-Arche, MB et al,
Adv. Mater. 28, 202102 (2021)

Band structure of KTO 2DEGs

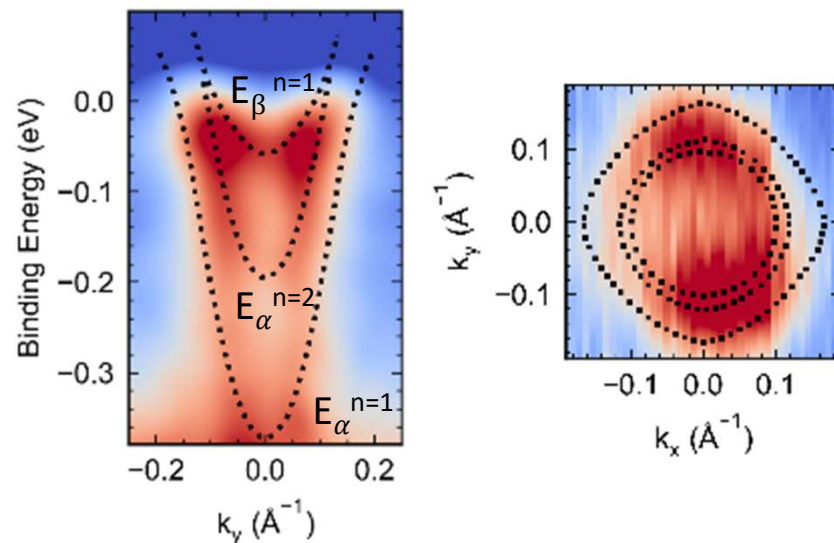
ARPES on (001) KTO surfaces



- Band structure resembles that of STO surface or STO 2DEGs
- Low-lying light bands with dominant d_{xy} character
- Heavy band with dominant $d_{xz/yz}$ character at higher energy
- Here, additional impurity band is observed
- Bands have lower mass than in STO 2DEGs

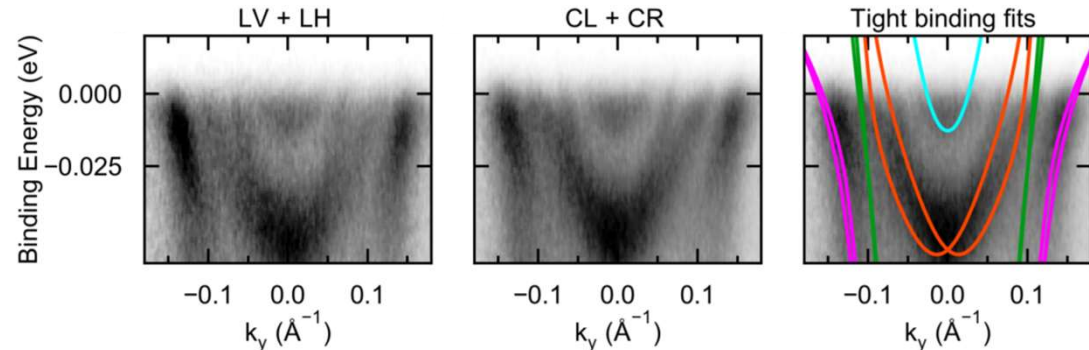
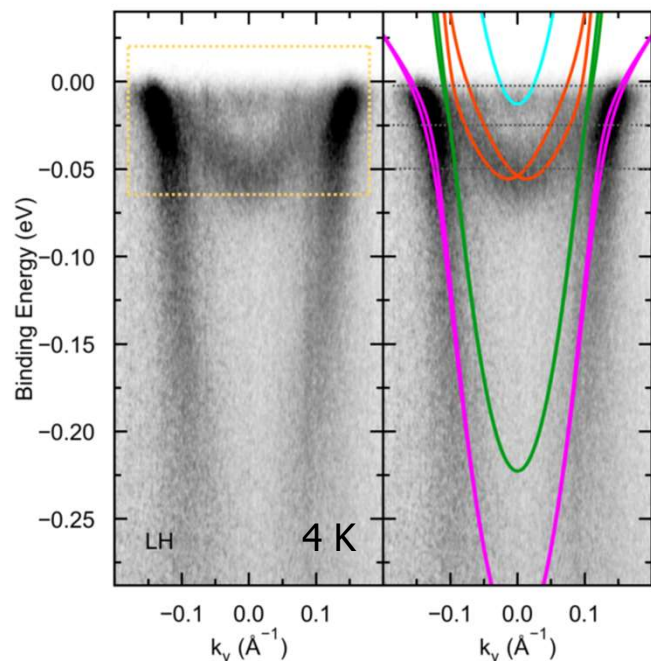
Santander-Syro, MB et al, PRB 86, 121107 (2012)

Direct visualization of the Rashba-split bands on KTO 2DEGs



- Growth of 1-2 Å of Al by MBE on KTO(001)
- ARPES at **room temperature** reveals same bands as in earlier literature (but no impurity band)

Cassiopée beamline, SOLEIL synchrotron, France



- Band structure comparable to KTO surface, with light (d_{xy}) and heavy ($d_{xz/yz}$) bands
- Orange band pair exhibits large Rashba splitting with $\alpha_R \approx 320$ meV·Å (one order higher than STO 2DEGs)
- **First direct visualization of Rashba splitting in perovskite oxides**

S. Varotto, MB et al. Nature Comm. 13, 6165 (2022)

1. SrTiO₃-based 2DEGs

1.1 Physics of bulk SrTiO₃

1.2 LaAlO₃/SrTiO₃ 2DEGs

1.3 Other SrTiO₃ 2DEGs

1.4 Electronic structure of SrTiO₃ 2DEGs

1.5 Superconductivity in SrTiO₃ 2DEGs

1.5 Introducing ferroic orders into SrTiO₃ 2DEGs

2. KTaO₃-based 2DEGs

2.1 Physics of bulk KTaO₃

2.2 KTaO₃ 2DEGs

2.3 Superconductivity in KTaO₃ 2DEGs

Search for superconductivity in KTO

Very Low-Temperature Search for Superconductivity in Semiconducting KTaO_3

J. R. Thompson

Department of Physics, The University of Tennessee, Knoxville, Tennessee, and Solid State Division, Oak Ridge National Laboratory,* Oak Ridge, Tennessee

L. A. Boatner

Solid State Division, Oak Ridge National Laboratory,* Oak Ridge, Tennessee

J. O. Thomson

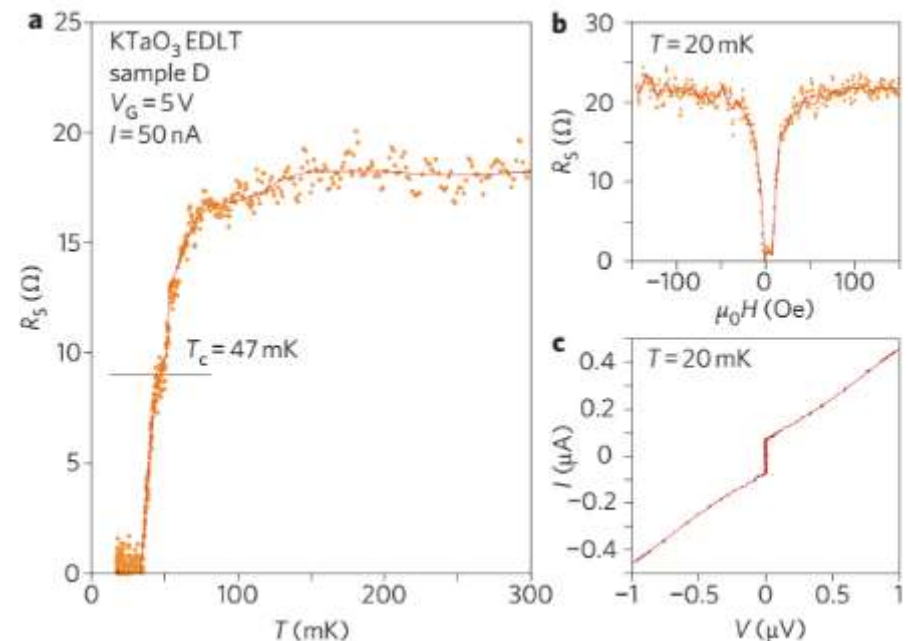
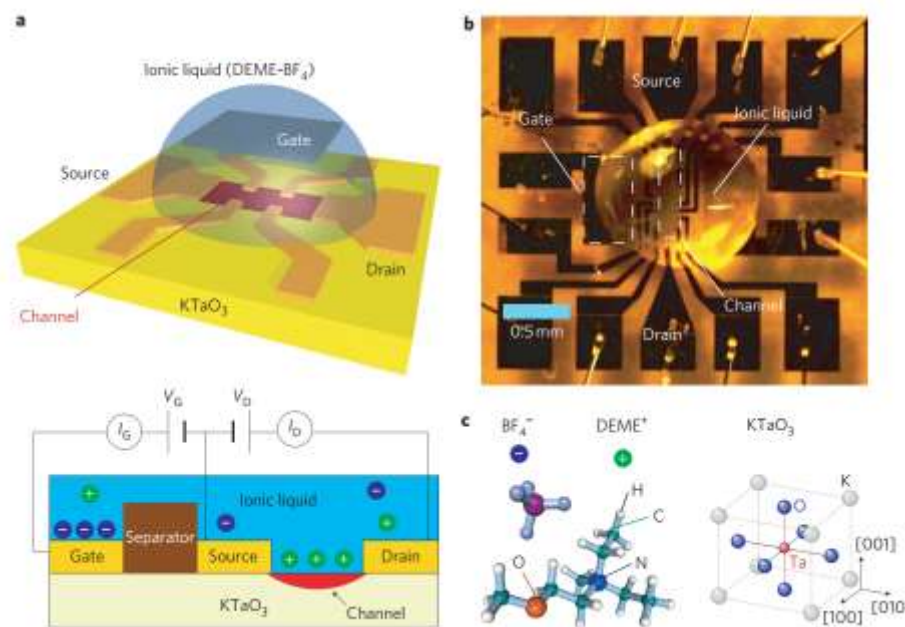
Department of Physics, The University of Tennessee, Knoxville, Tennessee

A series of attempts have been made to detect the presence of superconductivity in semiconducting potassium tantalate (KTaO_3) single crystals. Semiconducting potassium tantalate has a number of properties in common with semiconducting SrTiO_3 , which is superconducting below $\sim 0.3\text{ K}$, with a critical temperature T_c that varies as a function of the carrier concentration. Both KTaO_3 and SrTiO_3 are perovskite-structure oxides and both materials are so-called incipient ferroelectrics that are characterized by high dielectric constants at low temperature. These common properties suggest that superconductivity might also be observed in semiconducting potassium tantalate. In the temperature range from 0.01 to 4.0 K, however, no evidence was found for superconductivity in KTaO_3 in the presence of magnetic fields of 10^{-5} – 10^{-4} T (i.e., 0.1–1 Oe). Below 1.5 K, the search for superconductivity in KTaO_3 was carried out using a ^3He – ^4He dilution refrigerator equipped with a SQUID magnetometer and an ac magnetometer. The system response was verified by measuring the paramagnetic susceptibility of Dy_2O_3 -doped KTaO_3 . The failure to observe superconductivity in KTaO_3 , while SrTiO_3 is an established superconducting material, may be related to the fact that the latter substance assumes a tetragonal symmetry phase at 105 K, while KTaO_3 remains cubic to low temperatures.

No superconductivity found in KTO until...

Discovery of superconductivity in KTaO_3 by electrostatic carrier doping

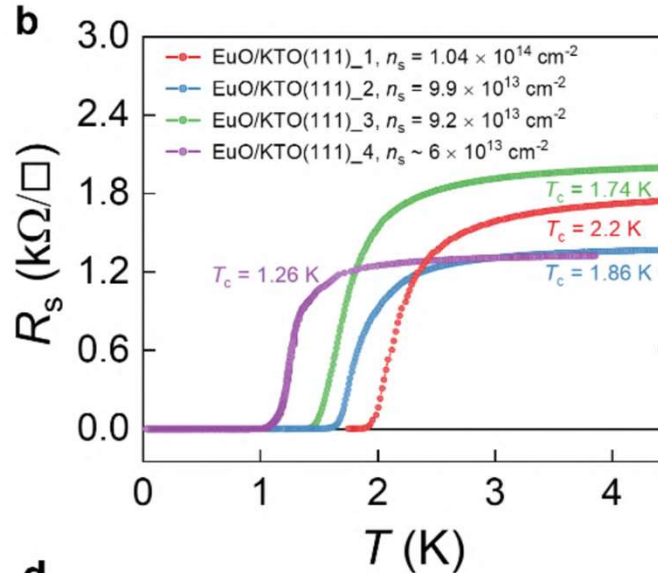
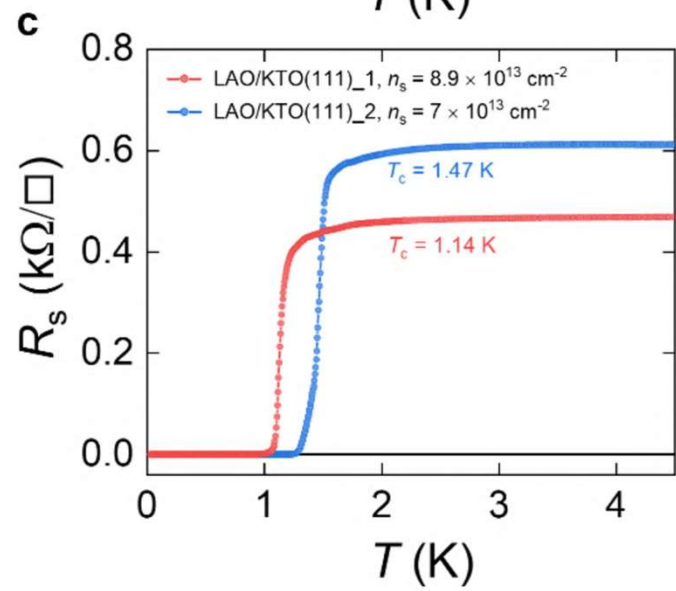
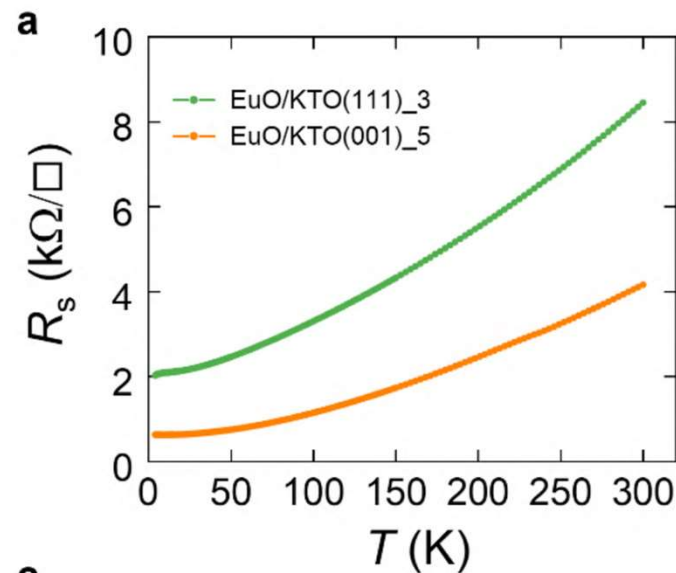
K. Ueno^{1,2}, S. Nakamura^{3,4}, H. Shimotani⁵, H. T. Yuan⁵, N. Kimura^{4,6}, T. Nojima^{3,4}, H. Aoki^{4,6}, Y. Iwasa^{5,7}
and M. Kawasaki^{1,5,7*}



- Ionic liquid doping induces superconductivity in KTO(001) with $T_C=47 \text{ mK}$, one order lower than in STO
- Critical carrier density about $4 \cdot 10^{14} \text{ cm}^{-2}$, about one order higher than in STO 2DEGs.

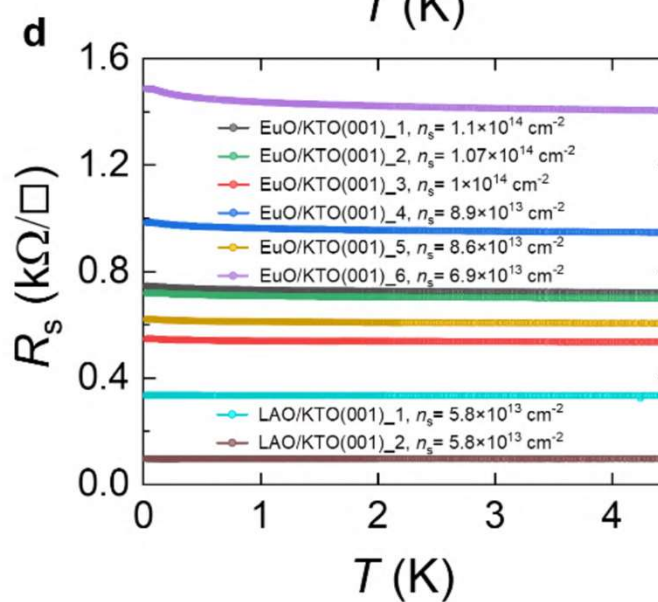
Ueno et al, Nature Nano. 6, 406 (2011)

Superconductivity in (111) KTO 2DEGs



First evidence of superconductivity in KTO (111) $T_C \sim 2$ K.

$$T_{C\text{ KTO}} > T_{C\text{ STO}}$$

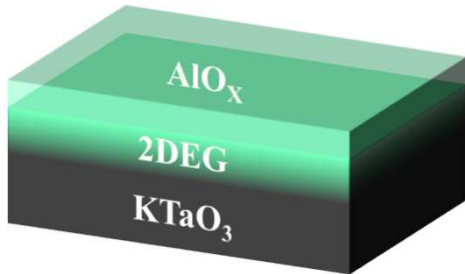


😢 KTO (001) : no SC

😊 KTO (111) : SC

Liu et al., Science 371, 716 (2021)

Formation of 2DEG at Al//KTO (111) interface

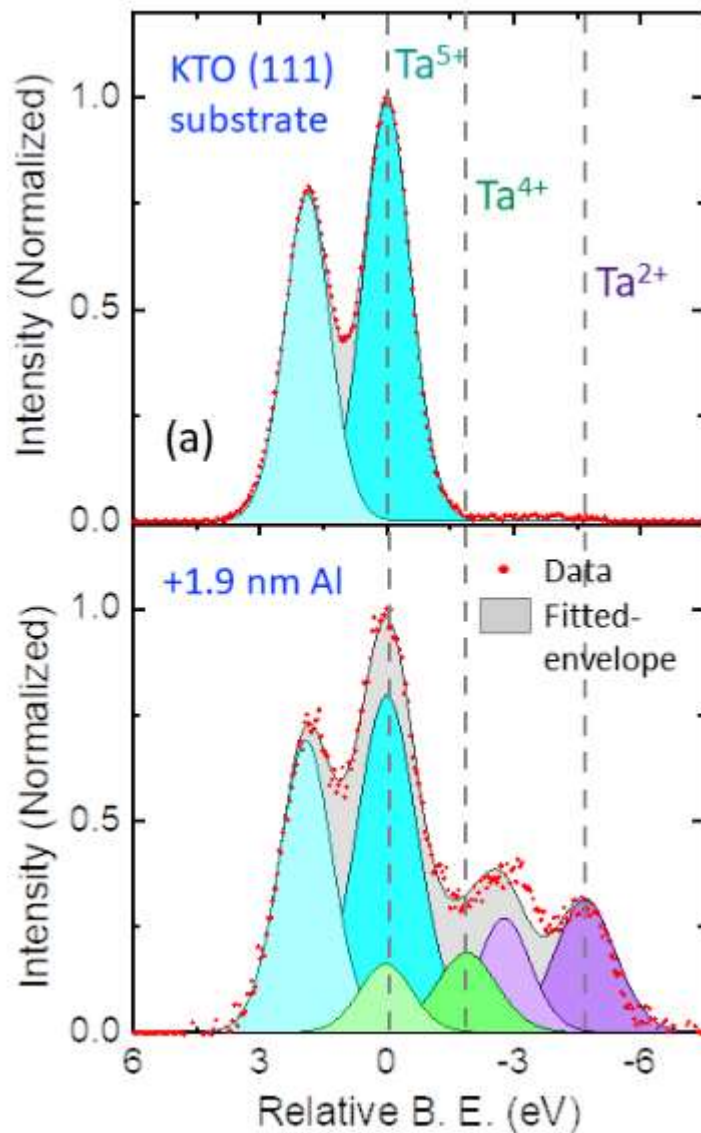


Sample structure

Deposition technique:
Sputtering

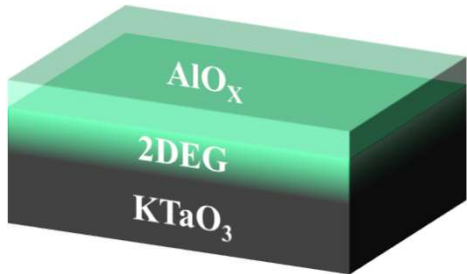
Metals used: **Al**

Pre-annealing: **600°C**
Growth temp: **500°C**



S. Mallik, MB et al, Nature Comm. 13, 4625 (2022)

Formation of 2DEG at Al//KTO (111) interface

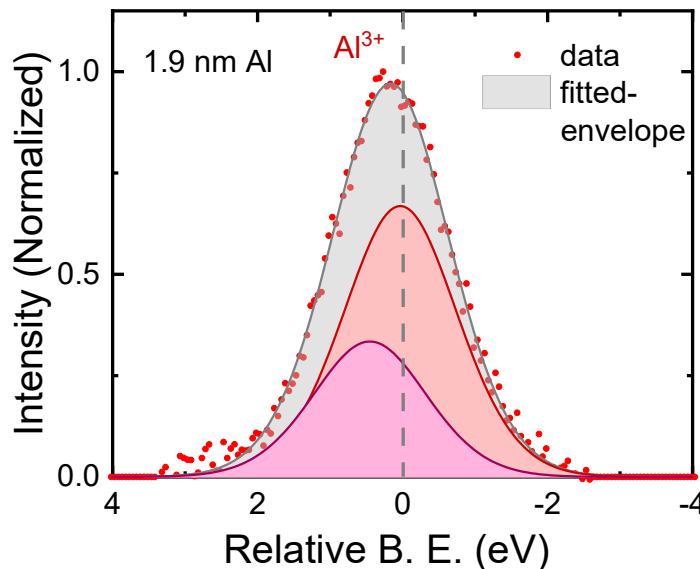


Sample structure

Deposition technique:
Sputtering

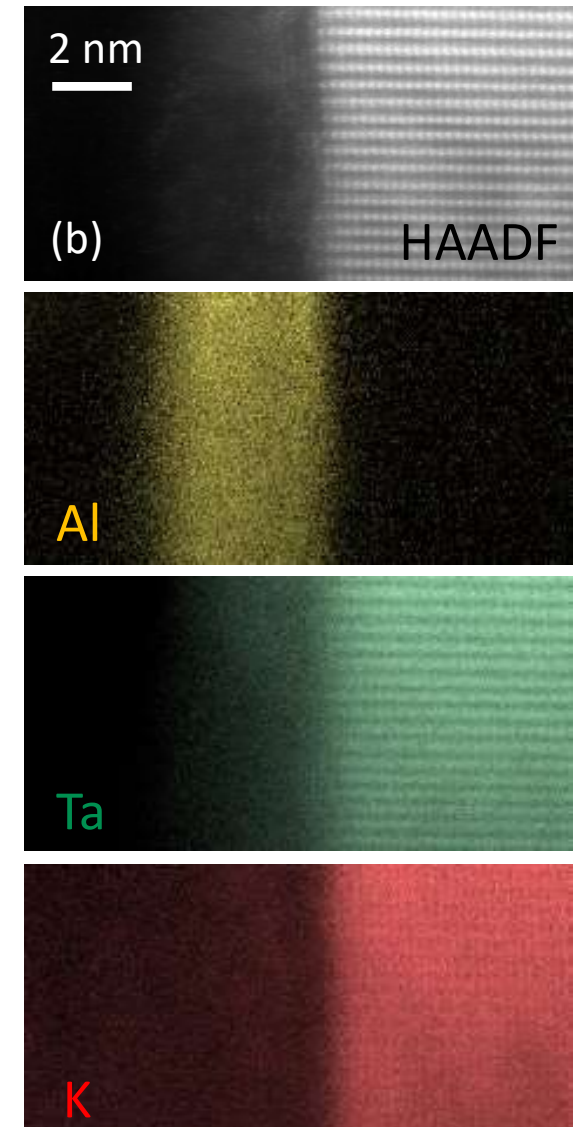
Metals used: **Al**

Pre-annealing: **600°C**
Growth temp: **500°C**



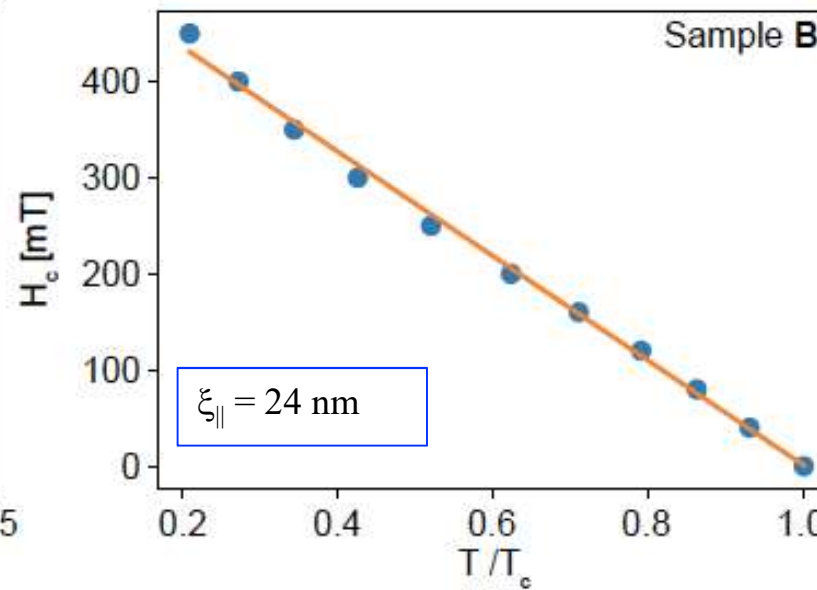
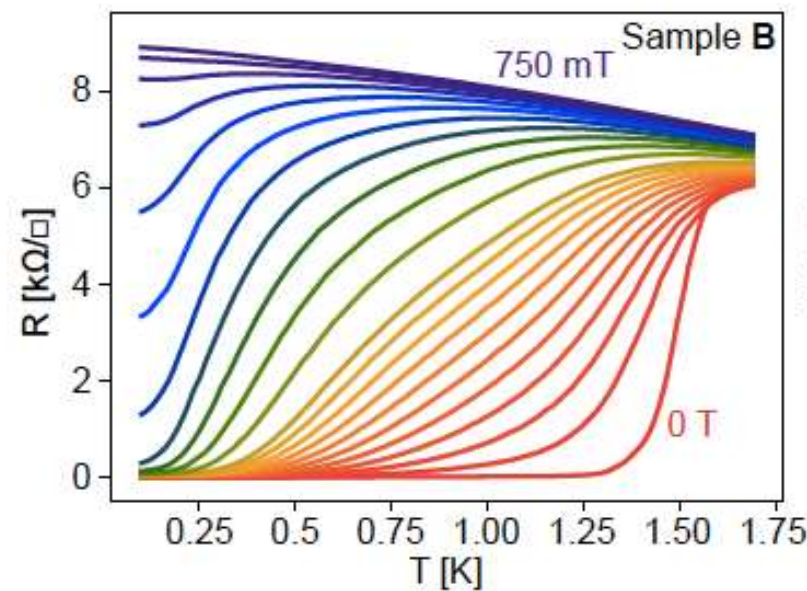
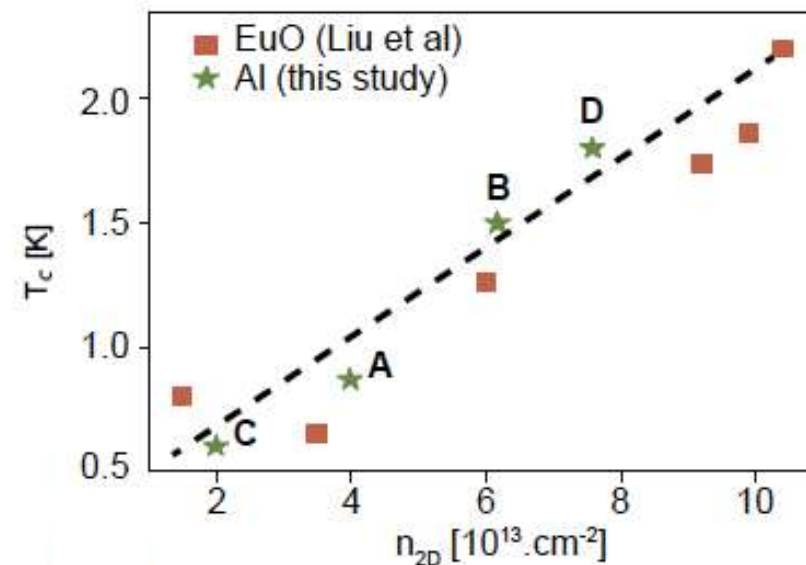
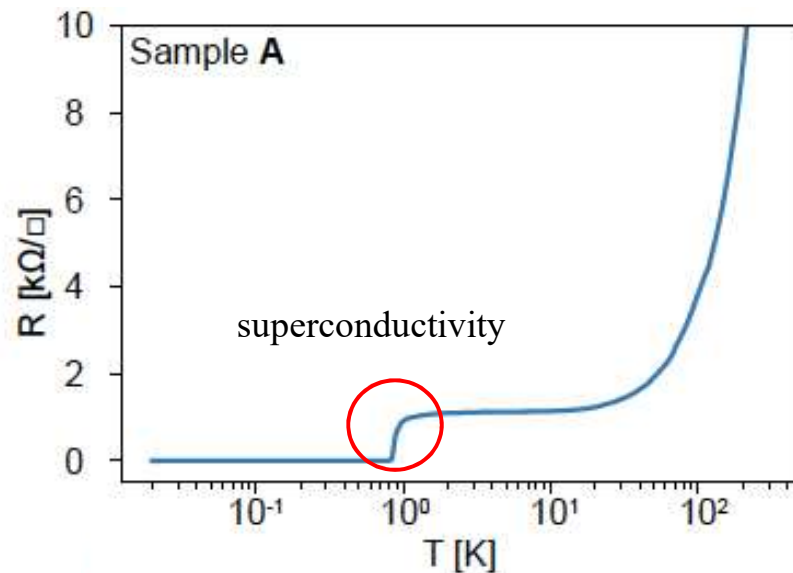
Fully oxidized Al

No interdiffusion of Al
into the substrate



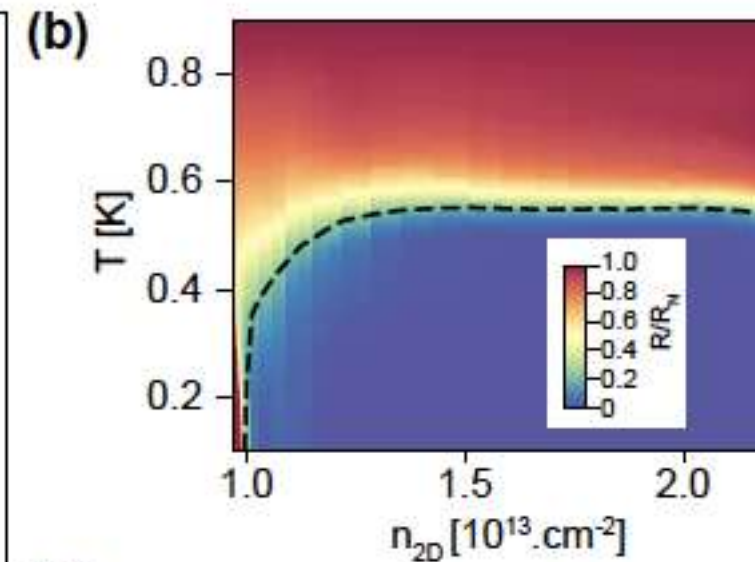
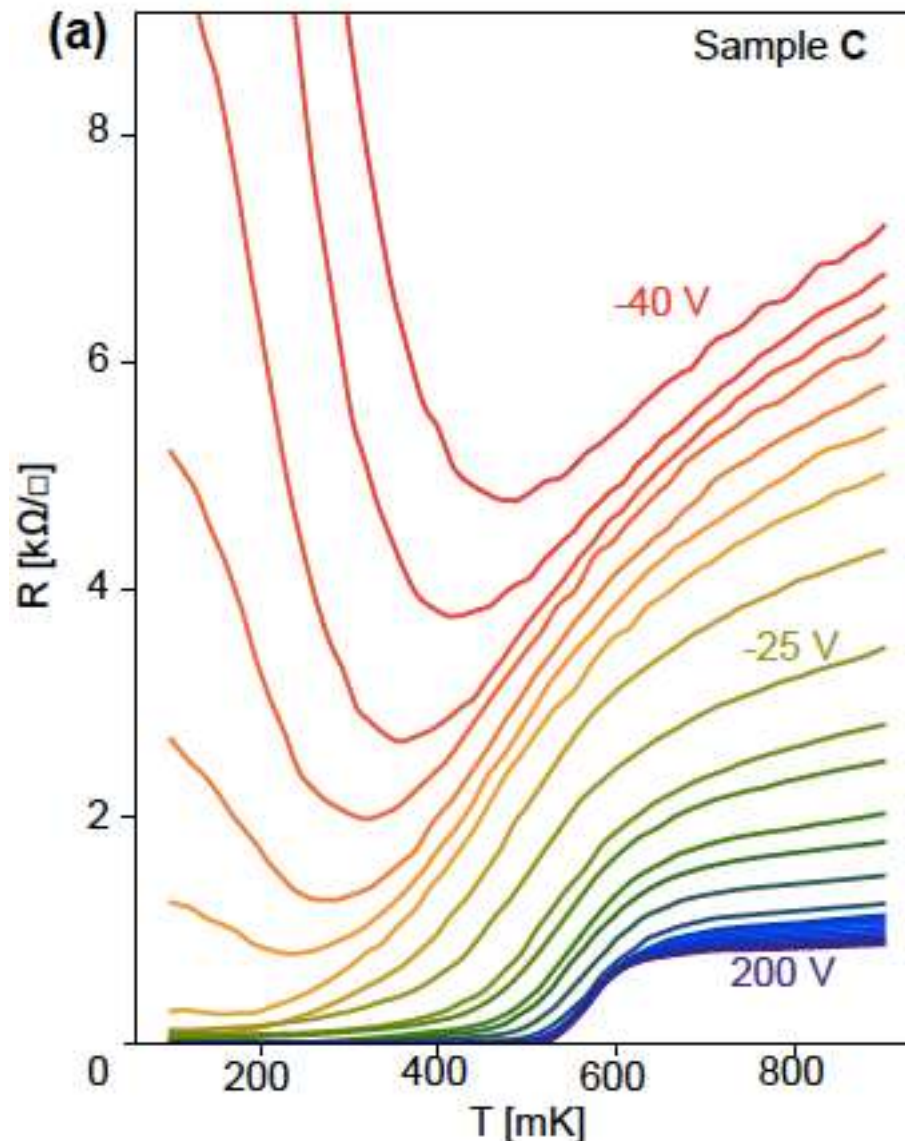
S. Mallik, MB et al, Nature Comm. 13, 4625 (2022)

Superconductivity at Al//KTO (111) interface



S. Mallik, MB et al, Nature Comm. 13, 4625 (2022)

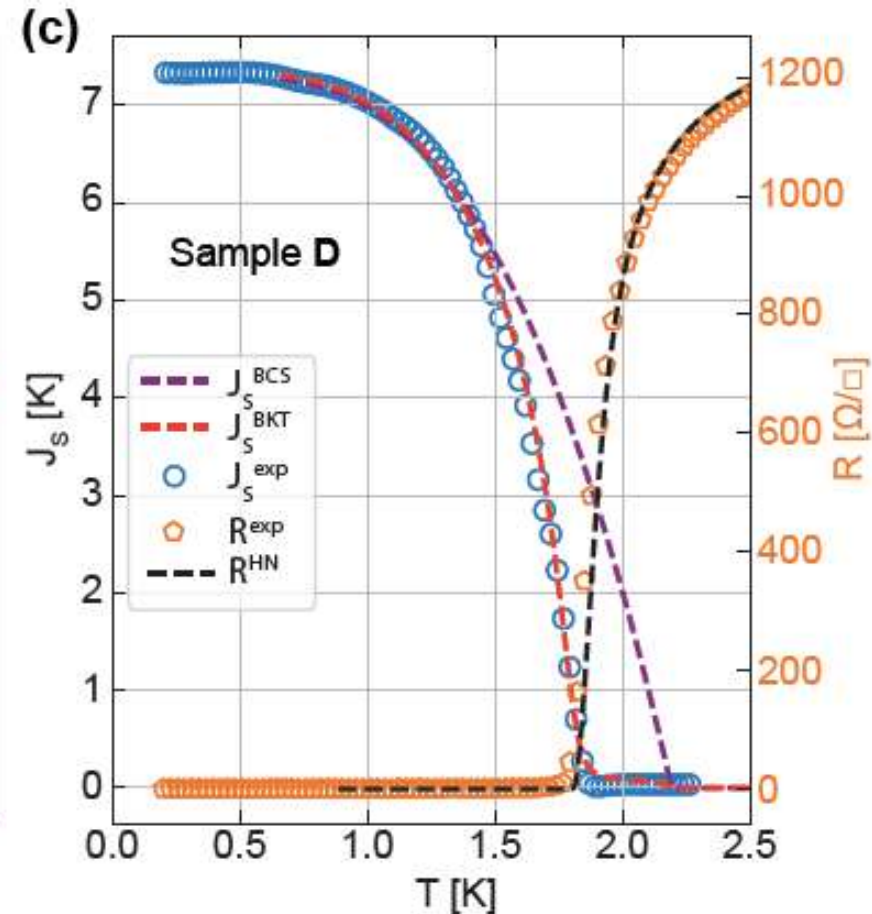
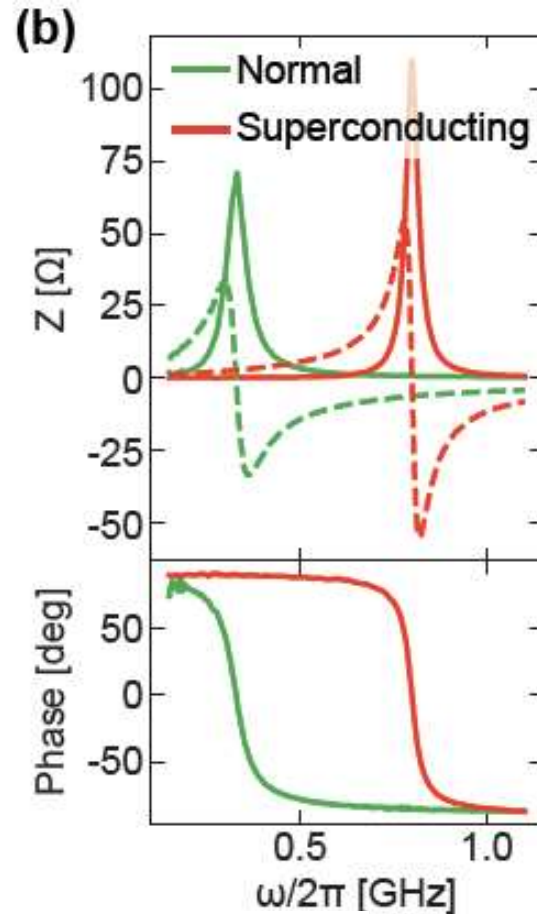
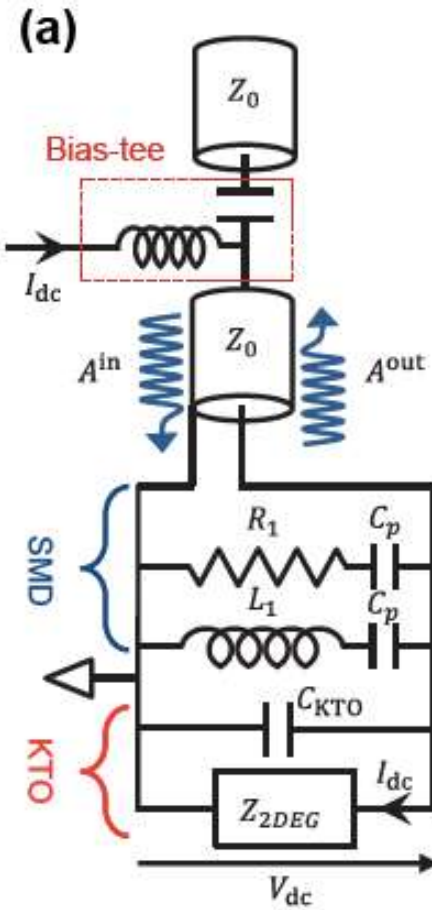
Superconductivity at Al//KTO (111) interface



- Disordered superconductivity below -25 V
- Possible to switch ON and OFF the SC with the gate voltage

S. Mallik, MB et al, Nature Comm. 13, 4625 (2022)

Superfluid stiffness measurements



Superfluid stiffness:

$$J_s(T) = \frac{\hbar^2}{4e^2 L_k(T)}$$

- The flattening of the J_s^{exp} curve below 1 K indicates a fully gapped behavior.
- Unlike STO, simple BCS model could not explain the nature of the $J_s(T)$ curve.

S. Mallik, MB et al, Nature Comm. 13, 4625 (2022)

Conclusions and perspectives

- Oxide interfaces have **unexpected electronic and magnetic properties**
- Some properties derive from the bulk of the compounds involved, **some are readily new**
- **Inversion symmetry breaking** is key to most new properties
- Both STO and KTO 2DEGs have Rashba SOC and are superconducting at low T
- Ferroic order can be introduced in these 2DEGs, expanding their functionalities
- Parameter space is huge and more **exotic phenomena** should arise from orbital and spin reconstruction (**topological effects**)



J. Varignon, MB et al., Nature Phys. 14, 322 (2018)
F. Trier, MB et al., Nature Rev. Mater. 7, 258 (2022)

Post-doc positions available !
If interested talk to me at
the School or email me at
manuel.bibes@cnrs-thales.fr